

# Production and Characterization of Fiber Reinforced Polymer Composites by Additive Manufacturing Method

Doctor of Philosophy  
in Materials Science and Engineering

by  
Alperen DOGRU  
ORCID 0000-0003-3730-3761

December, 2022

This is to certify that we have read the thesis **Production and Characterization of Fiber Reinforced Polymer Composites by Additive Manufacturing Method** submitted by **Alperen DOGRU**, and it has been judged to be successful, in scope and in quality, at the defense exam and accepted by our jury as a DOCTORAL THESIS.

**APPROVED BY:**

**Advisor:** **Prof. Dr. Mehmet Ozgur SEYDIBEYOGLU**  
İzmir Kâtip Çelebi University

**Committee Members:**

**Prof. Dr. İbrahim Etem SAKLAKOGLU**  
Ege University

**Assoc. Prof. Dr. Onur ERTUGRUL**  
İzmir Kâtip Çelebi University

**Assoc. Prof. Dr. Mehmet SARIKANAT**  
Ege University

**Asst. Prof. Dr. Aydın ÜLKER**  
İzmir Kâtip Çelebi University

**Date of Defense:** December 29, 2022

# Declaration of Authorship

I, **Alperen DOGRU**, declare that this thesis titled **Production and Characterization of Fiber Reinforced Polymer Composites by Additive Manufacturing Method** and the work presented in it are my own. I confirm that:

- This work was done wholly or mainly while in candidature for the Doctoral degree at this university.
- Where any part of this thesis has previously been submitted for a degree or any other qualification at this university or any other institution, this has been clearly stated.
- Where I have consulted the published work of others, this is always clearly attributed.
- Where I have quoted from the work of others, the source is always given. This thesis is entirely my own work, with the exception of such quotations.
- I have acknowledged all major sources of assistance.
- Where the thesis is based on work done by myself jointly with others, I have made clear exactly what was done by others and what I have contributed myself.

# Production and Characterization of Fiber Reinforced Polymer Composites by Additive Manufacturing Method

## Abstract

The production of polymer materials with additive manufacturing technology is an important issue that is a trend today. Studies are carried out on the production of high-performance polymer products with the additive manufacturing method. Currently, a wide variety of polymers can be processed in the Fused Filament Fabrication (FFF) method, one of the additive manufacturing methods. Pure polymers are generally preferred in the FFF method. Some polymers used in the FFF method show low mechanical properties, limiting their applications in the field of engineering. High-performance polymers are expensive to produce and difficult to process with FFF due to their high melting temperatures. For this reason, short fiber reinforcement was used to pure polymers' strength properties. To carry out production in the FFF method, short fiber-reinforced polymer matrix filaments were designed in the thesis study. Polyamide has been determined as a matrix material due to its wide application area and superior mechanical, thermal, and chemical properties. Designed filaments will be able to replace expensive and difficult-to-process materials, products that can be easily processed with standard FFF devices will be designed and testable products will be produced. The increase in the variety of materials used in this field will increase the

industrial usage area of the products produced by the FFF method and it will be possible to manufacture composite structures without injection molding, vacuum infusion, or pressure molding. With fiber-reinforced polymer filaments, it will be possible to produce low-cost products with complex geometries, especially in the aerospace, defense, automotive, and medical industries.

The most important problem in the production of fiber-reinforced polymer composites by the FFF method is the insufficient bonding of the layers and the formation of micro interfaces. Elimination of these defects will increase the mechanical performance of the final products produced by this method. In this context, carbon, glass, hybrid (carbon/glass) fiber reinforcements, and polyamide 6 matrix filaments were designed from the first stages of the thesis studies, and specimen production and characterizations were made. The mechanical properties of different production parameters examined with the FFF method process parameters were optimized. In the second stage, nanocellulose was added to glass and carbon fibers to improve the matrix-fiber interfaces and increase their mechanical properties. The same filaments were produced using modified fibers, and specimen production with the FFF method and characterizations were made. The designed hybrid composite structures are an innovative approach and their maximum tensile strength values are increased by 3 times compared to pure PA6.

**Keywords:** Hybrid Composites, Polymeric Composites, Polyamide, Nanocellulose, Fused Filament Fabrication, Additive Manufacturing

# Fiber Takviyeli Polimer Kompozitlerin Eklemeli İmalat Yöntemi ile Üretimi ve Karakterizasyonu

## Özet

Polimer malzemelerin eklemeli imalat teknolojisiyle üretilmesi günümüzde eğilim olan önemli bir konudur. Eklemeli imalat yöntemi ile yüksek performanslı polimer ürünlerin üretilmesi konusunda çalışmalar yapılmaktadır. Mevcut durumda eklemeli imalat yöntemlerinden erimiş filaman ekstrüzyonu (FFF) yönteminde çok çeşitli polimerler işlenebilmektedir. FFF yönteminde genel olarak saf polimerler tercih edilmektedir FFF yönteminde kullanılan bazı polimerler düşük mekanik özellikler göstermekte, mühendislik alanındaki uygulamaları kısıtlamaktadır. Yüksek performanslı polimerlerin üretilmesi ise oldukça pahalı ve erime sıcaklıklarının yüksek olması sebebiyle FFF ile işlenmesi zordur. Bu sebeple saf polimerlerin mukavemet özelliklerini iyileştirmek amacıyla kısa lif takviyesi yapılmıştır. FFF yönteminde üretim gerçekleştirebilmek için tez çalışmasında kısa lif katkılı polimer matrisli filamentler geliştirilmiştir. Geniş uygulama alanı, üstün mekanik, termal ve kimyasal özellikleri sebebiyle poliamide matris malzemesi olarak belirlenmiştir. Geliştirilen filamanlar pahalı ve işlenmesi zor malzemelerin yerini alabilecek, standart FFF cihazları ile kolay işlenebilen ürün geliştirilecek ve test edilebilir ürünlerin üretilmesi sağlanacaktır. Bu alanda kullanılan malzeme çeşitliliğinin artması FFF yöntemi ile üretilmiş ürünlerin endüstriyel kullanım alanını arttıracak ve kompozit yapıların plastik enjeksiyon, vakum infüzyon veya basınçlı kalıplama olmaksızın imal edilmesi sağlanacaktır. Lif takviyeli polimer filamanlar ile havacılık, savunma, otomotiv ve medikal sektörleri başta olmak üzere kompleks geometri ürünlerin düşük maliyetli olarak üretilmesine imkan sağlanacaktır.

Lif takviyeli polimer kompozit filamanların FFF yöntemi ile üretilmesinde karşılaşılan en önemli problem, katmanların yeterli birleşmemesi ve mikro ara yüzeylerin oluşmasıdır. Bu kusurların giderilmesi bu yöntem ile üretilen nihai ürünlerin mekanik performanslarını arttıracaktır. Bu kapsamda tez çalışmalarının ilk aşamalarından karbon, cam ve hibrit (karbon/cam) fiber takviyeleri poliamide 6 matrisli filamanlar geliştirilmiş, numune üretimleri ve karakterizasyonlar yapılmıştır. FFF yöntemi ile farklı üretim parametrelerinin mekanik özellikleri incelenmiş ve proses parametreleri optimize edilmiştir. İkinci aşamada ise matris-fiber ara yüzeylerini iyileştirmek ve mekanik özelliklerini arttırmak amacıyla cam ve karbon fiberlere nanoselüloz katkısı gerçekleştirilecektir. Modifiye edilmiş fiberler kullanılarak aynı filamentler geliştirilmiş, FFF yöntemi ile numune üretimi gerçekleştirilip karakterizasyonlar yapılmıştır. Geliştirilen hibrit kompozit yapılar yenilikçi bir yaklaşım olup maksimum çekme mukavemeti değerlerinde saf PA6'ya oranla 3 katı artış sağlanmıştır.

**Anahtar Kelimeler:** Hibrit Kompozitler, Polimerik Kompozitler, Poliamit, Nanoselüloz, Erimiş Filaman Ekstrüzyonu, Eklemeli İmalat

*Verba volant, Scripta manent, to the curious man in me and to my family who has  
always helped me...*



# Acknowledgment

I want to express my gratitude to my esteemed supervisor Prof. Dr. M Özgür SEYDİBEYOĞLU, whose character and science I have always taken as an example and whose knowledge and experience I have benefited greatly from. I am eternally grateful to him for his support and help throughout my studies, for providing solutions to every challenge, and for creating many opportunities to expand my horizons and increase the quality of my studies. I am also grateful to Prof. Dr. Cagri AYRANCI, who made great contributions to the realization of a part of the thesis, and whose knowledge and experience I benefited from during my time in his laboratories.

I heartily thank our only daughter, Pera DOĞRU who is our adventure partner, and my dear wife Özlem DOĞRU who did not spare her moral support from the beginning to the end of my doctoral process that did not leave me alone even miles away from our families by sacrificing her comfort and dreams, and to my mother Beyhan DOĞRU, and my father Kemal DOĞRU, who have made me come to these days by not refraining from any sacrifice and whose rights I will never be able to repay. I dedicate my thesis to them.

I would like to thank Prof. Dr. İbrahim Etem SAKLAKOĞLU and Associate Prof. Dr. Onur ERTUĞRUL in the thesis monitoring committee who closely followed all the processes of my thesis and guided me with their feedback.

I wish to show my appreciation to the members of the University of Alberta Multi-functional Composite Research Group for their contribution to the realization of the study. I would like to thank Dr. Didem KALE, Seçil YILANCIOĞLU, Mehmet Sadık EGELİ, Lecturer. Ayberk SÖZEN and Özay AKSOY that my esteemed supporters and friends, who somehow do not spare me their ideas, support, and help during my thesis work.

In addition, I would like to thank TÜBİTAK (2214-A) and İzmir Katip Çelebi University (2021-TDR-FEBE-0003) for the scholarship and project opportunities they provided in the realization of this thesis. I am so grateful to the University of Alberta

for its laboratory facilities and to Ege University where I have been working for many years.

Alperen DOĐRU

# Table of Contents

<b>Declaration of Authorship</b> .....	<b>ii</b>
<b>Abstract</b> .....	<b>iii</b>
<b>Özet</b> .....	<b>v</b>
<b>Acknowledgment</b> .....	<b>viii</b>
<b>List of Figures</b> .....	<b>xiii</b>
<b>List of Tables</b> .....	<b>xvii</b>
<b>List of Abbreviations</b> .....	<b>xix</b>
<b>List of Symbols</b> .....	<b>xxi</b>
<b>1 Introduction</b> .....	<b>1</b>
1.1 Polymer.....	1
1.1.1 Thermosetting Polymer.....	3
1.1.2 Thermoplastics.....	3
1.2 Polymeric Composite Materials.....	4
1.2.1 Thermoplastic Composites.....	5
1.2.2 Fiber Reinforced Thermoplastic Composites.....	6
1.2.3 Fibers.....	7
1.3 Hybrid Composites.....	11
1.3.1 Polyamide Matrix Hybrid Composites.....	12
1.4 Thermoplastic Composite Production Methods.....	13
1.4.1 Extrusion Process.....	15
1.5 Additive Manufacturing Technologies.....	16
1.5.1 Additive Manufacturing Methods.....	18

1.5.2 Fused Filament Fabrication (FFF).....	20
<b>2 Literature Review.....</b>	<b>22</b>
<b>3 Experimental .....</b>	<b>41</b>
3.1 Materials .....	41
3.1.1 PA6 Polymer .....	41
3.1.2 Carbon Fiber .....	42
3.1.3 Glass Fiber .....	43
3.1.4 Nano Cellulose.....	43
3.2 Short Fiber Reinforced (SFR) PA6 matrix Composites .....	44
3.2.1 SFR PA6 matrix Composites Compounding .....	45
3.2.2 SFR PA6 matrix Composites Filament Extrusion .....	47
3.2.3 SFR PA6 matrix Composites Production with FFF.....	49
3.3 Modified SFR PA6 matrix Composites.....	63
3.3.1 Modification of fibers with Nanocellulose .....	64
3.3.2 Modified SFR PA6 matrix Composites Compounding .....	66
3.3.3 SFR PA6 matrix Composites Filament Extrusion .....	67
3.3.4 Modified SFR PA6 matrix Composites Production with FFF.....	70
3.4 Mechanical Tests and Analysis .....	74
3.4.1 Thermal Analysis .....	74
3.4.2 Mechanical Testing .....	75
3.4.3 SEM .....	77
<b>4 Results and Discussion .....</b>	<b>79</b>
4.1 Results .....	79
4.1.1 Thermal Analysis .....	80
4.1.2 Mechanical Testing.....	87
4.1.3 Morphology.....	105
4.2 Discussion .....	109

4.2.1 TGA .....	109
4.2.2 DSC .....	110
4.2.3 Tensile Testing .....	111
4.2.4 Impact Testing .....	117
4.2.5 Compression Testing .....	119
4.2.6 SEM Analysis .....	121
<b>5 Conclusion.....</b>	<b>124</b>
<b>References .....</b>	<b>127</b>
<b>Curriculum Vitae .....</b>	<b>141</b>

# List of Figures

Figure 1.1 Classification of Polymers .....	2
Figure 1.2 Thermoplastic Polymers .....	6
Figure 1.3 Composite material reinforcement types	7
Figure 1.4 Carbon Fiber Image .....	9
Figure 1.5 Glass Fiber Image .....	9
Figure 1.6 Molecular structure of PA6 (left) and PA66 (right) .....	12
Figure 1.7 Twin-screw extruder .....	16
Figure 1.8 Single Screw Extruder .....	16
Figure 1.9 Material Based Additive manufacturing methods .....	19
Figure 1.10 Illustration of fused filament fabrication technique .....	21
Figure 2.1 FFF Device .....	24
Figure 2.2 AM Processes .....	24
Figure 2.3 FFF method diagram .....	25
Figure 2.4 (a) PLA Filament (b) TPU Filament.....	26
Figure 2.5 Unmanned Air Vehicle (UAV) propeller produced with FFF.....	31
Figure 2.6 Topology optimized aerospace part produced with AM .....	35
Figure 2.7 Thermal Annealing .....	36
Figure 2.8 Fiber Coating .....	36
Figure 3.1 Ultramid B40LN PA6 Pellet.....	42
Figure 3.2 Dowaksa AC4102 Short Carbon Fiber .....	42
Figure 3.3 Şisecam PA2short e-glass fiber .....	43
Figure 3.4 Slurry Nanocellulose .....	44
Figure 3.5 Short Fiber Reinforcement Composite Compounds.....	47
Figure 3.6 Single-screw Extruder .....	48
Figure 3.7 Laser Measuring Gauge.....	48
Figure 3.8 Single Screw Extrusion Parameters Setting Screens .....	49
Figure 3.9 Composite Filaments .....	49
Figure 3.10 Ultimaker 3 FFF Device .....	50

Figure 3.11 Ultimaker CC Printcore nozzle.....	51
Figure 3.12 ASTM D-638 Type5 Geometry.....	51
Figure 3.13 Infill patterns geometry for tensile specimens (-/+45°).....	52
Figure 3.14 Pure PA6 Tensile Test Specimens.....	53
Figure 3.15 PA6CF10 Tensile Test Specimens .....	54
Figure 3.16 PA6CF20 Tensile Test Specimens .....	55
Figure 3.17 PA6GF10 Tensile Test Specimens .....	56
Figure 3.18 PA6GF20 Tensile Test Specimens .....	57
Figure 3.19 PA6HF10 Tensile Test Specimens .....	58
Figure 3.20 PA6HF20 Tensile Test Specimens .....	59
Figure 3.21 ISO 179 Impact Charpy Geometry .....	60
Figure 3.22 Infill patterns geometries for impact specimens (0°/90°, -/+45°).....	60
Figure 3.23 Impact Charpy Test Specimens .....	61
Figure 3.24 ASTM D 695 Compression Test Geometry .....	61
Figure 3.25 Compression Test Specimens .....	62
Figure 3.26 Precision Balance.....	64
Figure 3.27 After Drying Process (a) Carbon fiber (b) Glass Fiber.....	65
Figure 3.28 Modified Short Fiber Reinforcement Composite Compounds.....	66
Figure 3.29 Vacuum Oven .....	67
Figure 3.30 Vacuumed Compounds.....	67
Figure 3.31 Single Screw Extruder .....	68
Figure 3.32 filabot airpath for cooling and filament spool system .....	68
Figure 3.33 Schematic representation of the single screw extrusion line .....	68
Figure 3.34 Single-screw extruder parameters adjusting screen.....	69
Figure 3.35 Filaments and Vacuumed filament spools.....	69
Figure 3.36 Ultimaker 3 FFF device and Ultimaker CC Printcore nozzle.....	70
Figure 3.37: Tensile Test Specimens for second stage .....	71
Figure 3.38 Impact Charpy Test Specimens .....	72
Figure 3.39 Compression Test Specimens .....	73
Figure 3.40 TA Intruments TGA Q50 Device.....	74
Figure 3.41 TA Instruments DSC Q100 Device .....	74
Figure 3.42 Zwick/Roell Z050 Tensile Testing Device.....	75
Figure 3.43 Instron 5966 Tensile Testing Device .....	75

Figure 3.44 CEAST Resil Impactor Device.....	76
Figure 3.45 Instron 5966 Compression Testing Device.....	76
Figure 3.46 Zeiss Sigma500 FESEM Device .....	77
Figure 3.47 Zeiss EVO MA10 .....	78
Figure 4.1 Pure PA6 Materials TGA Result .....	81
Figure 4.2 PA6CF10 Materials TGA Result.....	81
Figure 4.3 PA6CF20 Materials TGA Result.....	81
Figure 4.4 PA6GF10 Materials TGA Result.....	82
Figure 4.5 PA6GF20Materials TGA Result .....	82
Figure 4.6 PA6HF10 Materials TGA Result.....	82
Figure 4.7 PA6HF20 Materials TGA Result.....	83
Figure 4.8 PurePA6 Specimens DSC Results .....	83
Figure 4.9 PA6CF10 Specimens DSC Results .....	84
Figure 4.10 PA6CF20 Specimens DSC Results .....	84
Figure 4.11 PA6GF10 Specimens DSC Results .....	84
Figure 4.12 PA6GF20 Specimens DSC Results .....	85
Figure 4.13 PA6HF10 Specimens DSC Results .....	85
Figure 4.14 PA6HF20 Specimens DSC Results .....	85
Figure 4.15 Non-modified Specimens Tensile Test Results (Parameter 15).....	87
Figure 4.16 PurePA6 Specimens Tensile Test Results .....	88
Figure 4.17 PA6CF10 Specimens Tensile Test Results.....	89
Figure 4.18 PA6CF20 Specimens Tensile Test Results.....	90
Figure 4.19 PA6GF10 Specimens Tensile Test Results .....	91
Figure 4.20 PA6GF20 Specimens Tensile Test Results .....	92
Figure 4.21 PA6HF10 Specimens Tensile Test Results .....	93
Figure 4.22 PA6HF20 Specimens Tensile Test Results .....	94
Figure 4.23 PA6CF10c and PA6CF10 Specimens Tensile Test Results.....	97
Figure 4.24 PA6CF20c and PA6CF20 Specimens Tensile Test Results.....	97
Figure 4.25 PA6GF10c and PA6GF10 Specimens Tensile Test Results .....	98
Figure 4.26 PA6GF20c and PA6GF20 Specimens Tensile Test Results .....	98
Figure 4.27 PA6HF10c and PA6HF10 Specimens Tensile Test Results .....	99
Figure 4.28 PA6HF20c and PA6HF20 Specimens Tensile Test Results .....	99
Figure 4.29 Non-modified Specimens Impact Charpy Test Results.....	100



Figure 4.30 Modified Specimens Impact Charpy Test Results .....	101
Figure 4.31 Pure PA6 Compression Test Results .....	102
Figure 4.32 PA6 wt10% CF reinforcement Specimens Compression Test Results	102
Figure 4.33 PA6 wt20% CF reinforcement Specimens Compression Test Results	103
Figure 4.34 PA6 wt10% GF reinforcement Specimens Compression Test Results	103
Figure 4.35 PA6 wt20% GF reinforcement Specimens Compression Test Results	104
Figure 4.36 PA6 wt10% HF reinforcement Specimens Compression Test Results	104
Figure 4.37 PA6 wt20% HF reinforcement Specimens Compression Test Results	105
Figure 4.38 Non-modified Carbon Reinforcement Specimens SEM Images .....	106
Figure 4.39 Non-modified Glass Reinforcement Specimens SEM Images .....	106
Figure 4.40 Non-modified Hybrid Reinforcement Specimens SEM Images .....	107
Figure 4.41 Modified Carbon Reinforcement Specimens SEM Images .....	108
Figure 4.42 Modified Glass Reinforcement Specimens SEM Images .....	108
Figure 4.43 Modified Hybrid Reinforcement Specimens SEM Images .....	109
Figure 4.44 Spaces Between Layers in FFF Printed Specimen .....	111
Figure 4.45 PA6HF20 Specimen SEM Image .....	121
Figure 4.46 PA6GF10 Specimen SEM Image .....	122
Figure 4.47 PA6CF20 Specimen SEM Image .....	122
Figure 4.48 PA6HF10c Specimen SEM Image .....	123

# List of Tables

Table 1.1 Crystal Polymer Properties .....	4
Table 1.2 Typical properties of resins .....	5
Table 1.3 Polymer Matrix and Properties .....	6
Table 1.4 Fiber Types .....	8
Table 1.5 Typical properties of fibers .....	10
Table 1.6 Reason for using Hybrid Composite .....	12
Table 1.7 Processing methods for hybrid composites.....	14
Table 1.8 An overview of additive manufacturing .....	17
Table 1.9 Polymer Based Additive Manufacturing Methods.....	19
Table 2.1 Research of fiber-reinforced PLA and ABS matrix by the FFF .....	27
Table 2.2 Research of fiber-reinforced PA6 matrix by the FFF .....	33
Table 3.1 SFRThermoplastics Composite Compounds .....	44
Table 3.2 Single Screw Extrusion Parameters .....	49
Table 3.3 Mechanical Test Standards .....	50
Table 3.4 Fixed Parameters for FFF manufacturing .....	51
Table 3.5 FFF Parameters .....	52
Table 3.6 FFF Parameters for Impact Specimens .....	60
Table 3.7 FFF Parameters for Compression Specimens .....	62
Table 3.8 Modified SFR Thermoplastics Composite Compounds .....	63
Table 3.9 Single-screw extruder barrel temperature .....	69
Table 3.10 FFF process parameters for Tensile Specimens.....	71
Table 3.11 FFF Parameters for Impact Specimens .....	72
Table 3.12 FFF Parameters for Compression Specimens .....	73
Table 4.1 DSC results .....	86
Table 4.2 PurePA6 Specimens Tensile Test Results .....	88
Table 4.3 PA6CF10 Specimens Tensile Test Results.....	89
Table 4.4 PA6CF20 Specimens Tensile Test Results .....	90
Table 4.5 PA6GF10 Specimens Tensile Test Results.....	91
Table 4.6 PA6GF20 Specimens Tensile Test Results.....	92

Table 4.7 PA6HF10 Specimens Tensile Test Results.....	93
Table 4.8 PA6HF20 Specimens Tensile Test Results.....	94
Table 4.9 Non-modified Specimens Tensile test results .....	95
Table 4.10 All Average Tensile Results (13-14-15 parameters).....	96
Table 4.11 PA6CF10c Specimens Tensile Test Results .....	97
Table 4.12 PA6CF20c Specimens Tensile Test Results .....	97
Table 4.13 PA6GF10c Specimens Tensile Test Results .....	98
Table 4.14 PA6GF20c Specimens Tensile Test Results .....	98
Table 4.15 PA6HF10c Specimens Tensile Test Results .....	99
Table 4.16 PA6HF20c Specimens Tensile Test Results .....	99
Table 4.17 Non-modified Specimens Impact Charpy Test Results .....	100
Table 4.18 Modified Specimens Impact Charpy Test Results .....	101
Table 4.19 Non-Modified and Modified Specimens Average Charpy Results .....	119
Table 4.20 Specimens Average Compression Results .....	120

# List of Abbreviations

AM	Additive Manufacturing
FFF	Fused Filament Fabrication
PA	Polyamide
PP	Polypropylene
PC	Polycarbonates
PE	Polyethylene
PET	Polyethylene Terephthalate
PEK	Polyether Ketone
PEKK	Polyether Ketone Ketone
PES	Polyethersulfone
ABS	Acrylonitrile Butadiene Styrene
PLA	Polylactic acid
CNC	Cellulose Nanocrystals
CNF	Cellulose Nanofibrils
BC	Bacterial Cellulose
ECNF	Electrospun Cellulose Nanofibers
LOM	Laminated Object Manufacturing
StL	Stereolithography
SL	Sheet Lamination
DED	Directed Energy Deposition
DLP	Digital Light Processing
DIW	Direct Ink Writing

CLIP	Continuous Liquid Interface Production
MJP	Multi-jet
VP	Vat Photopolymerization
PBF	Powder Bed Fusion
BJ	Binder Jetting
MJ	Material Jetting
ME	Material Extrusion
SLS	Selective Laser Sintering
CAD	Computer-aided Deesign
CAM	Computer-aided Manufacturing
ASTM	American Society for Testing and Materials,
ISO	International Standards Organization
SEM	Scanning Electron Microscopy
TGA	Thermogravimetric Analysis
DSC	Differential Scanning Calorimetry
3D	Three Dimensional
STL	Standard Triangle Language
L/D	Length/Dimension
CF	Carbon Fiber
GF	Glass Fiber
HF	Hybrid Fiber
USA	United States
Rpm	Revolutions per minute
Tg	Glass Transition Temperature
Tc	Crystallization Temperature
Tm	Melting Temperature

# List of Symbols

C=O	Carbonyl group
(-OH)	Hydroxyl group
mm	millimeter
cP	Centipoise
$\eta$	Viscosity
pa.s	Pascal-second
°C	Celcius
MPa	Megapascal
GPa	Gigapascal
m/s	Meter per second
mm/s	Milimeter per second
Nm	Newton-meter
W/g	Watt per gram
J	Joule
kJ	Kilojoule
kJ/m <sup>2</sup>	Kilojoule/squaremeter
nm	Nanometer
$\mu\text{m}$	Micrometer
kV	Kilovoltage
Hz	Hertz

# Chapter 1

## 1 Introduction

In this section, the definitions, advantages, and disadvantages of polymer materials and their types, composite materials, fiber reinforcements, thermoplastic composite production methods and additive manufacturing technologies are explained clearly. Classification of polymers, the importance of thermoplastics for a sustainable and clean world, the development of composite materials in human history, the place of composite materials in our lives, and their sectoral usage areas are discussed. The benefits of thermoplastic composites, types of reinforcing structures that make up composite materials, fiber types, particles, and hybrid structures are explained. In addition, the production methods of thermoplastic composite materials are briefly explained.

Additive manufacturing technologies, which are one of the innovative production methods of today, and fused filament fabrication (FFF) technologies, which are one of the new generation production methods of polymer matrix composites, and their innovative aspects are mentioned. The benefits of using fiber reinforced composite structures in additive manufacturing technologies, which are being used extensively in polymer production, are mentioned. Finally, the most used FFF method in the production of polymers by additive manufacturing is explained.

### 1.1 Polymer

The fact is that most of the technological developments are achieved in parallel with the developments in materials science. Engineering comes to life based on materials science. Materials, which can have many different properties such as conductivity, transparency, strength, thermal resistance, etc., direct the life of humanity in many

different areas of use. Regardless of the field, the usage limits of the products depend on the materials rather than the design geometry. Polymeric materials, which have been the subject of extensive research in recent years, find use in many new areas and play a role in determining product performance (1). Polymers have a wide range of applications, from simple parts in our daily life to complex industrial products (2). So much so that it is difficult to imagine today's world without polymers. Polymer materials have unique properties not found in conventional materials such as lightness, flexibility, corrosion resistance, transparency, and easy processing (3).

Polymers are one of the materials first introduced by JJ Berzelius in 1833 (4). The structures of polymers consist of long molecules, macromolecules in the form of chains (2). Polymers are familiar plastics and rubber materials. They are mostly organic compounds based on hydrogen, carbon and other non-metallic elements. (5). Typically, polymers contain various additives. Additives are distinguished in the following categories: antistatic agents, binding agents, fillers, extenders, flame retardants, lubricants, pigments, plasticizers, supplements, and stabilizers (3).

Polymer materials are divided into four main groups depending on origin of source, structure, molecular forces and mode of polymerization (2). Polymers can be categorized for better understanding as shown in Figure 1.1.

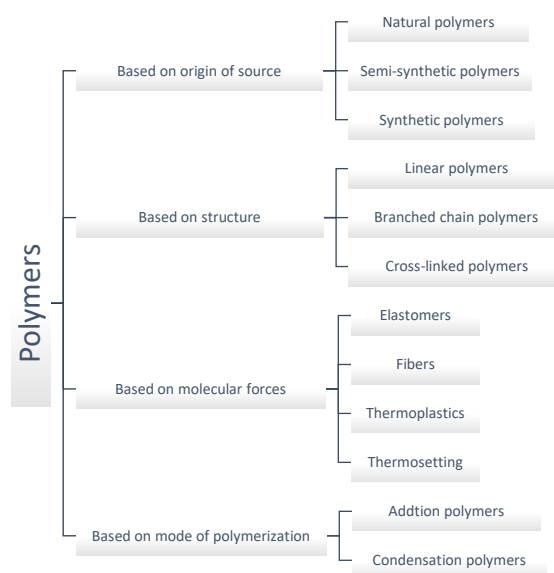


Figure 1.1: Classification of Polymers (2,6)



Although polymers are divided into 4 main groups, molecular forces are more important in terms of industrial application. This group; It consists of 4 different categories: elastomers, fibers, thermoplastics and thermosetting plastics. Thermoplastic or thermosetting materials can be processed with different methods. Table 2 contains some properties of thermoplastic and thermosetting materials and examples of different polymer matrix materials used in industry.

### 1.1.1 Thermosetting Polymer

They are formed as a result of a chemical reaction with two steps. They are first produced as chains of macromolecules such as reactive thermoplastics. In the second stage, these macromolecular chains, which they have with the effect of temperature and pressure, form a cross-link (3). The cross-linking of thermosetting polymers strengthens the molecular bonds and makes the polymer durable. Thermosetting polymers do not soften when heated, due to the cross-linking molecular bonds they have. As these polymers are reheated, they do not become fluid, but rather decompose with an increase in temperature (7,8). Thermosetting polymers, which are widely used in the polymer industry today, have recycling problems (9).

### 1.1.2 Thermoplastics

Polymers that soften or melt when heated are called thermoplastic polymers. These polymers are suitable to form flow with temperature increase (10). The macromolecules that make up the thermoplastic polymers are bonded to each other by weak van der Waals force (3).

When thermoplastic polymers are heated, the intermolecular forces are greatly reduced, so the material begins to soften. With the increase in temperature, the material becomes flexible and becomes a viscous liquid at high temperatures. It becomes solid again when allowed to cool (3). This cycle can be repeated many times, which is an advantage for recycling. However, of course, with more than one heating-cooling cycle, the properties of thermoplastic polymers degrade (11).

Thermoplastic materials are divided into two groups according to the arrangement of the macromolecules they have. These are called crystalline and amorphous structures.

In the crystalline structure, macromolecules are characterized in an ordered array, while in the amorphous structure, the macromolecules are randomly arranged (12,13). Polymers such as polyamide can have a high degree of crystallinity. However, it is not possible to make a perfect crystalline thermoplastic because of the complex structures. That's why it can be called semi-crystalline (14). The crystallization of polymers is largely dependent on the thermal processes during their production and results from the more intense aggregation of macromolecules. Crystal structure affects the mechanical properties of polymers (15). The characteristic of crystal polymers are given in table 1.1.

Table 1.1: Crystal Polymer Properties (15)

<b>Characteristic</b>	<b>Value</b>
Hardness	High
Coefficient of Friction	Low
Impact resistance	High
Ability to add reinforcements	High
Frictional resistance	High

## 1.2 Polymeric Composite Materials

From the mud and straw used in the construction of adobe houses by human beings to the carbon fiber-reinforced epoxy materials used in the construction of today's aircraft, composites are at many points in our lives (16). These engineering materials, which are insoluble in each other, consist of more than one component, and have chemically distinctive properties, are formed by matrix and reinforcement components. Composite materials are called reinforced plastics when they are produced with a polymer-based matrix. In the composite material, the matrix phase keeps the reinforcement phase together and provides continuity. The reinforcement phase gives the material extra properties such as conductivity, strength, and hardness. Polymeric composite materials are frequently used in many engineering applications, especially in the aerospace industry. The polymer matrix and reinforcing components that form the composite structure transfer their advantageous properties to the final product it creates, resulting in an excellent structural material.

Polymer matrix composites are divided into thermosetting and thermoplastic according to the matrix type. Thermoplastics, which are solid at room temperature, can be reformed with heat. However, thermosetting, which is liquid at room temperature, degrades if it is reheated after curing. It has higher strength due to its thermosetting cross-linked structure. Thermoplastics such as polyamide (PA), polypropylene (PP), polyether ether ketone (PEEK), polyethersulfone (PES), and polycarbonate (PC) provide superior fracture toughness, high hardness, and impact resistance, long shelf life, and easy recyclability. Some of the polymer matrix types used in composites are given in Table 1.2.

Table 1.2: Typical properties of resins (17)

<b>Resin type</b>	<b>Density (gm/cm<sup>3</sup>)</b>	<b>Young's modulus (GPa)</b>	<b>Poisson's ratio</b>	<b>Tensile strength / yield (MPa)</b>	<b>Tensile failure strain (%)</b>
Polyester <sup>s)</sup>	1.21	3.6	0.36	60	2.5
Vinyl ester <sup>s)</sup>	1.12	3.4	-	83	5
Epoxy <sup>s)</sup>	1.20	3.2	0.37	85	5
Polycarbonate (PC) <sup>p)</sup>	1.20	2.3	0.41	60	100
Polyethersulphone (PES) <sup>p)</sup>	1.35	2.8	0.42	84	60
Polyether-ether ketone (PEEK) <sup>p)</sup>	1.30	3.7	0.39	92	50
Polyamide 6 (PA6) <sup>p)</sup>	1.13	2.4	0.42	78	90

<sup>s)</sup> thermosetting, <sup>p)</sup> thermoplastic

### 1.2.1 Thermoplastic Composites

Both thermoplastics and thermosetting polymers can be reinforced with different reinforcing elements, thereby developing new materials with unique properties (18,19). The properties and sample polymer types of thermosetting and thermoplastic materials are given in Table 1.3.

Table 1.3: Polymer Matrix and Properties

	Thermosetting	Thermoplastic
Properties	High stiffness and strength Adhesion properties	Better impact resistance Higher fracture toughness Moderate stiffness and strength
Examples	Epoxy Polyester Bismaleimide Vinyl ester	Polyamide (PA) Polycarbonates (PC) Polyethylene (PE) Polyethylene Terephthalate (PET) Polyether ketone (PEK) Polyether ketone ketone (PEKK)

In Figure 1.2, thermoplastics used industrially are shown with their properties and classifications. While some properties of thermoplastic polymers have limits, their application limits are only up to the imagination of the designer. In addition, reinforcement can be added to improve the strength properties (20). Reinforcements can be made as discontinuous fiber, continuous fiber, particulate and structural.

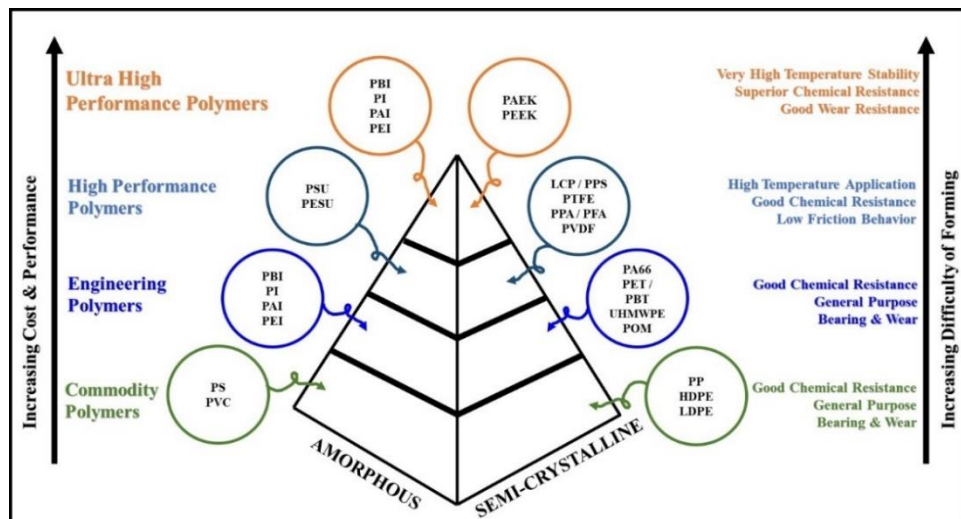


Figure 1.2: Thermoplastic Polymers

### 1.2.2 Fiber Reinforced Thermoplastic Composites

Fiber-reinforced thermoplastic composite materials are composite materials that provide desired parameters such as high strength, high rigidity, low density, high corrosion resistance, and lightness. They are used in many products in the automotive,

aerospace, defense, and maritime sectors. In addition, considering that today's products are tomorrow's garbage, recycling is an important parameter and humanity is facing it more and more every day. The recycling advantages of thermoplastic matrices are critical to green manufacturing.

Thermoplastic composite materials are expected to have improved structural properties as well as the advantages of recycling. In composite structures where recyclable thermoplastic materials are used as matrix material, different fiber reinforcements are performed to improve the structural properties.

### 1.2.3 Fibers

It is possible to produce functional products by changing many properties with fiber reinforcement. Reinforcement of thermoplastic polymers with fibers is a frequently applied method. Different fiber types, different surface modifications, different diameters and lengths can be used for reinforcement. The increase in fiber percentage or fiber diameters and lengths do not affect the material properties linearly. It has certain threshold values. In different production processes, the threshold values are also different depending on the application areas.

Fibers can be in discontinuous (a) or continuous (b, c, d) form as seen in Figure 1.3. Continuous fibers can be given different forms with different weaving types. In short fiber reinforcements, fiber type, percentage, length, and diameter are variable. In many cases different surface modifications can be applied. Fiber surface properties are critical, especially for matrix fiber interface bonds. Short fiber reinforcements are often used in conjunction with a thermoplastic matrix (15).

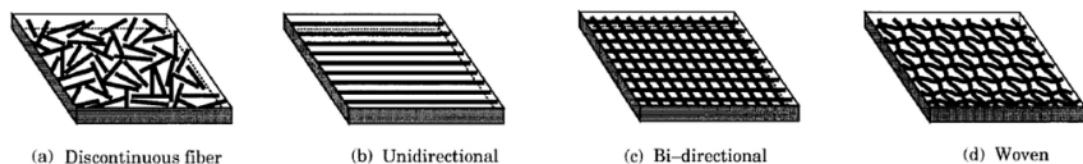


Figure 1.3: Composite material reinforcement types (21)

Fibers used for reinforcement are divided into two as natural and synthetic according to their sources. Natural fibers are produced from renewable resources, synthetic fibers

can be organic or inorganic, and are usually synthesized from petroleum-based products. Natural fibers are named after their origin, regardless of whether they are derived from plants, animals, or minerals (22). Compared with synthetic fibers, natural fibers have disadvantages such as low resistance to moisture absorption, thermal degradation and weathering, lower durability, poor interfacial adhesion (23).

Table 1.4: Fiber Types

<b>FIBERS</b>			<b>FIBERS</b>	
<b>Natural Fibers</b>			<b>Synthetic Fibers</b>	
<b>Animal</b>	<b>Cellulose</b>	<b>Mineral</b>	<b>Organic</b>	<b>Inorganic</b>
Silk	Jute	Asbestos	Aramid	Glass
Wool	Flax		Polyethylene	Carbon
Hair	Hemp		Polyester	Boron Aramid
	Kenaf			
	Wood			
	Cotton			
	Stalk			
	Bamboo			

### 1.2.3.1. Synthetic Fibers

Polymeric composites reinforced with synthetic fiber are widely used in automotive, construction, sports equipment, household appliances, electronic components, defense industry, aerospace industries, wind turbine blades, boats, etc. they are used in most applications. Carbon and glass fibers are synthetic fibers that are used extensively for reinforcement in polymeric composites.

Carbon fiber was started to be developed by DuPont in 1952, and patent applications were made for the first time in 1959 and 1962 by a team led by Dr. Shindo at the Osaka Research Institute on the production of carbon fiber from polyacrylonitrile (PAN) fibers. Carbon fibers can be prepared from polymeric materials such as PAN, cellulose, pitch and polyvinylchloride. However, PAN-based carbon fibers are dominant among them, due to the fact that they have the best strength values and the production technologies are developed in this area. Carbon fiber is one of the most resistant and toughest materials commercially available. It can maintain its mechanical properties even at high temperatures. Carbon fiber is a corrosion and fire resistant material. It

represents prestige and luxury. Its main disadvantages are its high cost and complex manufacturing process.



Figure 1.4: Carbon Fiber Image

Glass fiber was patented by Owens Corning in 1935 and commercial product was produced by Ray Greene in 1942 with the first fiberglass sailing boat with epoxy matrix (24). Glass fiber has a high strength to weight ratio and low production cost. It also shows good chemical resistance. Glass fibers are classified as general purpose (E-Glass) and special purpose (S-glass, D-glass, A-glass, ECR-glass). Most of the glass fibers produced are E-glass. E glass (lime aluminum borosilicate) has relatively good tensile and compressive strength, toughness, electrical property and low cost, but its fatigue strength is poor.



Figure 1.5: Glass Fiber Image

While the use of glass fiber in polymer matrix composites is 84%, natural fibers are around 10% and carbon fiber is 6% (25). The high cost of carbon fiber limits its use. The main reason for the widespread use of glass fibers is their low cost. Although polyester and nylon thermoplastic fibers are widely used, they can also be used in hybrid form with glass fibers when necessary (26). The fiber types are listed in Table 1.5. As a result, functional composite products can be produced with appropriate design and material selection.

Table 1.5: Typical properties of fibers (17)

<b>Fiber type</b>	<b>Density (gm/cm<sup>3</sup>)</b>	<b>Young's modulus (GPa)</b>	<b>Poisson's ratio</b>	<b>Tensile strength (GPa)</b>	<b>Failure strain (%)</b>	<b>Relative cost</b>
Carbon Fiber	1.74-1.81	248-345	-	3.1-4.5	0.9-1.8	45-50
E-glass	2.55	72	0.2	2.4	3	1
S-glass	2.5	88	0.2	3.4	3.5	8
Aramid	1.45	124	-	2.8	2.5	15

### 1.2.3.2. Cellulose Fibers

Natural fibers are derived from plants, animals, and minerals. Composite materials with a wide variety of properties can be produced by combining these raw materials, which can be converted into filaments, non-woven fabrics, paper, or yarn, with a suitable matrix. Natural fibers are generally divided into three types: animal fibers, plant fibers and mineral fibers (35). Cellulose is the main component of the type called plant fiber. For this reason, they are called cellulose fibers. It is found in plant-based materials such as cellulose, wood, cotton, hemp. The most important industrial resource is wood (27). Cellulose acts as a reinforcing phase in plant structure and is one of the most abundant biopolymers on earth. Cellulose can also be synthesized by algae, tunicas, and some bacteria (28). Despite its chemical simplicity, the physical and morphological structure of natural cellulose in different plant species is also complex and shows heterogeneous properties.

Natural cellulose fibers are an attractive option for several reasons:

- There is a huge resource in the world
- Less wear occurs in the production processes of natural fibers compared to synthetic fibers
- They do not cause respiratory and other health problems that synthetic fibers have
- Some natural fibers have very high strength values

In addition to the diversity of the fibers, the differences in their physical dimensions also affect their performance. Especially with the emergence of nanotechnology,



which is made possible by advanced microscope techniques, the use of various nano-sized materials in polymer composites and other composites has been discovered and applied. Among the many nanomaterials, nanocellulose has been one of the most important to be presented as the “future of materials” and numerous publications, including many research papers, have been published in the last two decades. The addition of nanometer-sized materials into polymers for reinforcement is an innovative field.

Cellulose particles that have at least one dimension at the nanoscale (1-100 nm) are called nanocellulose. Depending on the manufacturing conditions affecting their size, composition, and properties, nanocellulose can be divided into two main categories: (i) cellulose nanocrystals (CNC) and (ii) cellulose nanofibrils (CNF). CNC and CNF are very commonly used because they are produced by breaking down cellulose fibers into nanoscale particles (top-down). Bacterial cellulose (BC) and electrospun cellulose nanofibers (ECNF) are costly and not widely used because they are produced by bottom-up of low molecular weight nanofibers. Regardless of the type, nanocelluloses exhibit hydrophilicity, relatively large specific surface area, large surface chemical modification potential (29).

### 1.3 Hybrid Composites

Hybrid composites are materials in which one type of reinforcing materials is incorporated into two similar or different polymer matrix mixtures, or a particular polymer matrix is reinforced with more than one reinforcing material (30). They are multifunctional materials used in advanced structural parts and intended for more than one characteristic benefit from the materials in their content.

Hybrid Composite materials can have the following forms (31);

- a. Hybrid composite system with at least two reinforcing fibers
- b. Hybrid composite system with fibers and micron-nano scale particles
- c. Hybrid composite system containing at least two different nanomaterials

Hybrid nanocomposites are obtained by adding nano-sized filler in addition to fiber-reinforced or nanoparticle-doped polymer matrix composites. Hybrid structures bring

together the optimum properties of the materials that form the composition, ensuring that the properties expected from the final products are met. Hybrid structures are preferred for the reasons given in Table 1.6.

Table 1.6: Reason for using Hybrid Composite

Reducing the Cost
Improve the Interface
Determine Thermal Properties
Determine Conductivity Properties
Determine Mechanical Properties

Recent research has shown that the addition of organically modified nanoclays into cured epoxy resins results in a 60% reduction in hydrogen permeability, improved compatibility with liquid oxygen, and increased resistance to microcracking (72-74). It has been found that the bio and/or synthetic nano additive improves the strength, and thermal resistance and reduces the water absorption rate of hybrid composites.

### 1.3.1 Polyamide Matrix Hybrid Composites

Polyamide which has a crystalline structure is made up of recurring amide links, such as  $-\text{CO}-\text{NH}-$ . Polyamides can be found in nature as polypeptides. Also, polyamides can be seen commercially as nylon and aramids. The term nylon has been discovered by Dupont in 1928 (32). But today, nylons are categorized into the aliphatic PAs while aramids are classified in PAs containing aromatic diamines and aromatic dicarboxylic acids (33).

The most widely used PA types are PA 6 and PA66 whose molecular structures are shown in figure 1.6. The monomer of PA 6 is Caprolactum while the monomer of PA66 is Hexamethylene Diamine/Adipic Acid. Polyamide 12, Polyamide 69, Polyamide 6-10, Polyamide 6-12, Polyamide 46, Polyamide 1212 are some of the polyamide types found in literature (32).

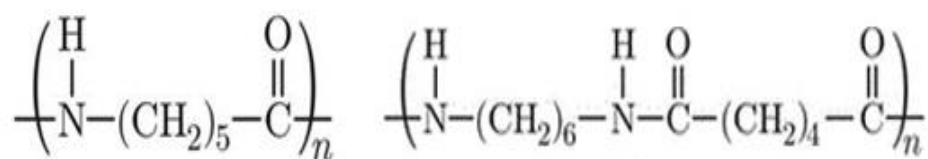


Figure 1.6: Molecular structure of PA6 (left) and PA66 (right)

Polyamide, which is included in the classification of engineering polymers, has found wide application in many different industries in recent years. Polyamide matrix composites have thermal and chemical stability(34). In addition, thanks to their mechanical properties, they have been used in different applications in many transportation vehicles such as maritime, aerospace, and automotive. Polyamide is among the most durable engineering polymers thanks to its high fatigue strength and thermal resistance (35).

The composites reinforced with fiber or particles, in which polyamide is used as a matrix material, have a wide range of applications. Today, the production of functional, low-cost, hybrid composites with expected properties is among the topical topics. In this context, there are many hybrid studies created with polyamides blended with different polymers (36).

To increase the mechanical properties of polyamide matrix composites, many studies have been carried out on the addition of different reinforcements. Reinforcement of the polyamide matrix with fibers such as glass and carbon durable, thermal resistance (up to 230 degrees (33)) and allows the production of composites with high fatigue strength. It is an innovative application to create hybrid structures by adding different fibers together to the polyamide matrix or adding nano additives together with the fibers. Szakacs et al. conducted studies on hybrid composites with carbon nanotube and microfiber doped PA6 matrix (37). In this study, it was observed that the microfiber additive helped the homogeneous distribution of carbon nano tubes in the polyamide. In addition, it was determined that the presence of carbon nanotubes reduces residual deformation. In the study of Cho et al, hybrid composite production was carried out by adding carbon fiber reinforcement coated with graphene oxide-carbon nanotube to the PA66 matrix. It has been observed that the graphene oxide-carbon nano tube treatment improves the interfacial bonding by forming hydrogen bonds. This resulted in a 136% increase in tensile strength (37).

## 1.4 Thermoplastic Composite Production Methods

Thermoplastic matrix composites have many advantages and disadvantages compared to thermosetting matrix composites.

- Cooling is not required in thermoplastic matrix composites.
- Parts can be shaped and joined by heating.
- Parts can be remolded and recycled.

The transition from the use of a thermosetting matrix to the use of thermoplastic has brought innovations related to production processes. Control of the crosslinking reaction is the basis of forming in thermosetting matrix composites. Therefore, chemical reactions at all production stages affect the properties of thermosetting composites. In thermoplastic matrix composite materials, rheological control is more important than chemical reaction. Thermosetting polymers have a viscosity of less than 100pa.s, while thermoplastics have a viscosity of 500-5000 pa.s. The high viscosity effect of thermoplastics has a critical importance in determining the production method. This situation especially makes it difficult to realize the homogeneous distribution of the fibers in the matrix.

There are several methods of combining matrix and fiber in thermoplastic composites. These; melt impregnation, mixing, powder impregnation and solvent impregnation. After these methods used in compound preparation processes, fiber reinforced thermoplastic matrix raw materials are produced.

Thermosetting matrix composites can be produced by a wide variety of methods including autoclave molding, cold pressing, compression molding, hand lay-up, hydraulic press, vacuum bagging, and infusion methods. (30), (36–38). Extrusion, injection molding and thermoforming are widely used as manufacturing techniques in thermoplastic composites (39,40). Other production methods are sputtering, filament winding, pultrusion and additive manufacturing (41, 42).

Table 1.7: Processing methods for hybrid composites

<b>Thermosetting Processing</b>	<b>Thermoplastic Processing</b>
Autoclave Molding	Extrusion
Cold Pressing	Injection Molding
Compression Molding	Thermoforming
Hand-Layup	Additive Manufacturing
Vacuum Bagging	Prepreg
Vacuum Assisted Resin Transfer Molding	
Spray Up	
Filament Winding	
Pultrusion	

Extrusion, injection molding, thermoforming, prepreg and additive manufacturing methods are used in the forming processes of thermoplastic matrix composites. The final product geometry is the most important component in selecting the process. In addition, the production volume plays a critical role in determining the process. To successfully manufacture a product, the process must be cost-effective and reliable. The cost-effective component is highly dependent on production speed, consumables, and infrastructure requirements. For reliability, all post-production parts are expected to be of the same quality. The part should be able to be shaped in the desired geometry, the tolerances are expected to be at the expected values during shaping and it is expected to exhibit the mechanical properties determined during the design. Different production methods are used in line with these requirements.

### 1.4.1 Extrusion Process

Extrusion is the most important and oldest transformation and shaping process of thermoplastic polymers. After the polymerization process, the formulation or production of the finished or semi-finished product is carried out. The development of the single screw extrusion configuration, derived from the Archimedean screw principle, began in rubber production in the 1880s and later in the production of polymers in the 1940s. Today, it is widely used in the production of finished or semi-finished products, which are then subjected to a second process. Extruders are the basis of profile extrusion, film blowing, calendaring, blow molding and injection molding processes.

Extrusion is the process of melting and homogenizing the raw material before passing the molten polymer through a die or transferring it under pressure to a die. The screw or screws rotating in the barrel with the controlled heated sections enable the polymer to be transferred to produce the final product or semi-product with similar cross-sectional geometry.

To produce thermoplastic composite raw material after polymerization, twin-screw extruders are used in the compound preparation process by melt impregnation. The twin-screw extrusion process was developed in the early 20th century alongside the single-screw extrusion process. A twin-screw extruder, by definition, consists of two parallel configurations of screws that rotate in a shape of eight in a barrel. Twin screw

extruders are used in the formulation processes of polymers, joining polymers and manufacturing complex materials with special applications.

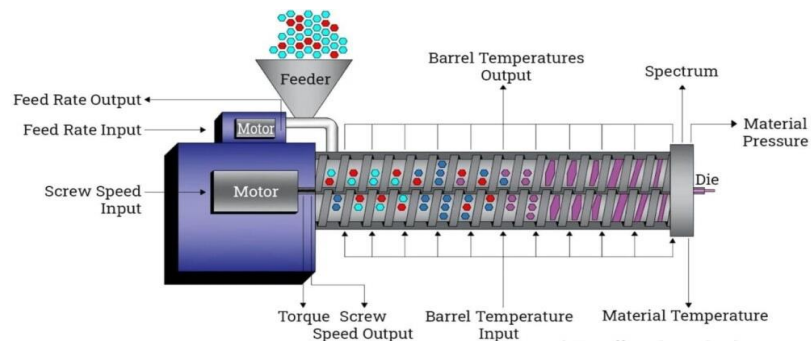


Figure 1.7: Twin-screw extruder

Single screw extruders, on the other hand, are used in the processes of passing the access polymer through the molds or transferring the polymer into a mold by pressure to produce profiles with similar cross-sectional geometry. With extrusion processes, products with many production volumes can be produced. In the production of the final product using single screw extrusion, it is carried out by pushing the molten polymer through an equipment called a die that will give the final shape to the product.

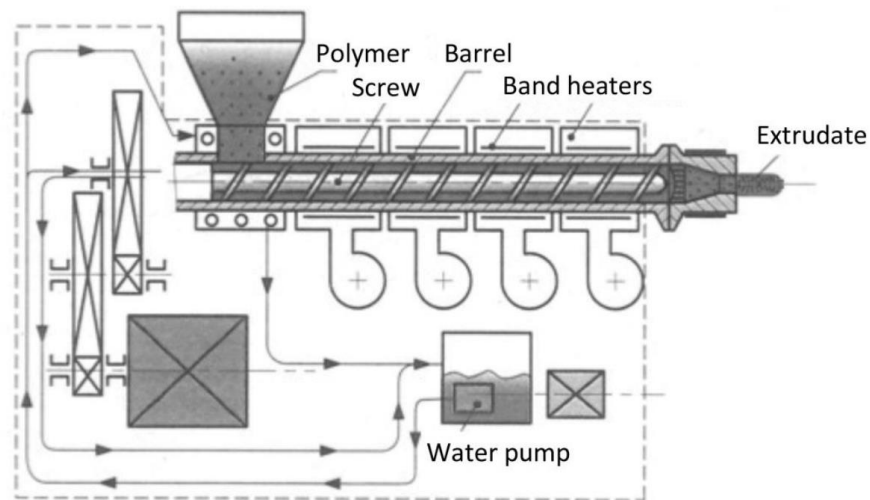


Figure 1.8: Single Screw Extruder

## 1.5 Additive Manufacturing Technologies

Additive manufacturing, known as three-dimensional printing, is a production system in which the material is combined layer by layer, unlike the forming processes by reducing material from solid raw materials in traditional production methods. Additive

manufacturing is used in a variety of industries to quickly produce a prototype of a system or part prior to final product or commercialization. Additive manufacturing reduces the cost of production by shortening lead times and using a small number of parts. A product in which three-dimensional computer-aided design (CAD) data is created with additive manufacturing methods can be produced directly without the need for tools, molds, and apparatus. In addition, additive manufacturing simplifies the production processes of objects with complex geometries and provides design freedom. Provides additive manufacturing methods, lightweight designs, assembly-free parts, on-site manufacturing, direct production of directional materials, structural internal supports, and personalized products (38,39).

Table 1.8: An overview of additive manufacturing

<b>Advantageous</b>	<b>Limitations</b>
<ul style="list-style-type: none"> <li>• Low-cost production depending on production size</li> <li>• Nearly net shape production</li> <li>• Production of unique and complex shapes</li> <li>• Reduced part assembly necessity</li> <li>• Minimum material waste</li> <li>• Short time to market (reduced lead time)</li> <li>• Green manufacturing capability</li> <li>• Lightweight production possibility</li> <li>• Tooling and fixturing elimination</li> <li>• Reduced scrap</li> </ul>	<ul style="list-style-type: none"> <li>• High first time buy cost of AM equipment, material, and software</li> <li>• Low reliability regarding mass production</li> <li>• Lack of global certification and standardizations</li> <li>• Limited component size and building volume</li> <li>• Low production speed compared to the traditional manufacturing process</li> <li>• Costly for high-volume production</li> <li>• Limited material option</li> <li>• Defects, e.g. porosity, hot cracking, warping</li> <li>• Unsatisfactory dimensional accuracy</li> </ul>

Compared to traditional manufacturing methods, many advantages make additive manufacturing methods to be preferred. With additive manufacturing, lattice geometries can be created and the potential to produce topology optimized designs is very high. In this way, lighter and functional parts can be produced. Structures that cannot be produced with traditional production methods or that can be produced with several different sub-processes and require post-production assembly can be produced integrated in a single operation with additive manufacturing. Contrary to processing

with volume reduction in traditional methods, the use of lower volume raw materials in additive manufacturing methods, where the part is produced layer by layer, provides material savings. In addition to the advantages of additive manufacturing technology, it also has some disadvantages and limitations. These are: High initial investment costs and system prices, the need for post-production processes to improve the surface quality of the final product, improve the mechanical properties of the final product depending on the material and method, low precision, and limited dimensions of the parts that can be produced depending on the machine dimensions.

### 1.5.1 Additive Manufacturing Methods

The production of objects drawn in the CAD program with additive manufacturing was first carried out in the 1980s. These first models, produced for prototype purposes, enabled the ideas developed by the engineers to become reality. With this developed method, time and cost savings were achieved, and human-induced problems were minimized (40). In addition, any shape that is difficult to process with traditional methods can be produced by additive manufacturing. Although additive manufacturing technologies are developing for the production sector today, they are frequently used by scientists, doctors, and artists. In addition, with the developments in the field of materials, additive manufacturing methods and the usability of the products produced with these methods are increasing (41,42).

Numerous additive manufacturing methods are now available; They differ in the way the layers are combined to form parts, the principle of operation and the materials that can be used. Some methods melt or soften solid or powdered materials to produce layers, while others use liquid materials. Additive manufacturing technologies are classified by the International Standards Organization/American Society for Testing and Materials Standards (ISO/ASTM 52900:2015) according to their working principle, type of material used and energy type (43). Additive manufacturing methods can be divided into three as solid, liquid and powder based on the raw material they are used. These methods are summarized in figure 1.9.



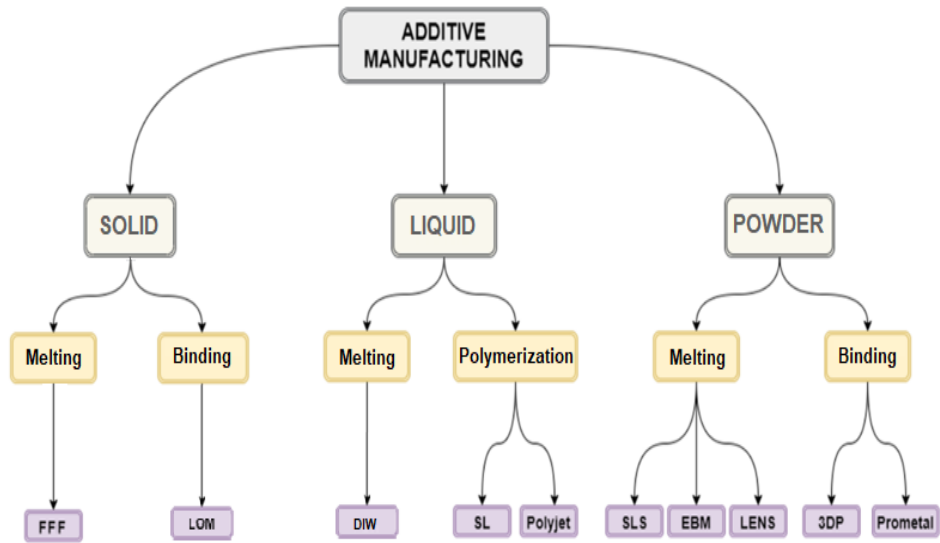


Figure 1.9: Material Based Additive manufacturing methods (41)

The ISO/ASTM 52900:2015 standard defines all commercially available additive manufacturing processes in seven main categories. These categories are Directed Energy Deposition (DED), Vat Photopolymerization (VP), Powder Bed Fusion (PBF), Binder Jetting (BJ), Material Jetting (MJ), Sheet Lamination (SL), and Material Extrusion (ME) (44). Considering the materials used in all these methods, the methods in which polymeric materials can be used as raw materials are as in table 1.9.

Table 1.9: Polymer Based Additive Manufacturing Methods

Methods	ASTM Classification	Materials	Process
<b>Stereolitografi (StL)</b>			
<b>Digital Light Processing (DLP)</b> <b>Continuous Liquid Interface Production (CLIP)</b>	Vat Photopolymerization	Liquid	Polymerization
<b>Polyjet</b> <b>Multi-jet (MJP)</b>	Material Jetting	Liquid	Polymerization
<b>3D Printing (3DP)</b>	Binder Jetting	Powder	Binding (ink)
<b>Selective Laser Sintering (SLS)</b>	Powder Bed Fusion	Powder	Melting
<b>Laminated object manufacturing (LOM)</b>	Sheet Lamination	Solid	Binding (heat)
<b>Fused Filament Fabrication (FFF)</b>	Material Extrusion	Solid	Melting
<b>Direct Ink Writing (DIW)</b>		Liquid	Melting

There are advantages and disadvantages to the methods of additive manufacturing and part production using solid, liquid, or powdered polymer raw materials. A wide variety of thermoplastic polymer materials can be processed with additive manufacturing methods. Some polymers used show low mechanical properties, limiting their applications in engineering. High-performance polymers are expensive to produce and difficult to process due to their high melting temperatures. Fiber and particle reinforcement to thermoplastic polymers has been a method used for many years to increase their various physical properties. Fiber-reinforced polymers are known to exhibit superior mechanical properties when compared to pure polymers. Composite material development using additive manufacturing methods is the focus of most published research studies. Fiber reinforcement can greatly improve the properties of polymer matrix composite parts produced by additive manufacturing. Stereolithography (SL), laminated object manufacturing (LOM), fused deposition modeling (FFM), and selective laser sintering (SLS) methods are currently used in the additive manufacturing of fiber-reinforced polymeric composites.

### 1.5.2 Fused Filament Fabrication (FFF)

With intensive research and development in the fields of materials, processes, software, and equipment, additive manufacturing technologies are used more intensively, directly or indirectly, in the manufacture of equipment, functional parts, and molds (45). More than 50% of the parts produced by additive manufacturing are polymer materials (46). The most preferred additive manufacturing method in the production of polymer products are fused filament fabrication (FFF), which is included in the material extrusion heading (47). Significant advances have been made in the FFF method since 2013 (48) (45). The FFF method is the most efficient and fastest growing technology among other additive manufacturing technologies, thanks to its low cost and printing capability (49). The raw material used in the FFF method is in filament form (43). The FFF method is like conventional polymer extrusion processes, except that the extruder is mounted vertically in a drawing system instead of remaining fixed in a horizontal position. This extruder is expressed as a nozzle and the region to be processed in each layer and the transition to the next layer is made according to the 3D Cartesian coordinate system (43,44,50). In the FFF method, the polymer fed as a filament is melted by a heated nozzle. The filament is pushed into the nozzle by a gear

wheel to generate extrusion pressure. Because the pressure is constant, the extruded material flows at a constant rate and exits the nozzle of a fixed cross-sectional diameter (48). The extruded material is in a semi-solid state when it leaves the nozzle (51). Before solidification, it adheres to the previous layer, the material solidifies keeping its shape and the process continues layer by layer (48).

Polymers are widely used as filament materials in additive manufacturing methods due to their favorable mechanical properties (high strength/weight ratio, hardness, ductility and durability) (52). Thermoplastic polymers such as acrylonitrile butadiene styrene (ABS), polylactic acid (PLA), polycarbonate (PC), polyamide (PA), Polyetheretherketone (PEEK) and Polyetherketoneketone (PEKK) are used as raw materials of the FFF method (53)(50). The most preferred polymers in the FFF method are ABS, PLA and PA (45,49,54,55).

Products printed from pure thermoplastics show lower mechanical properties in terms of strength and functionality compared to many load-bearing parts. These disadvantages limit the production of the parts to be used as the final product from pure polymers by the FFF method. As a result, high-performance composite raw materials need to be developed, especially for printing load-bearing parts with the FFF method (56). In addition, there are new research areas for the development of thermoplastic-based composites due to recycling and environmental problems of thermosetting polymer matrix composites (57). Thermoplastics such as PLA, ABS, PC, and PA processed with the FFF method produce solutions in certain areas in this regard. The use of materials with fiber reinforcement in the thermoplastic matrix in the FFF method is the focus of research in this field.

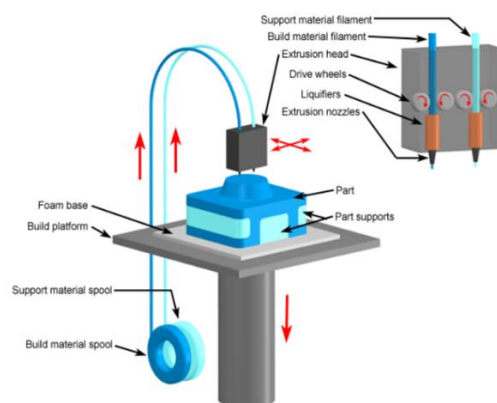


Figure 1.10: Illustration of fused filament fabrication technique (58)

# Chapter 2

## 2 Literature Review

In this section, literature studies and recent commercial developments in Additive Manufacturing (AM) technologies are discussed. The production of fiber-reinforced thermoplastic composites by AM methods and the studies carried out specifically for FFF are discussed. The advantages of the FFF method, the benefits of producing materials with higher strength properties with this method, and the opportunities offered by AM are explained. In addition, literature information on the importance of reinforcing fiber selection and the effect of fiber-matrix interface on mechanical properties has been shared. Finally, the motivation and goals in the production of thermoplastic matrix fiber-reinforced hybrid composite structures developed with the thesis study are summarized.

This thesis aims to develop new composite filaments to be used in structural applications that can be processed with AM. When the information documents of the commercially available ABS and PLA filaments used in the FFF method were examined, it was determined that the tensile strengths vary between 20-65 MPa. In addition, in the literature studies, it has been observed that materials with tensile strengths ranging from 30 to 80 MPa have been developed in studies where PLA and ABS polymers are reinforced with carbon and glass fibers. With the composite filaments developed in the thesis study, products with high mechanical properties will be produced. In this context, carbon, glass, and hybrid short fiber reinforced polyamide matrix polymer composite filament material that can be processed by the FFF method have been developed. In addition, nanocellulose was added to improve the matrix-fiber interface. It is aimed that the developed filament has better mechanical properties than PLA and ABS matrix composite filaments and pure Polyamide filament and can be

easily processed with the FFF method. Thanks to the reinforced fibers, nano additives and polyamide matrix used in the development of these new filaments, it will be possible to produce complex shaped products with significant strength values. Recyclable products will be produced thanks to the use of thermoplastic matrix.

With the increasing confidence and interest in AM methods, the design concept is changing to make better use of this technology. While traditional manufacturing methods use simple shapes and solid, linear lines to create parts, AM can produce complex structures. There are many restrictions in producing parts with complex geometry with conventional manufacturing methods. It is difficult to produce these parts in one piece and without assembly with conventional manufacturing methods. In addition, the geometrical structures of the topology optimized parts cause obstacles in conventional manufacturing. With the use of the developed materials in AM methods and the possibility of using them in certain areas, the restrictions will be removed. With AM technologies, the factors limiting the design are overcome.

AM is a term formerly called rapid prototyping and now commonly referred to as 3D Printing (43). AM is defined as "a layer-by-layer material manufacturing process for making objects from 3D model data, unlike subtractive manufacturing methodologies" (59). AM has been used since the 1980s for rapid prototyping in industrial applications. With the developing production, software and material technology, it is now used for prototyping as well as molding, short run production and mass production applications. AM is versatile and flexible and also can be customizable, and personalized. Therefore AM is suitable for industrial production in many industries (60). Today, AM methods are changing all production methods. All-to-one processes have changed from one-to-all. This manufacturing concept has influenced many components, from design geometry to material selection. Compared with traditional methods, AM can shorten the design cycle, provide efficiency, material flexibility, design flexibility, reduce production costs, and increase competitiveness (61).

Preferred methods for producing polymer products with AM are indicated in chapter 1. In the AM of fiber-reinforced polymeric composites, SL, LOM, FFF, and SLS methods are used today. The most popular process of shaping polymers with AM is FFF (62). It can also produce fiber-reinforced polymeric composites.



Figure 2.1: FFF Device

The FFF method is similar to conventional polymer extrusion processes, except that the extruder is mounted vertically so that it moves in a cartesian system rather than staying in a fixed horizontal position (43,44,50). In the FFF method, filament-shaped polymer or polymeric composite raw material is fed from the nozzle to the production table (bed table). To liquefy the polymer and feed it to the bed table in a fluid manner, the nozzle is heated according to the melting point of the polymer. To extrude the molten polymer or polymeric composite from the heat-controlled nozzle, the filament-shaped raw material is pushed by a gear wheel that generates the extrusion pressure (48). The extruded material is in a semi-solid state when it leaves the nozzle (51). It adheres to the previous layer before solidification. The material solidifies keeping its shape and the process continues layer by layer (48).

FFF systems, which are included in the Material Extrusion classification among AM technologies, express the process of combining the materials whose temperature is increased up to the melting point in the production of the physical model in layers (63). The CAD data of the part to be produced is sliced in layers using various Computer Aided Manufacturing (CAM) programs and the material is extruded in a controlled manner with a nozzle heated to the solid sections in the relevant layer (41).

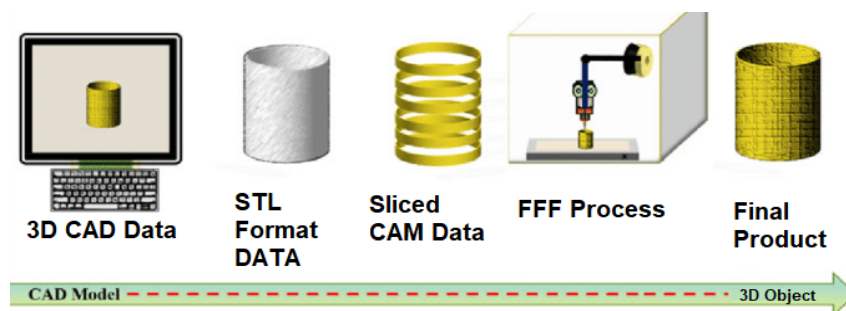


Figure 2.2: AM Processes

Although the variety of materials that can be used in AM technologies is increasing day by day, it currently has a limited material variety compared to other methods. Thermoplastics such as PLA, ABS, PC, and PA processed with the FFF method provide solutions in certain areas. Products printed using pure thermoplastic with the FFF method exhibit lower mechanical properties in terms of strength and functionality than many load-bearing parts. These disadvantages limit the production of the parts to be used as the final product from pure polymers by the FFF method. As a result, it is necessary to develop new raw materials, especially for the production of high-performance components carrying loads with the FFF method (56). The use of fiber-reinforced polymeric composites in this area creates new opportunities. In addition, there are new research areas for the development of thermoplastic-based composites due to the recycling of thermoset polymer matrix composites and environmental problems (57).

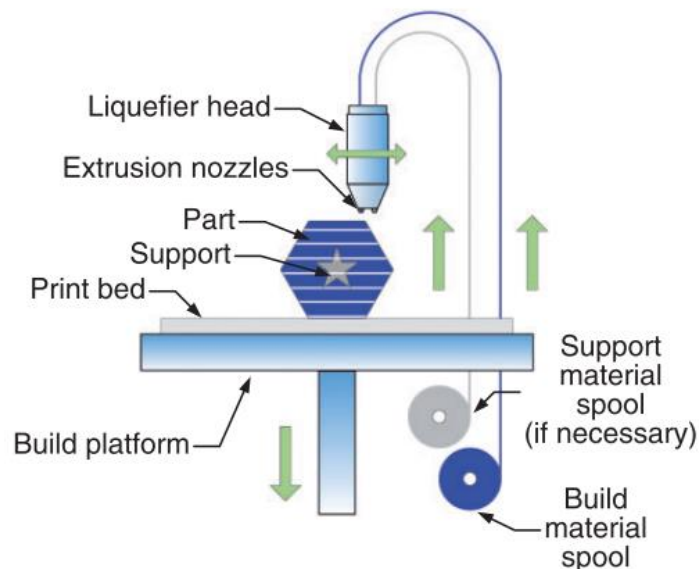


Figure 2.3: FFF method diagram (64)

While early AM methods focused on producing rapid prototypes for functional testing from pure plastic materials, AM can now be used to produce final products with emerging technologies (43). Although AM has gained attention in the last three decades, most of the reviewed published articles focused on the introduction of machining techniques and the production of pure polymer materials. However, in the last few years significant gains have been made in the development of fiber-reinforced polymer composite filaments with improved performance.

The variety of materials used in the AM method is increasing day by day and research is carried out on new-generation materials. Today, AM methods are used in many different industries, especially in the aerospace, defense, automotive and medical sectors, to develop prototypes and even to produce final products. New AM processes are being developed with studies in these areas.

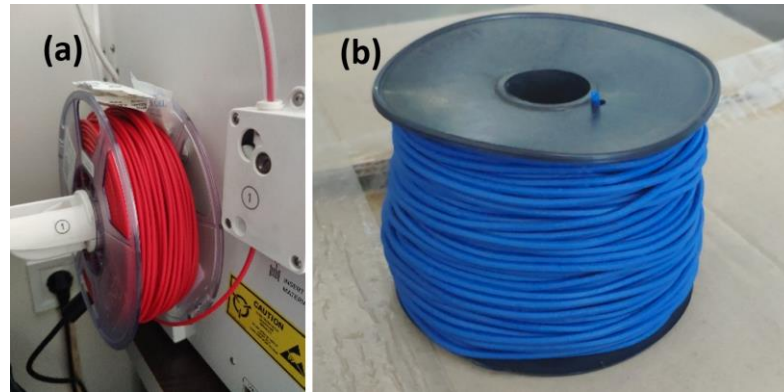


Figure 2.4: (a) PLA Filament (b) TPU Filament

Reinforcing the polymer matrix with fiber is a widely used method in industries such as aerospace, automotive, wind turbine, and medical (64). In addition, when the literature is examined, it is seen that the production of fiber-reinforced polymer matrix materials by the FFF method is a new research topic. Different research groups in this field have studied the mechanical properties, manufacturing processes, and defects of different polymer matrices.

Recently, more advanced 3D printing filaments have become available. Some of these are powdered metals and wood-based filaments, highly flexible filaments (thermoplastic polyurethane - TPU), shape memory filaments, and 3D printing filaments reinforced with graphene, carbon nanotube, and carbon fibers combined with PLA matrix. New advanced 3D printing filaments offer a wide range of mechanical, thermal, and electrical properties as well as a wide range of surface properties (65). As can be seen from the table, there are studies on short fiber reinforced PLA and ABS matrix in the literature.

Zhong et al. research the processability and mechanical properties of short glass fiber reinforced ABS matrix composites with FFF. They concluded that the composite filaments prepared were compatible with the FFF method, compared to pure ABS, the short glass fiber reinforced ABS composite significantly increased strength, reduced



shrinkage and increased surface hardness. By increasing the ratio of glass fiber in the composite filament, it increased the strength under linear load but weakened the adhesion strength between the layers (66).

Table 2.1: Research on the usage of fiber-reinforced PLA and ABS matrix by the FFF method's

Researchers	Matrix Material	Fiber	Tensile Strength	Research Focus	Deficiencies
<b>Zhong et al.</b> (66)	ABS	Short Glass Fiber	58.6 MPa	Tensile strength Surface hardness	Layers not merging
<b>Shofner et al.</b> (67)	ABS	Nano Carbon Fiber	37.4 MPa	Tensile strength Dynamic mechanical analysis	Layers not merging
<b>Tekinalp et al.</b> (68)	ABS	Short Carbon Fiber	65 MPa	Tensile strength Microstructure analysis	Pore formation and improvement of the interface
<b>Love et al.</b> (69)	ABS	Short Carbon Fiber	70.69 MPa	Thermal deformation Geometric tolerances	Thermal size changes
<b>Ning et al.</b> (64)	ABS	Powder Carbon Fiber	43 MPa	Tensile- Flexural strength Microstructure analysis	Pore formation
<b>Ning et al.</b> (70)	ABS	Short Carbon Fiber	32.3 MPa	Process parameters	Effect of parameters
<b>Anwer and Naguib</b> (71)	PLA	Nano Carbon Fiber	80 MPa	Mechanical, morphological, thermal characterization	Weak interface
<b>Ivey et al.</b> (65)	PLA	Short Carbon Fiber	60.6 MPa	Effect of annealing and carbon fiber additive on mechanical properties	Annealing does not affect mechanical properties Finding large gaps
<b>Ferreira et al.</b> (72)	PLA	Short Carbon Fiber	53.4 MPa	Mechanical tests Microstructure analysis of damages	Fragility increased
<b>Papon and Haque</b> (73)	PLA	Nano Carbon Fiber	42 MPa	Microstructure analysis Tensile strength	Agglomeration Gap formation depending on the printing direction
<b>Papon and Haque</b> (56)	PLA	Powder Carbon Fiber	54.64 MPa	Microstructure analysis Fracture toughness	Weak interface at high carbon ratios

Shofner et al. research the processability and mechanical performance of vapor grown carbon nanofibers reinforced ABS matrix composites with FFF. In specimens containing 10% nanoscale fiber by weight, uniaxial tensile strength was observed to increase by an average of 33%. It was determined that the increase in the tensile

strength varies according to the printing parameters of the specimens and the degree of melting between the layers. The results of tensile tests and dynamic mechanical analysis have shown that nanoscale short carbon fibers provide additional stiffness and strength, although they do not affect the viscous response of ABS. In addition, it was observed that the transition between layers in the specimens and the fiber / matrix interface is not ideal, therefore, the transition from ductility to brittleness (67).

Tekinalp et al research the FFF processability, microstructure, and mechanical performance of short carbon fiber reinforced ABS matrix composites. They compared the composites produced by conventional pressure molding with the FFF method. They research the effects of process and fiber ratio on cavity formation, average fiber length, and fiber orientation distribution, and consequently the effects of the final specimens on tensile strength and modulus. As a result, it concluded that highly dispersed and highly oriented carbon fibers composite filaments can be processed by the FFF method. Tensile strength of specimens produced with FFF increased by 115% and young's modulus increased by around 700%. With the FFF method, specimens with high fiber orientation (around 91.5%) could be produced in the printing direction. In contrast, specimens produced by pressure molding have very low fiber orientation. When the microstructure properties and mechanical properties are associated, it has been demonstrated that the specimen produced with FFF shows relatively high porosity compared to that produced by pressure molding, but the specimens in both production methods show similar tensile strength and modulus. This phenomenon is explained by fiber orientation, dispersion and pore form (68).

Love et al. to research the production of short carbon fiber reinforced ABS matrix composites with different FFF devices and different fiber ratios in terms of thermal deformation and geometric tolerance. They concluded that the addition of carbon fiber provides rigidity in the manufactured part, significantly reduces twisting, increases strength and stiffness (69).

Ning et al. examined the tensile and flexural properties of different sizes of carbon fiber powder reinforced ABS matrix composites produced by the FFF method. The effects of carbon fiber sizes and carbon fiber content on mechanical properties and porosity were compared. Carbon fiber reinforcement increased tensile strength and young's modulus, while reducing toughness, yield strength and ductility. In addition,

carbon fiber reinforcement increased flexural strength and flexural modulus. The highest porosity was found in the specimen containing 10 percent carbon fiber (64). Ning et al. In another study, carbon fiber reinforced ABS filament has been processed with different processing parameters by FFF method and examined its mechanical properties. In this study, it has been determined that the printing pattern, printing speed, layer thickness and nozzle temperature affect the mechanical properties of the specimens (70).

Anwer and Naguib investigated the mechanical, morphological, and thermal characteristics of PLA matrix composites with different ratios of carbon nanofiber reinforced produced by FFF and injection method. In the specimens containing 15% carbon reinforcement, it was observed that young's modulus increased by 50 percent, carbon nano fiber additive did not significantly affect the glass transition, crystallization occurred with carbon nano fiber additive. In addition, SEM morphology showed that most fiber surfaces are not covered with the matrix, so the stress transfer between the matrix and the fiber under high load is weak (71).

Ivey et al. made mechanical comparisons of specimens produced by FFF method using pure PLA filaments and short carbon fiber reinforced PLA matrix composite filaments. Post-production samples applied annealing at different temperatures and examined the effects of this process on mechanical properties. Annealing was observed to increase crystallinity in both specimens' groups, but statistically significant effect of annealing on mechanical properties was not observed. It has been determined that the addition of carbon fiber to the PLA filament provides a significant increase in tensile properties. In addition, it has been determined that carbon fiber reinforcement causes high gaps in the material in microstructure analysis since the carbon fiber causes clogging of the printing nozzle (65).

Ferreira et al. examined young's modulus, Poisson ratio, shear modulus, and strength properties of the 15 percent short carbon fiber reinforced PLA matrix composites in the direction of printing and perpendicular to the direction of printing. Mechanical tests were carried out in ASTM D638-10 and ASTM D3518-13 standards and damaged surfaces were examined with SEM after the test. Different fiber orientations and fiber lengths were observed, explaining the differences in strength properties with microstructure analysis and evaluation of the data obtained. In this study, unlike other

studies, shears properties were also examined. It was observed that with the carbon fiber reinforcement, young's modulus increased 2.2 times in the printing direction, 1.25 times in the perpendicular direction to the printing direction, and 1.16 times in the shear module. In addition, it has been determined that the elongation in carbon fiber additive samples is reduced and the carbon additive makes the material more brittle. In addition, it has been determined that the elongation in carbon fiber reinforcement specimens is reduced and the carbon reinforcement makes the material more brittle (72).

Papon and Haque examined the processability in FFF method, microstructure, and mechanical performance of carbon nano-fiber reinforced PLA matrix composites. It has been observed that at different ratios (0.5-1%) of carbon nanofiber reinforced PLA composites, young's modulus and yield strength increase as the concentration increases. It has been stated that the highest fracture and tensile strengths are in the specimen of 0.5% and possibly agglomeration occurs in the specimen of 1%. In addition, it was observed that the strain decreased compared to pure PLA. Papon et al. examined the gaps between the layers with microstructure analysis. Two dominant gap geometries, similar to the triangle and diamond configuration, were observed and it was determined that the direction and size of the print played a role in this (73).

Papon and Haque investigated the relationship between the fiber content and fracture toughness of PLA matrix composites reinforced with carbon fiber powder produced by the FFF method and different nozzle designs. It has been determined that PLA samples reinforced with carbon fiber powder show high fracture properties compared to pure polymer. In microstructure analysis, it was observed that the design of the new type of square nozzle significantly increased the bonding between the extruded material lines and that homogeneous parts were produced. In high fiber ratios, no improvement was observed in the fracture properties. It is stated that this is due to weak interfacial binding between the fiber and PLA matrix, microcrack formation and internal cavities (56).

All these literature studies show that important developments have been achieved in recent years and the applicability of the FFF method in the production of functional parts. In addition, studies on this subject have shown that PLA, a completely bio-based thermoplastic polymer with many desirable properties such as easy processability,

strength, hardness, and biodegradability, can be used in material processing with the FFF method (74). However, its inherent brittleness and low thermal tolerance prevent PLA from replacing traditional thermoplastic polymers such as PA, PC, and ABS for high-strength applications (75). In addition, the use of unreinforced polymer filaments with low elastic modulus and mechanical properties in the FFF method limits the use of parts produced by this method in wider areas in industry and research environments (65). Reinforcing with different types and proportions of fiber is an industrial method used to strengthen polymer materials (71). Literature studies also show that fiber reinforcement made to PLA and ABS materials for the FFF method increases their mechanical properties and expands the area of use.

The major shortcomings encountered in the studies on fiber-reinforced polymer filaments were noted as a void formation during processing with FFF, insufficient bonding between matrix and reinforcement, and layer separation. In this case, it limits the applicability of filaments in many areas and causes them to have lower properties. Shofner et al. stated that more work can be done on process optimization and better fiber/matrix bonding with the use of composite filaments with the FFF method, and different matrices and fibers can be used (67), Tekinalp et al. stated that interfacial bonding between the fiber/matrix can be improved by applying surface modification to reduce the pore formation that occurs during printing and to reduce the fracture of the fibers during printing (68), and Ning et al. stated that it can be worked on by optimizing the processing parameters to reduce pore formation (64,70). These statements can be defined as the next steps necessary for the processes of the FFF method to reach their full potential. In the thesis study, these research outputs were considered in determining the goals and objectives.

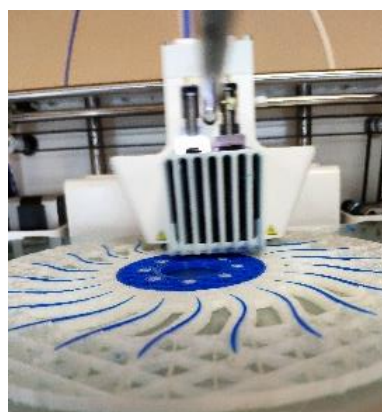


Figure 2.5: Unmanned Air Vehicle (UAV) propeller produced with FFF

The application area is expanding with the use of engineering polymers in AM methods instead of polymers with low mechanical properties such as PLA and ABS. PA polymers, which are included in the classification of engineering polymers and have a wide application area in many industries, especially in automotive, aerospace defense, and space in recent years, have been commercialized for use in AM methods by producing them as filaments. PA is a critical material for many applications thanks to its mechanical properties and thermal and chemical stability.

When the studies on the strengthening of the PA matrix with fiber reinforcement are examined, it is seen that there are very few short fiber-reinforced studies and there are many issues that need to be studied. Continuous fiber reinforcement was observed in most of the PA matrix composite filaments. As can be seen from the table, there are a limited number of studies on the short fiber-reinforced PA matrix in the literature.

Melenka et al. Have studies on continuous Kevlar fiber reinforced PA matrix composite filaments produced by AM. In their studies, the effect of Kevlar fiber ratio on its elastic properties was researched. It was stated that the mechanical properties of composites increased due to the increase in Kevlar fiber ratio (76).

Dickson et al. studied the tensile and flexural properties of nylon matrix composite filaments reinforced with different types of continuous fibers (carbon, glass and kevlar). They compared specimens produced with different filling patterns in the FFF method. They observed that 3D printed laminated composites with isotropic filling patterns had better tensile performance than concentric fill patterns (77).

Justo et al. conducted tensile, compression, and shear tests for glass fiber reinforced and carbon fiber reinforced PA matrix composite filaments. They found that fiber composites oriented in the direction of loading undoubtedly have higher mechanical properties (78).

Peng et al. researched the mechanical properties of PA matrix composites reinforced with both short and continuous carbon fibers and produced using the FFF process. They examined filaments with continuous carbon fiber reinforced and short fiber reinforced polyamide matrix by thermal, mechanical, and morphological analysis. The short fiber reinforced product examined is a standard product belonging to the brand Markforged. For this reason, there is no data on the effect of fiber ratios on the analysis.

They observed that there is a good interface between the short carbon fiber and the PA matrix (79).

Table 2.2: Research on the usage of fiber-reinforced PA6 matrix by the FFF method's

Researchers	Matrix Material	Fiber	Tensile Strength	Research Focus	Deficiencies
<b>Melenka et al.</b> (76)	PA6	Continuous Kevlar Fiber	> 80 MPa	Tensile strength	Fiber rates
<b>Dickson et al.</b> (77)	PA6	Continuous Carbon Fiber Continuous Glass Fiber Continuous Kevlar Fiber	216 MPa 194 MPa 150 MPa	Tensile strength  Flexural Modulus	Infill geometry (better results in isotropic filling pattern)
<b>Justo et al.</b> (78)	PA6	Continuous Carbon Fiber  Continuous Glass Fiber	600 MPa  500 MPa	Tensile strength  Compressive In-plane shearing	Fiber oriented
<b>Peng et al.</b> (79)	PA6	Short Carbon Fiber (Markeforged)  Continuous Carbon Fiber	37 MPa 515 MPa	Mechanical, morphological, thermal characterization	Good interface between the short carbon fiber and the PA matrix.
<b>Miguel Araya-Calvo et al.</b> (80)	PA6	Continuous Carbon Fiber	~2 GPa  ~5 GPa	Compressive Modulus  Flexural Modulus	Fiber oriented
<b>Yunchao Jia et al.</b> (54)	Pure PA6	-	-	FFF Process parameters	Shape Stability
<b>Basavaraj et al.</b> (81)	Nylon 618	-	-	FFF Process Parameters	For ultimate tensile strength 0.1mm layer thickness, 300 orientation angle and 1.2mm shell thickness
<b>Claudio Badini et al.</b> (82)	PA12 PA11	Short Carbon Fiber  (Windform®)	82 MPa	FFF Process parameters	Superior strength and stiffness were observed in the direction of fiber alignment.

Miguel Araya-Calvo et al. carried out compression and flexural tests of continuous carbon fiber reinforced PA6 matrix composites produced by FFF method. They observed that the flexural data is larger than the compression data and the specimens can accommodate greater loads in the flexural. They observed that the PA6 matrix avoids fiber bucking effects. They stated that the uniform distribution of the fibers improves the adhesion of the layers and increases the mechanical properties (80).

Yunchao Jia et al. Studied the warping of pure PA6-based FFF products after printing due to the shrinkage stress caused by the crystallization of PA6. To solve this problem,

they added maleic anhydride-grafted poly (ethylene octen) (POE-g-MAH) to PA6 to disrupt crystallization and reduce shrinkage stress. In addition, hard polystyrene (PS) with good fluidity was added. They observed that the product with 60% PA6 and 40% POE-g-MAH content by weight provides the best shape stability. The filament used in FDM must have sufficient hardness and good melt fluidity. For this reason, PS which has rigid chain segments and low shear viscosity as the filler material was added to improve the shape stability. Specimens containing 20% PS by weight were found to exhibit the best shape stability (54).

C K Basavaraj et al. researched the production parameters of Nylon 618 filament by FFF method. They compared the mechanical properties of specimens produced in different layer thicknesses and orientations. For ultimate tensile strength 0.1 mm layer thickness, 300 orientation angle, and 1.2 mm shell thickness (81).

Claudio Badini et al. Studied the short carbon fiber reinforced filament with a PA11 and PA12 matrix. Materials are produced in SLS and FFF methods. The mechanical properties of the samples produced in different printing directions were compared. Superior strength and stiffness were observed in the direction of fiber alignment (82).

Although researchers have studied various aspects of 3D-printed fiber-reinforced composites, these studies mostly involve PLA and ABS matrices. In Peng et al.'s work, there are structures in which short and continuous carbon fibers are used together with the same fiber-different length. In studies with PA matrix, there are no studies in which short fiber reinforced, different fibers together or nanoparticle reinforced fiber reinforced hybrid composites are used.

The focus of most of the published research studies on composite material developed for use in the FFF method is the mechanical characterization of printed fiber-reinforced polymers by comparison with pure polymer material. Short fibers (56,65,66,68–70,72) (83–85), nanofibers (67,71,73) (85) and continuous fibers (78,86,95–98,87–94) were used. The fibers have been combined with thermoplastic matrix materials such as PA, PLA, ABS, PPS, and PEI for most of the references cited (48). While research studies have been conducted on continuous fiber reinforced composites with PA matrix (87,88,98–100), studies involving short fibers are limited. A study on the effect of change in short fiber ratios is not included in the literature. In addition, adding



nanoscale reinforcement for interfacial improvement in short fiber-reinforced PA matrix composites is a completely innovative approach.

The productive design approach revolutionizes with AM, allowing to creation of new and complex shapes that can be optimized for budget, materials, production method, stability, flexibility, durability, and many different factors (101). One of the most fundamental issues of productive design is topology optimization. Topology optimization includes designs based on reducing the amount of material used without sacrificing the strength expected from the part, thus increasing the production speed while reducing material costs and weight (102). AM methods provide important advantages in this regard (103). With AM, each revision in part geometry can find numerous applications as seen Figure 2.6. The composite filaments to be developed will find wide usage areas thanks to their mechanical properties and will positively affect the material parameters in topology optimization in application areas.

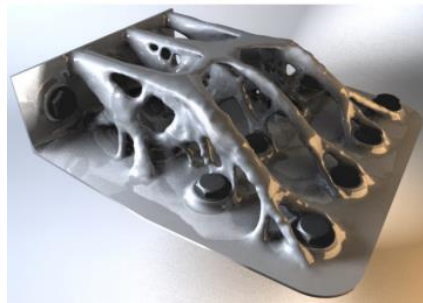


Figure 2.6: Topology optimized aerospace part produced with AM (structural bracket element) (101)

The developed composite filaments can be used in many different industries. The most interesting of these is the aerospace industry. Because innovations in AM in the field of topology will provide significant weight reductions. In the aerospace industry, the concept of payload refers to the load that the aircraft can carry, apart from the weight of its components and fuel. Every load reduced from aircraft components turns into a payload, increasing profitability and fuel savings (104). UAV technology, which is one of the sub-sectors of the aerospace industry, is one of the important areas of today. The UAV industry is an area that has become widespread with the interest of model aircraft clubs and hobbyists after World War II and features have been used for the problems of daily life since the 2000s. The FFF method creates important advantages for this area where mostly polymer materials are used. AM creates important

advantages in the production of parts of UAVs with complex geometry (105). In this way, the disposable load that UAVs can carry increases.

Thermoplastics, which create sustainable resources for the future of our world thanks to their recyclability, are the most up-to-date subject of polymer composites' matrix preferences (57,106–108). When the literature studies are examined, it is seen that there are studies on the use of PLA and ABS matrix and fiber-reinforced filaments in AM. However, studies with polyamide matrix fiber reinforcement are very few in the literature. PA has higher mechanical properties than conventional matrix materials. PA6, named Nylon 6, which is the most widely used among PA types, is translucent or opaque white in color, thermoplastic, lightweight, has good toughness, and chemical resistance, and good mechanical properties (14). PA6 is a thermoplastic polymer widely used in many industries and many applications, such as food packaging, household goods, the textile industry, and the electrical industry (109).

When the fracture surfaces of the fiber reinforced structures were examined by scanning electron microscopy, it was observed that there were microstructures at the matrix fiber interfaces, and it was determined that this had an effect on the mechanical properties (110) (111)(70). To improve this situation, FFF application under pressure, fiber coating (110), and thermal annealing (112) studies such as.

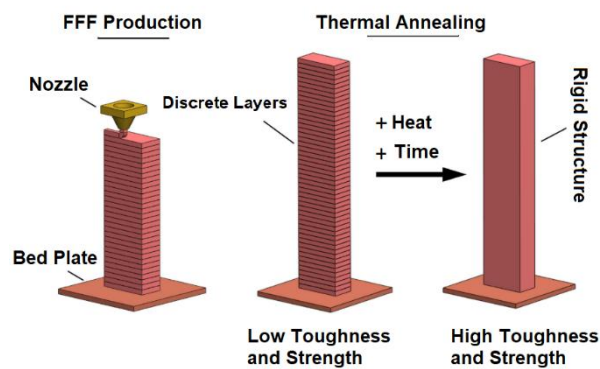


Figure 2.7: Thermal Annealing (112)

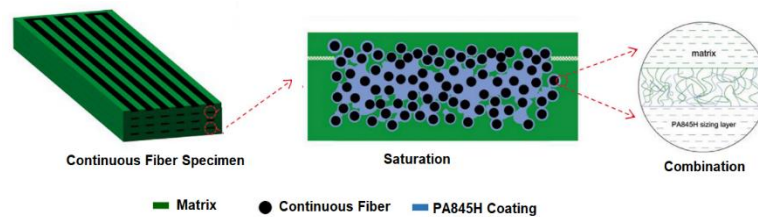


Figure 2.8: Fiber Coating (110)

Carbon-based nanomaterials (single, double, and multi-walled carbon nanotubes, carbon black, and graphene) are widely used in nanocomposites due to their excellent mechanical properties. The introduction of nanometer-sized materials into polymers for mechanical reinforcement is a well-developed field of study. It can also be a solution for microstructures at the interface in fiber-reinforced structures. The production of carbon nanomaterials, their incorporation into nanocomposites, and their disposal at the end of their useful life pose potential health and environmental problems, as well as large surface volume ratios, the potential for harmful biological interactions (113,114). On the other hand, adding alternative reinforcement materials obtained from renewable resources such as nanocellulose to composite structures is an innovative approach. In conjunction with renewability, nanocellulose offers biodegradability, low cost, and significantly fewer potential health issues (115).

Nanocellulose offers high surface area (150-600 m<sup>2</sup>g<sup>-1</sup>) (116,117), high aspect ratio and impressive mechanical properties ( elastic modulus of approximately 160 GPa (118) and 300 GPa tensile strength (118). Because of these properties, there is growing literature on the development of nanocellulose composites. Considerations regarding the selection of nanocellulose/polymer couples and machining methods have been reviewed in various studies (119)(120). In addition, there are many polymers industries-related multinational companies working to improve existing products or potentially use nanocellulose with new polymers. The interest of the companies producing in this field in nanocellulose is increasing day by day.

The surface chemistry of nanocellulose is naturally composed of polar hydroxyl groups and charged ionic groups resulting from the nanocellulose isolation process (121). Therefore, there are numerous examples of the incorporation of nanocellulose into various polar, hydrophilic polymers such as polyvinyl alcohol (PVA) (122), PLA (123), polyethylene oxide (PEO) (124) and polyurethane (PU) (125). Difficulties in making nanocellulose compatible with thermoplastic matrices have limited its use in industrial applications. The poor compatibility between nanocellulose and hydrophobic polymer matrices often causes agglomeration of the nanomaterial during mixing (120). Strong intermolecular hydrogen bonding causes the self-self-aggregate of nanocellulose in the mixing process with polar polymer matrices (120). CNC(Cellulose NanoCrystal) compound with Polyethylene (PE) (126), polypropylene

(PP) (127), polyvinyl chloride (PVC) (128), polystyrene (PS) (129) and polyamide 6 (PA6) (130) further studies are needed to further demonstrate and exploit the benefits of nanocellulose reinforcement in such polymers.

Yousefian and Rodrigue succeeded in that spray-dried CNC particles were combined with PA6 using a thermal extrusion process at 220°C. They observed a 23% increase in elastic modulus and an 11% increase in tensile strength with a 3% CNC additive by weight. Heat treatment of composite materials is industrially essential. However, nanocellulose is known to have a low thermal decomposition temperature, which limits its use in thermal processing with polymers such as PA6, which exhibit a relatively high melting temperature ( $T_m \sim 220^\circ\text{C}$ ). Another study by Corrêa et al. discussed the thermal compatibility of CNC in melt mixing processes. Corrêa et al. used PA6 as a carrier polymer for the CNC. They showed that coating the freeze-dried CNC with PA6 in formic acid increased the thermal stability of the CNC and observed well-dispersed nanocellulose crystals. Composites prepared by melting/combining coated CNC and PA6 affected the mechanical properties. The addition of 1% by weight CNC to the PA6 matrix, and 45% in elastic modulus resulted in an increase. No change was observed in the tensile strength. These studies demonstrated the potential of nanocellulose additives to improve the mechanical properties of PA6. Studies on optimizing their interactions in PA6 through chemical modification of nanocellulose have not yet been performed. Numerous ways have been followed to replace nanocellulose. Acetylation (131), esterification (132), etherification (133) and cationic surfactants (133,134) are the most common modifications to increase adhesion between nanocellulose and engineering thermoplastic polymers. Among the modifications mentioned above, the esterification of nanocellulose is considered the most effective. This modification has been indicated as an effective way to improve both the thermal properties of nanocellulose and the mechanical properties of the resulting composite (135). The main objective of this research project is to investigate the effect of a hydrophobic coating on the nanocellulose surface on the mechanical properties of the resulting hybrid composite filaments.

When PA6 properties are examined, it has high mechanical properties compared to other filament materials and durable parts can be produced. In addition, when the features of the FFF devices in the market are examined, it is seen that the PA6 is

compatible with the FFF system. For this reason, PA6 material was determined as the matrix material in the thesis study. It is aimed that the composite filaments to be developed with the research are quickly processed with the FFF method and have similar mechanical properties to their commercial competitors. It is well known that short carbon fibers blended with thermoplastic polymers significantly improve the strength of the polymer material and therefore have the potential to improve the mechanical properties of the FFF part. Thus, hybrid composite structures reinforced with carbon and glass and nanocellulose added to the PA6 matrix were produced.

It is seen in all research that AM methods are inevitable for design geometry, rapid prototyping, and demounted production. With its technological infrastructure, AM methods have a critical role in the transformation of Industry 4.0. New filament materials, products with increased mechanical properties, developed to expand the field of use of the FFF method and increase its effectiveness will be maintained for the use of the AM method in a wider area with the filament to be developed.

The thesis study was carried out to gain the ability to produce thermoplastic matrix composites with the FFF method and to ensure the production of durable parts. In the first stage, glass, carbon, and glass/carbon hybrid reinforced PA6 matrix filaments were developed to increase their mechanical properties. Thermal properties of fiber-reinforced compounds were analyzed to determine production parameters by extruder and FFF method. Characterization and thermal analysis of the developed filaments were made. The structures in which carbon fiber, glass fiber, and carbon/glass fibers are used as hybrids were produced with the FFF method in different parameters. Also, the compounds were prepared by different fiber proportions and the effect of fiber proportions was tested for mechanical properties. Optimization of FFF production parameters was carried out by examining its mechanical and morphological properties. One of the important factors affecting the mechanical properties in fiber-reinforced structures is matrix fiber interface bonding. In this context, in the second stage, the fibers were modified with nanocellulose to improve the interface. The same compounds were produced again using modified carbon and glass fibers. Compounds again were turned into filaments to be used in the FFF method. Specimens' productions were carried out by the FFF method using the optimized parameters in the first stage. Mechanical test specimens were produced from PA6 filaments reinforced with

nanocellulose-modified short fibers. The mechanical, thermal, and morphological properties of the specimens were investigated. Hybrid composite filament production was carried out, which can be used in the FFF method, which will enable the production of qualified products, which will enable the production of products with similar mechanical properties at a lower cost, and fiber-matrix interface improvement with nano additives has been carried out.

Critical points in this study;

- Production of carbon and glass fiber-reinforced polyamide compounds
- Fiber orientation, homogeneous distribution of fibers
- Adding nanomaterials for the interfacial improvement of the fibers
- Production of filaments in suitable diameter tolerances
- Production of test specimens from filaments by the FFF method

# Chapter 3

## 3 Experimental

In this section, the properties of the PA6 polymer used as the matrix material, the properties and effects of the carbon fiber and glass fiber reinforcements, and why carbon and glass fibers are chosen as the reinforcement material are explained. In the properties of nanocellulose used for interfacial improvement, the processes applied to gain hydrophobic properties of nanocellulose and the stages of modifying the fiber with nanocellulose are mentioned.

The working principles of the twin-screw extruders used in the compound preparation processes, the short fiber additive ratios realized in the first stage, and the preparation processes of the nanocellulose additive in the second stage are mentioned. It is explained that the filament form needed for production by the FFF method is produced with a single-screw extruder. Finally, the parameters used in the FFF method, the effects of these parameters, and the production of specimens are mentioned.

### 3.1 Materials

#### 3.1.1 PA6 Polymer

PA6, also called nylon 6, is translucent or opaque white in color, thermoplastic, light, has good toughness, resistant to chemicals and good mechanical properties (56), (66), (43), (140). Compared to other materials used in the FFF method, PA6 has high mechanical properties and durable parts can be produced (79). In addition, when the features of the FFF devices on the market are examined, it is seen that the PA6 is compatible with the FFF system. PA6 is preferred in many engineering applications, especially in the automotive sector. PA6 is a polymer matrix that creates opportunities

for thermoplastic composites thanks to its physical properties. PA6 is a thermoplastic polymer widely used in many industries and applications such as food packaging, household appliances, textile industry and electrical industry (109). For all these reasons, PA6 material was determined as the matrix material in the thesis study.

The PA6 polymer used as the matrix material in the thesis study is the Ultramid B40LN product of BASF company. This product has a density of 1.13 g/cm<sup>3</sup> and its relative viscosity value is 4. This PA6 product was chosen because of its suitability for the extrusion process and its superior chemical resistance and mechanical properties. The dimensions of the cylindrical PA6 pellets are between 2-2.5 mm.



Figure 3.1: Ultramid B40LN PA6 Pellet

This product, which is used in extrusion processes, has suitable viscosity values for filament production and production with FFF method. Relative viscosity value between 3 and 8 is ideal for extrusion processing (138). Similar values are valid for feeding sufficient material from the nozzle in the FFF method.

### 3.1.2 Carbon Fiber

In the thesis study, AC4102 chopped fiber product of Dowaksa company was used as carbon fiber reinforcement in all compound productions. Chopped fibers have 1.76 g/cm<sup>3</sup> density, 4200 MPa tensile strength, and 240 GPa tensile modulus values. Fiber diameters are 7  $\mu$  and lengths are 6 mm. It has been chosen because it is suitable to produce PA6 compound, which carbon fibers have proper sizing for PA.



Figure 3.2: Dowaksa AC4102 Short Carbon Fiber



### 3.1.3 Glass Fiber

As glass fiber reinforcement, PA2 e-glass product of Şişecam company was used. Due to its low alkaline ratio, its electrical insulation is very good compared to other glass types. Its strength is quite high. Water resistance is quite good. E-glass is generally used in composites developed for humid environments. Due to these physical properties and e-glass fiber was preferred. In addition, these e-glass fiber products of Şişecam were preferred because they have special sizing for PA6 compound. The fiber diameters are  $11\mu$  and the length is 4.5 mm.



Figure 3.3: Şişecam PA2short e-glass fiber

With the filaments to be produced using carbon and glass fiber products, specimen production will be carried out in the FFF device. A special nozzle with a diameter of 0.6 mm was used in specimen production with the FFF device. For this reason, short fiber lengths are very important in order not to cause clogging of nozzle. In addition, Dowaksa AC4102 and Şişecam PA2 products were preferred for this reason.

### 3.1.4 Nano Cellulose

Nanocellulose is derived from cellulose, the essential component of plant cell walls and the world's most abundant natural polymer. Composed of nanofibrils isolated from cellulose fibers found in wood and grass, nanocellulose exhibits several properties that make it an attractive and versatile biomaterial suitable for many uses. Nanocellulose is a hydrophilic material. Nanocellulose offers high surface area (150-600  $m^2g^{-1}$ ) (116,117), high aspect ratio and impressive mechanical properties (elastic modulus of about 160 GPa, and 300 GPa tensile strength (118).

Nanocellulose produced by the University of Maine was used in the thesis study. Nanocellulose in slurry form containing 11.5% nanocellulose and 88.5% water by

weight was supplied from the University of Maine. Nanocelluloses are small, rod-like particles obtained from wood pulp and the resulting is about 5-20 nanometers (nm) in diameter and 150-200 nm in length. It has a density of 1.5 g/cm<sup>3</sup> in its dry form and 1 g/cm<sup>3</sup> in the form of aqueous gel. It is white in color and odorless.



Figure 3.4: Slurry Nanocellulose

The main purpose of this thesis study is to investigate the contribution of short fiber reinforcement ratios and lean fibers and hybrid forms of these fibers to the mechanical properties and the effect of nanocellulose surface modification on the mechanical properties of the resulting composites in the specimens produced by the FFF method.

### 3.2 Short Fiber Reinforced PA6 matrix Composites

In the first stage of the thesis study, short fiber reinforcement was made to the PA6 matrix at the rates specified in table 3.1. To examine the effect of fiber additive ratios on the mechanical properties of the specimens produced by the FFF method, PurePA6 control group and fiber reinforcements at 10% and 20% by weight were performed.

Table 3.1: Short Fiber Reinforcement Thermoplastics Composite Compounds

<i>Compound No</i>	<i>Code</i>	<i>Matrix</i>	<i>Fiber</i>	<i>Fiber Ratio</i>
<i>1</i>	PurePA6	Pure Polyamide (PA6)	-	-
<i>2</i>	PA6CF10	Polyamide (PA6)	Carbon Fiber	10%
<i>3</i>	PA6CF20	Polyamide (PA6)	Carbon Fiber	20%
<i>4</i>	PA6GF10	Polyamide (PA6)	Glass Fiber	10%
<i>5</i>	PA6GF20	Polyamide (PA6)	Glass Fiber	20%
<i>6</i>	PA6HF10	Polyamide (PA6)	Carbon Fiber	5%
			Glass Fiber	5%
<i>7</i>	PA6HF20	Polyamide (PA6)	Carbon Fiber	10%
			Glass Fiber	10%

When the cost of carbon fiber is compared with glass fiber, a rate of 3 times is encountered. In addition, the cost per weight of glass fiber is cheaper than the matrix material PA6. For this reason, glass fiber reinforcement is a parameter that makes the compounds cheaper. In this context, the effect of glass fiber additives on mechanical properties in hybrid form was investigated. Compound production processes were carried out in a twin-screw extruder. The produced compounds were brought into filament form with a single-screw extruder to be produced by the FFF method. Finally, tensile, compression, and impact test specimens were produced with the FFF method, and mechanical tests, thermal and morphological analyzes were performed on the produced specimens. By using the findings obtained after this study, the interface improvement phase was started. The objectives of this study are;

- To ensure homogeneous distribution of reinforcing structures in composite compounds,
- To ensure that the length of short fiber reinforcements in composite compounds is less than 6 mm,
- To determine the necessary parameters to produce composite filaments and to standardize the production,
- Determining the mechanical and morphological characterizations of the composite filaments and determining the structural properties efficiently,
- Contributing to the literature on composite manufacturing with additive manufacturing
- To raise awareness about the performance improvements that these capabilities can provide in related industrial products.

### 3.2.1 Short Fiber Reinforced PA6 matrix Composites

#### Compounding

Polymeric composites are greatly affected by applied force, deformation, temperature, humidity, and time. The main feature of this behavior is the viscoelastic response. The crystal structure of thermoplastic polymers provides higher impact strength compared to thermosets (12). The wide range of fracture stresses in thermoplastics is due to large variations in the amount of crystallinity. The crystal structure of the thermoplastic

matrix changes drastically with the addition of reinforcement materials (139). To ensure the flow of a thermoplastic matrix during manufacture, the matrix must be heated to a temperature above its melting point. Increasing temperature decreases the viscosity of the polymer, but degradation is inevitable at higher temperatures. For this reason, performing the process at the appropriate temperature is critical for thermoplastics.

Compounds were produced with twin-screw extruder in Eurotec company. Since the homogeneous distribution of the fibers is a critical issue, Eurotec company, which is experienced in polyamide production, was preferred.

PurePA6 and compounds with 6 different fiber ratios were produced with a twin-screw extruder. Twin-screw extruders are classified according to screw rotation direction and size configuration. Twin-screw extruders are called co-rotating if both screws rotate in the same direction and counter-rotating if they rotate in opposite directions. To obtain a homogeneous mixture, an extruder with a counter-rotating screw configuration was used. A twin screw extruder unit with a diameter of 18 mm was used in the production of the compound. Pre-drying was carried out at 80°C for 24 hours.

The screw system is the focus of the extrusion process and determines the performance. The flow of the polymer is due to the action of the screw vanes, which are in contact with the inner wall of the sleeve and enable the transfer of the polymer. It is desirable that the transferred polymer does not stick to the screw and adheres to the sleeve part. Adhesion of the polymer to the screw inhibits the progression of the extrusion, while the adhesion of the polymer to the sleeve improves flow. In general, a screw is divided into four different, but interconnected sections. These four sections are, in order, the solids transport zone, the melting retardation zone, the mixing zone, and the mold zone.

The parameters in compound production are as follows; the feeding zone is 25°C, the melt retarding zone is 190°C, the mixing and conveying is 220°C and the die head temperature is 225°C.

The prepared compounds were vacuumed and stored in their bags until the next process. The purpose of this is that the polymeric matrix is not affected by moisture. The target in the compound preparation process is to have a homogeneous fiber

distribution and to prepare fiber-reinforced compounds at the rates determined by weight. The fiber distributions were analyzed by SEM analysis and the results were shared in the chapter 4. Reinforced fiber ratios by weight were confirmed by Thermogravimetric Analysis (TGA) shared in same chapter.

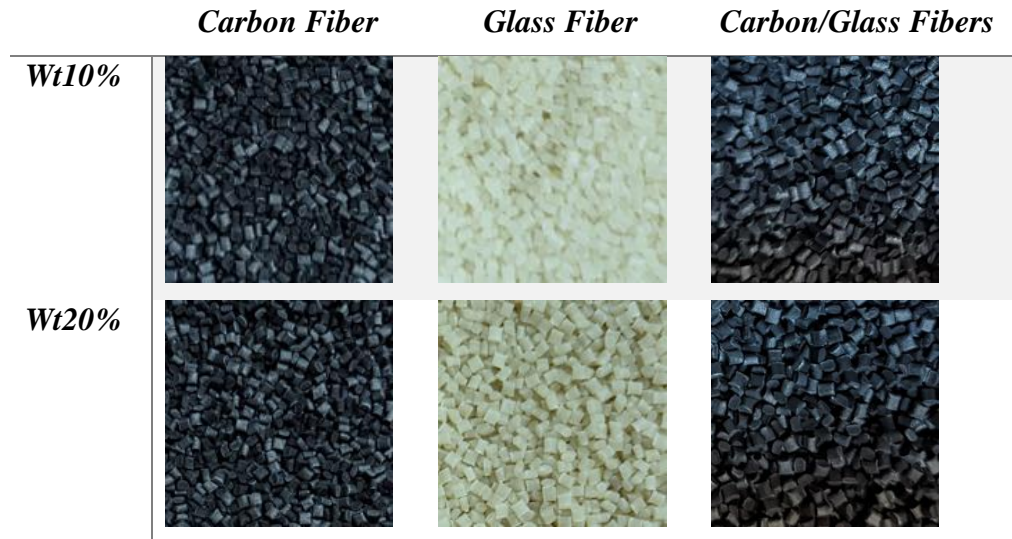


Figure 3.5: Short Fiber Reinforcement Composite Compounds

### 3.2.2 Short Fiber Reinforced PA6 matrix Composites Filament Extrusion

The control group PurePA6 and compounds with 6 different fiber ratios were shaped into filament form with a single-screw extruder in EG Plastic Company. The filament production was carried out in the SJ brand 35 mm diameter single screw extruder with 35:25 L/D ratio shown in Figure 3.6. Thermal properties (glass transition/melting/crystallization/decomposition temperatures) were investigated by Differential Scanning Calorimetry (DSC) to determine the extrusion parameters of the composite compounds turned into filaments for specimens' production in the FFF method.



Figure 3.6: Single-screw Extruder

Since the filament diameter of the device to be used in specimen production with FFF is 2.85 mm, all products were produced in these dimensions. Line continuity and diameter control in filament production was carried out with the laser measuring instrument seen in figure 3.7. Filaments with a diameter of 2.85 mm were produced with a tolerance of  $\pm 0.15$  mm.



Figure 3.7: Laser Measuring Gauge

In single screw extruders, it is desirable that the polymer does not stick to the screw and adheres to the sleeve part. Adhesion of the polymer to the screw inhibits the progression of the extrusion, while the adhesion of the polymer to the sleeve improves flow. In general, a screw is divided into four different, but interconnected sections. These four sections are respectively: the solids transport zone (Z1), the melting retardation zone (Z2), the melting zone (Z3), and the mold zone. Thermal properties

(glass transition/melting/crystallization/decomposition temperatures) of composite compounds were investigated with DSC to determine the necessary parameters for filament production by single screw extrusion. Considering the data shared in the chapter 4, the parameters in Table 3.2 were determined for the extrusion process.

Table 3.2: Single Screw Extrusion Parameters

<i>Compounds</i>	<i>Single Screw Extrusion Zones Parameters</i>			
	<i>Z1 °C</i>	<i>Z2 °C</i>	<i>Z3 °C</i>	<i>DIE °C</i>
PurePA6 Compound	200	220	220	180
Wt10% Compounds	230	235	225	220
Wt20% Compounds	225	230	220	210



Figure3.8: Single Screw Extrusion Parameters Setting Screens

Line continuity was ensured by winding 10% glass, 10% carbon, 10% hybrid (carbon/glass), 20% glass, 20% carbon, and 20% hybrid (carbon/glass) fiber reinforced filaments by weight on reels. Produced filaments are seen in figure 3.9.



Figure 3.9: Composite Filaments

### 3.2.3 Short Fiber Reinforced PA6 matrix Composites

#### Production with FFF

The test specimens were produced with the FFF method using 7 different filaments produced. Tensile, compression, and impact test specimens were produced to determine and compare the mechanical properties of composite parts produced by the

FFF method. The standards used for all tests are listed in table 3.3. Drawings of all test specimens according to the dimensions in the relevant standards were made with the AutoCAD Fusion360 CAD program. Parameters and part positioning required to produce the drawn parts in the FFF device were carried out with the CURA CAM program. The parts that were drawn in the CAD program and exported in "Standard Triangle Language (stl)" format were converted into the "gcode" file required to produce the FFF device in the CAM program.

Table 3.3: Mechanical Test Standards

<i>Test</i>	<i>Designation</i>	<i>Standard</i>
<i>Tensile</i>	ASTM D-638-14	Standard Test Method for Tensile Properties of Plastics
<i>Compression</i>	ASTM D-695-15	Standard Test Method for Compressive Properties of Rigid Plastics
<i>Impact (Charpy)</i>	ISO-179	Plastics – Determination of Charpy Impact Properties

The Ultimaker 3 device in the Ege University Aviation Vocational School Composite Laboratory was used to produce the specimens by the FFF method.



Figure 3.10: Ultimaker 3 FFF Device

All specimens were produced with the ultimaker CC printcore on the 0.6 mm diameter sapphire tipped as seen in figure 3.11. Since carbon and glass fibers have abrasive effects, a sapphire tip special nozzle is preferred. In addition, considering the lengths of the fibers preferred in the preparation of compounds, 0.6 mm gives better performance to prevent clogging.





Figure 3.11: Ultimaker CC Printcore nozzle

There are many parameters used in production with the FFF method. Of these parameters, those affecting the mechanical property were chosen as variables for optimization. To observe the mechanical effects in all specimens, the specimens were produced at 100% infill rate and in materials flow. The printing speed determines the amount of material to be extruded from the nozzle tip per unit of time. Bed temperature is critical to ensure that the first layer in production adheres to the table. In the experiments on different geometries, the most suitable parameters were determined as in table 3.4. Print speed is fixed at 50mm/s and bed temperature at 80°C.

Table 3.4: Fixed Parameters for FFF manufacturing

<b>Infill Percentage</b>	100%
<b>Infill Pattern</b>	<i>-/+45 Degrees</i>
<b>Print Speed</b>	50mm/S
<b>Flow Rate</b>	100%
<b>Bed Temperature</b>	80°C

### 3.2.3.1 Tensile Specimens

To compare the tensile properties of the parts produced by the FFF method, specimens were produced in ASTM D-638 Type 5 geometry as in figure 3.12.

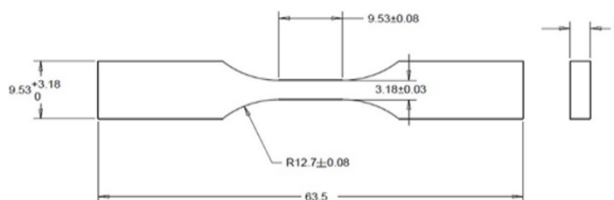


Figure 3.12: ASTM D-638 Type5 Geometry

Tensile test specimens were all produced with the same infill pattern. Infill pattern was selected as  $\pm 45$  in tensile test specimens. The effect of the infill pattern on the

mechanical properties was discussed in the impact test. The visual of the  $\pm 45^\circ$  orientation in the tensile test specimen is indicated in figure 3.13.

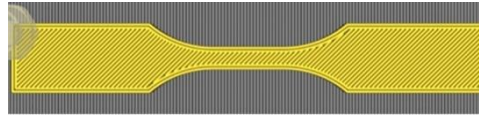


Figure 3.13: Infill patterns geometry for tensile specimens ( $\pm 45^\circ$ )

To optimize the production parameters with FFF, the nozzle temperature and layer thickness were taken as variables. The nozzle temperature was changed in the range of 235-275 °C and the layer thicknesses were changed in the range of 0.1-0.3mm. These two variables are the main parameters that affect the mechanical properties. All tensile test specimens were produced in 15 different parameters. Production parameters are in table-3.5.

Table 3.5: FFF Parameters

<i>PARAMETERS NO</i>	<i>LAYER HEIGHT (MM)</i>	<i>NOZZLE TEMPERATURE (°C)</i>
<i>1</i>	0.3	235
<i>2</i>	0.2	235
<i>3</i>	0.1	235
<i>4</i>	0.3	245
<i>5</i>	0.2	245
<i>6</i>	0.1	245
<i>7</i>	0.3	255
<i>8</i>	0.2	255
<i>9</i>	0.1	255
<i>10</i>	0.3	265
<i>11</i>	0.2	265
<i>12</i>	0.1	265
<i>13</i>	0.3	275
<i>14</i>	0.2	275
<i>15</i>	0.1	275

To observe the standard deviation values, 5 specimens were produced from each material configuration and parameter.

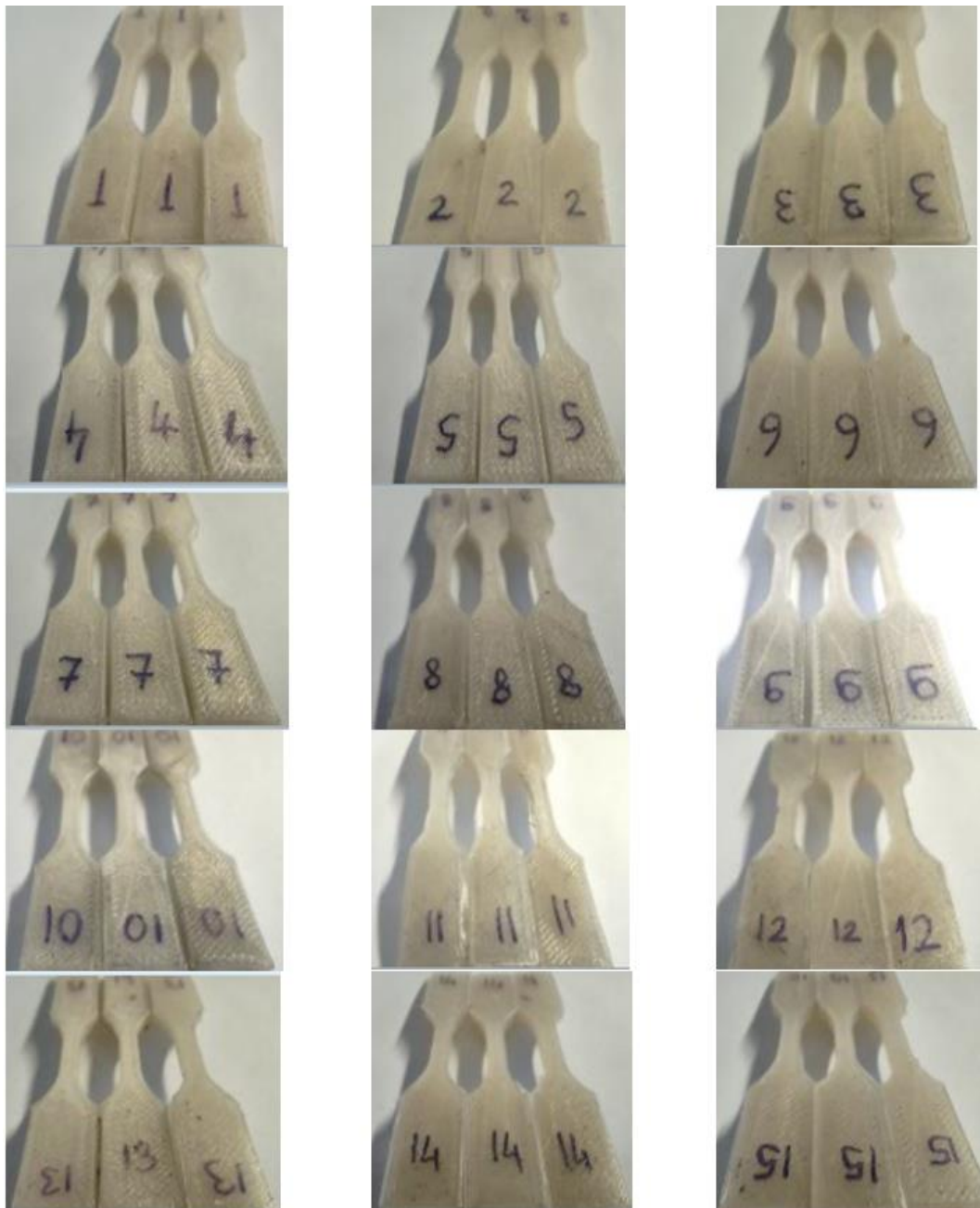


Figure 3.14: Pure PA6 Tensile Test Specimens



Figure 3.15: PA6CF10 Tensile Test Specimens

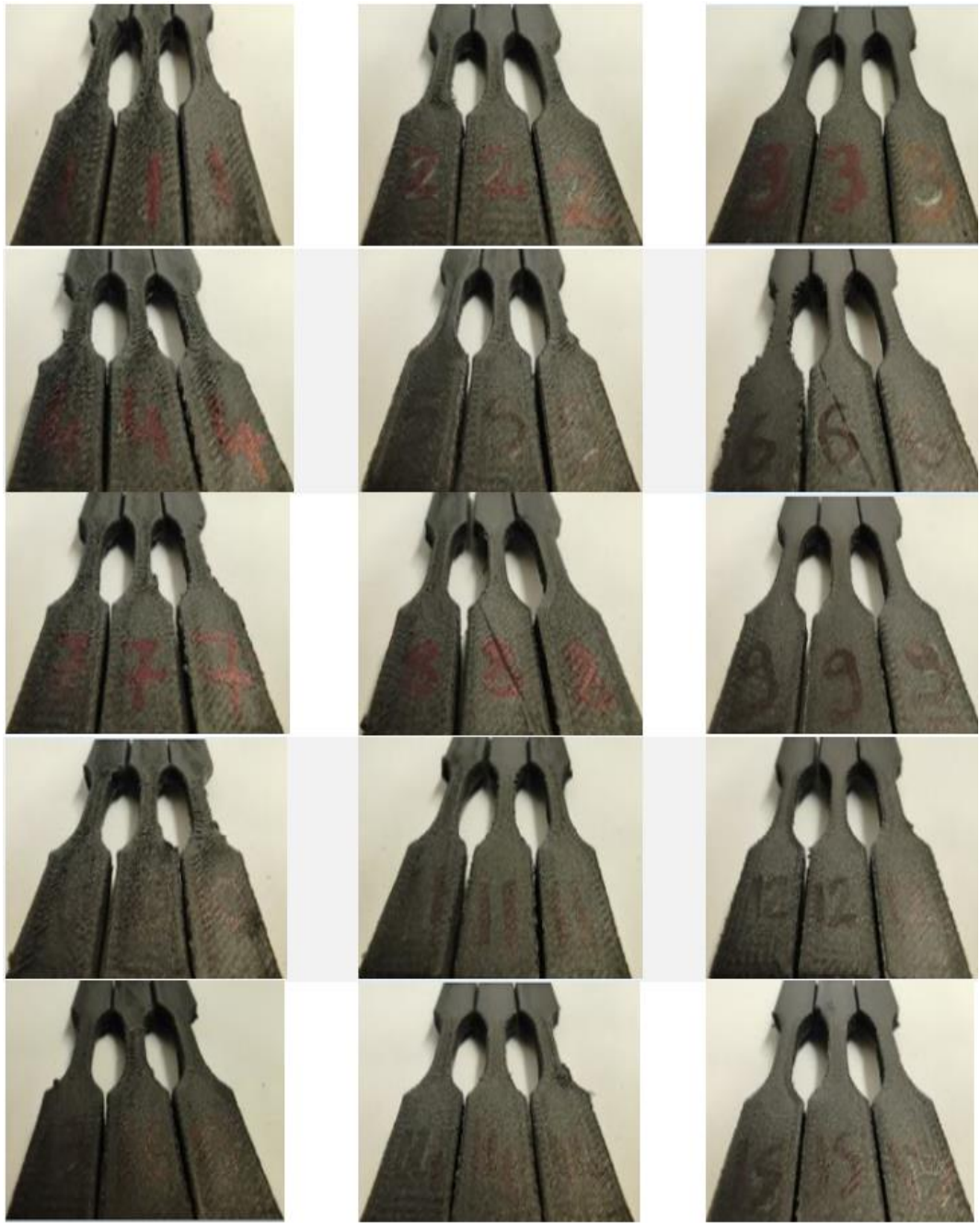


Figure 3.16: PA6CF20 Tensile Test Specimens

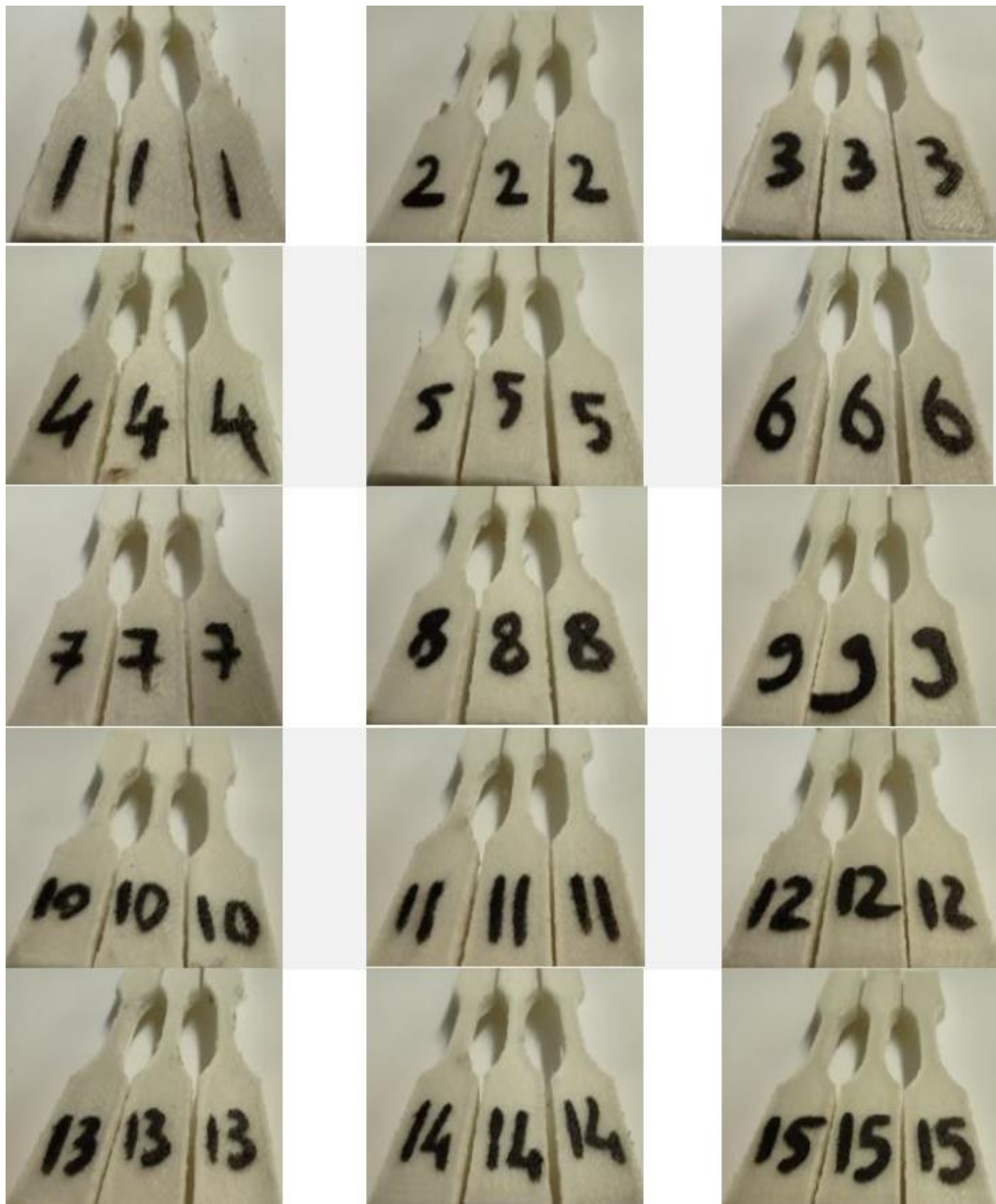


Figure 3.17: PA6GF10 Tensile Test Specimens



Figure 3.18: PA6GF20 Tensile Test Specimens

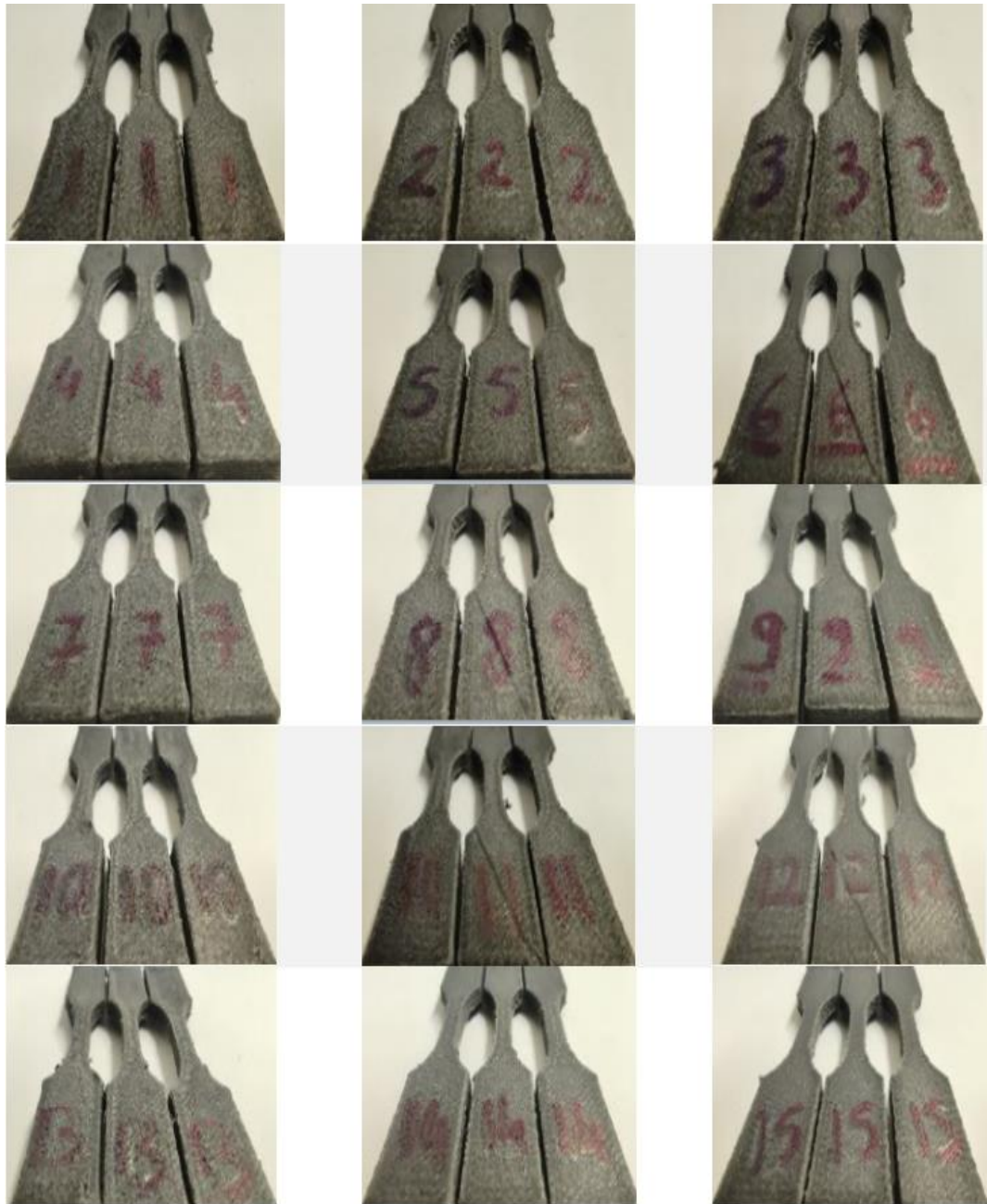


Figure 3.19: PA6HF10 Tensile Test Specimens



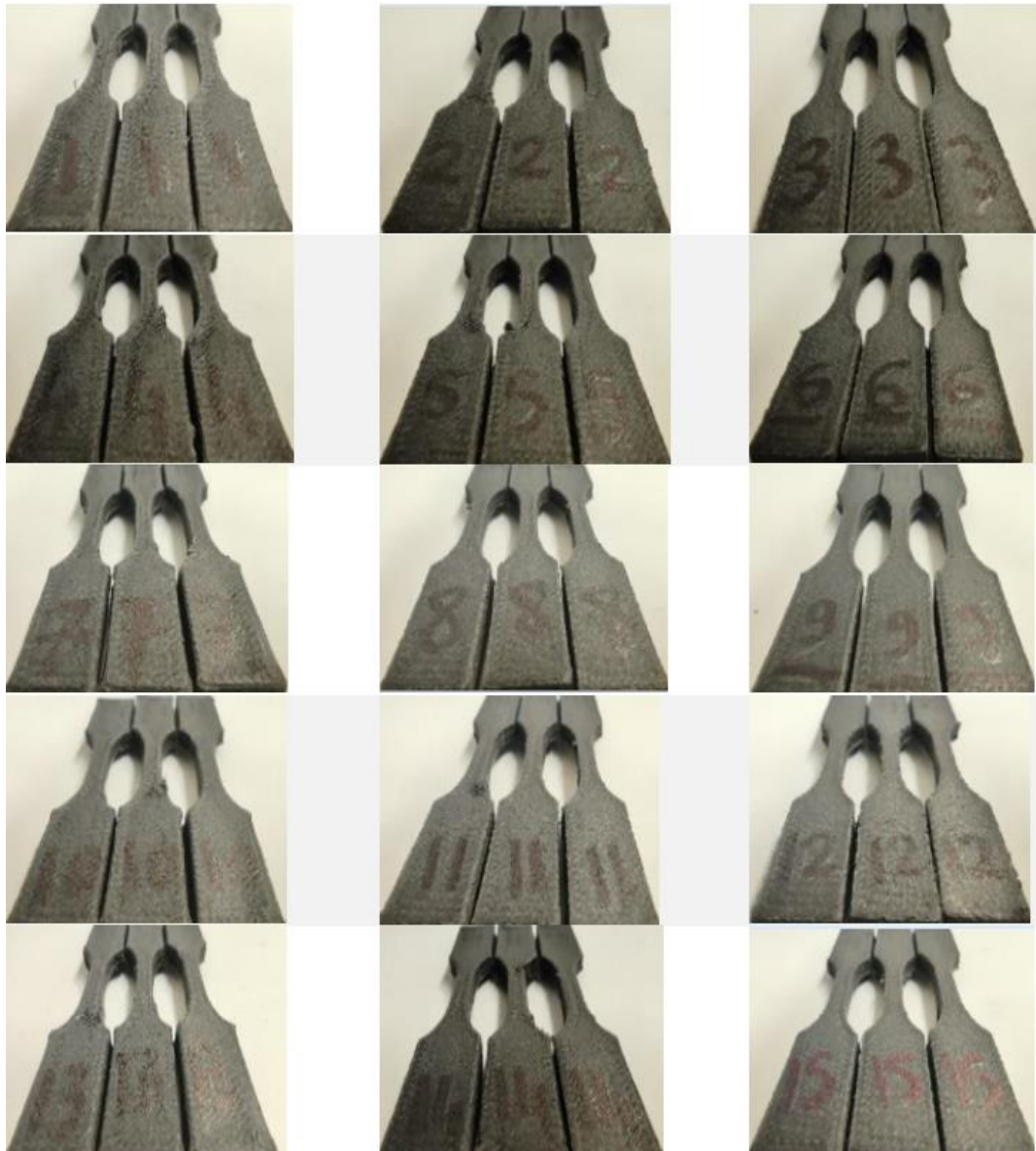


Figure 3.20: PA6HF20 Tensile Test Specimens

Tensile test specimens of 7 different composite materials produced in 15 different parameters were tested by ASTM D638 standard. In the microstructural analysis, these materials were expected to contain a maximum of 10% porosity and the tensile strength of carbon, glass and hybrid fiber reinforced filaments was higher than the pure ones.

### 3.2.3.2 Impact Specimens

The highest tensile strength was obtained in parameter 15 in all of the specimens' groups whose tensile test results were shared in the Results and Discussion chapter. Impact test specimens were produced to examine the effect of the infill pattern by considering the production parameters with the highest tensile strength.

To compare the impact properties of the parts produced by the FFF method, production was carried out in the unnotched specimen geometry in the ISO 179 standard shown as in figure 3.21.

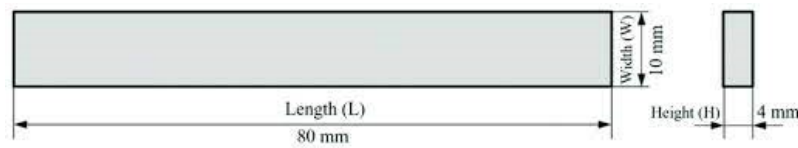


Figure 3.21: ISO 179 Impact Charpy Geometry

Impact test specimens were produced with two different infill patterns. Specimen production was carried out at the nozzle temperature and layer thickness parameters, where the highest tensile strength was obtained. This is parameter 15.

Table 3.6: FFF Parameters for Impact Specimens

<i>PARAMETERS NO</i>	<i>LAYER HEIGHT (MM)</i>	<i>NOZZLE TEMPERATURE (°C)</i>
<i>15</i>	0.1	275

The effect of the infill pattern on the mechanical properties was discussed in the impact test. Two different impact specimens with 0/90 and -/+ 45 orientation were produced from each composite compound. Images of infill patterns are shown in figure 3.22.

<i>View</i>				
<i>Direction</i>	<b>0°</b>	<b>90°</b>	<b>-45°</b>	<b>+45°</b>
<i>Infill Pattern</i>	<b>0°/90°</b>	<b>-/+45°</b>		

Figure 3.22: Infill patterns geometries for impact specimens (0°/90°, -/+45°)

To observe the standard deviation values, 5 specimens were produced for each material configuration and different infill patterns. One of each of the produced specimens is

seen in figure 3.23. The specimens on the left are those with an orientation of 0/90, and the specimens on the right have an orientation of -/+45.

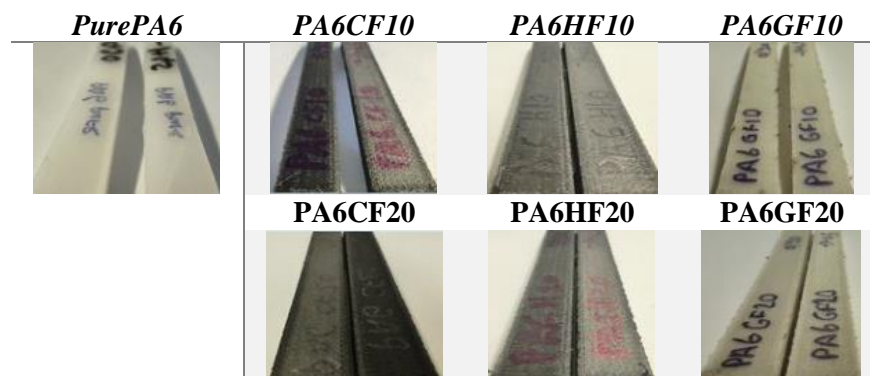


Figure 3.23: Impact Charpy Test Specimens

### 3.2.3.3 Compression Specimens

The weakest axis of the parts produced by the FFF method is the z-axis. For this reason, the tensile strengths in the z-axis are quite low (140). Compression test specimens were produced to observe the effect of this disadvantageous situation in the tensile direction in the compression direction. To examine the effect of different layer thicknesses on the compressive strength at the nozzle temperature with the highest tensile strength, the specimens were produced with parameters numbers 13, 14 and 15.

To compare the compression properties of the parts produced by the FFF method, production was carried out in the specimen geometry in the ASTM D 695 standard shown in figure 3.24.

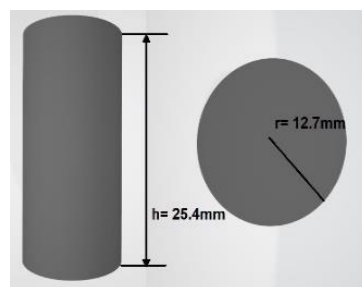


Figure 3.24: ASTM D 695 Compression Test Geometry

Compression test specimens are produced in a single infill pattern as they have circular cross-sections. Specimens' production was carried out in different layer thicknesses at the nozzle temperature where the highest tensile strength was obtained.

Table 3.7: FFF Parameters for Compression Specimens

<i>PARAMETERS NO</i>	<i>LAYER HEIGHT (MM)</i>	<i>NOZZLE TEMPERATURE (°C)</i>
13	0.3	275
14	0.2	275
15	0.1	275

To observe the standard deviation values, 5 specimens were produced for each material configuration and different layer thicknesses. Produced specimens are shown in figure 3.25.



Figure 3.25: Compression Test Specimens

### 3.3 Modified Short Fiber Reinforced PA6 matrix Composites

The studies in this part of the thesis study were carried out at the University of Alberta, Edmonton, AB Canada with the support of TUBİTAK 2214A. Nanocellulose was added to the short fiber reinforced PA6 matrix polymeric composite materials which improved at the first stage of thesis studies, to increase their strength properties and improve their interfaces. In this context, all composite compounds produced in the first stage were re-produced using nanocellulose-modified fibers. The surfaces of the fibers used in the compound production were modified with nanocellulose. Compounds with 1% nanocellulose additive by weight are given in table 3.8.

Table 3.8: Modified Short Fiber Reinforcement Thermoplastics Composite Compounds

<i>Compound No</i>	<i>Code</i>	<i>Matrix</i>	<i>Fiber</i>	<i>Fiber Ratio</i>	<i>NC Ratio</i>
1	PurePA6	Pure Polyamide (PA6)	-	-	
2	PA6CF10c	Polyamide (PA6)	Carbon Fiber	10%	
3	PA6CF20c	Polyamide (PA6)	Carbon Fiber	20%	
4	PA6GF10c	Polyamide (PA6)	Glass Fiber	10%	% 1
5	PA6GF20c	Polyamide (PA6)	Glass Fiber	20%	
6	PA6HF10c	Polyamide (PA6)	Carbon Fiber	5%	
			Glass Fiber	5%	
7	PA6HF20c	Polyamide (PA6)	Carbon Fiber	10%	
			Glass Fiber	10%	

6 hybrid composite structures containing PA6CF+nanocellulose, PA6GF+nanocellulose, and PA6HF+nanocellulose with two different fiber reinforcement ratios, 10% and 20% by weight, were created. There is no previous study about producing short carbon, glass, and hybrid (carbon/glass) fiber reinforced PA6 matrix specimens using the FFF. Developing a hybrid composite structure with nanocellulose additive is an entirely innovative approach.

At this stage of the thesis, carbon, glass, and hybrid (carbon/glass) fiber hybrid composite compounds modified with PA6 matrix and nanocellulose were produced, and filaments were produced using these compounds. In all these processes, the characterizations of compounds and filaments were made. The tests of the parts produced with these composite filaments were carried out and the production parameters were determined. Pure PA6, carbon, glass, and hybrid composite structures produced in the first stages of the doctoral thesis were compared with hybrid composite structures modified with nanocellulose.

### 3.3.1 Modification of fibers with Nanocellulose

The nanocellulose product produced by the University of Maine, which is used in interface improvement, is a slurry product containing 11.5% nanocellulose and 88.5% water by weight. With this product, surface modifications of carbon and glass fibers to be used in compound preparation were carried out.

Cellulose is a hydrophilic material. For this reason, it is very easily affected by humidity. In their study, Hajian et al. suggested that esterification is the best method to impart hydrophobic properties to cellulose (141). For this reason, nanocelluloses were kept in a citric acid solution at 50 °C for 20 minutes, as stated in Hajian's study. Hajian et al. used chloroform to reduce viscosity and to benefit the contact of cellulose with the mixture and stated that the toluene solution had the same effect. In our thesis study, nanocelluloses surfaces treated with citric acid were mixed mechanically with glass in figure 5 (b) and carbon fibers in figure 5 (a) in a toluene solution. This process was carried out to homogeneously coat the nanocellulose on the fiber surface. Nanocellulose was added at a rate of 1% by weight. Sartorius brand precision balance was used to determine the weight ratios.



Figure 3.26: Precision Balance

By the additive ratios, 6 different compounds were produced with the fibers coated with nanocellulose. Finally, before the compounding process, each composition was kept in a vacuum oven at 80 degrees for 48 hours for drying.

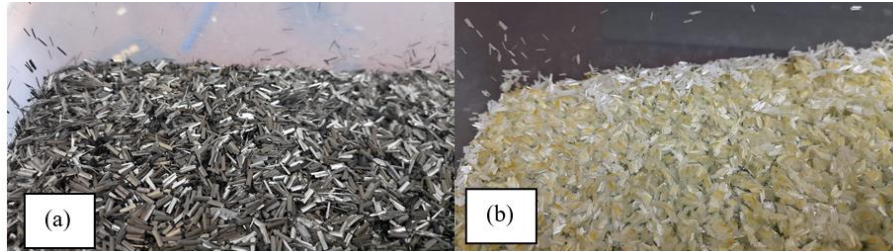


Figure 3.27: After Drying Process (a) Carbon fiber (b) Glass Fiber

Fibers modified with nanocellulose were taken into vacuum bags and sent to Eurotec Company for compound production. Compound preparation processes were carried out in a twin-screw extruder. The prepared compounds were brought into filament form with a single-screw extruder to be produced by the FFF method. Finally, tensile, compression, and impact test specimens were produced with the FFF method, and mechanical tests, thermal and morphological analyzes were performed on the produced specimens. This study was compared with the results obtained after the first stage.

The objectives of this study are;

- To ensure homogeneous distribution of reinforcing structures in composite compounds,
- To ensure that the length of short fiber reinforcements in composite compounds is less than 6mm,
- Determining the mechanical and morphological characterizations of the composite filaments and determining the structural properties efficiently,
- To determine the effect of interface improvement on mechanical properties,
- Contributing to the literature on additive manufacturing and hybrid composite manufacturing,
- To raise awareness about the performance improvements that these capabilities can provide in related industrial products.

### 3.3.2 Modified Short Fiber Reinforced PA6 matrix Composites Compounding

As in the first stage of the thesis, the compounds were produced in Eurotec Company with a twin-screw extruder. Since the homogeneous distribution of the fibers is a critical issue, Eurotec company, which is experienced in polyamide production, was preferred.

Since the filament production will be carried out in a different single-screw device, PurePA6 pellets were used again in this study. Nanocellulose modified fibers and compounds with 6 different ratios were produced with a twin-screw extruder. To obtain a homogeneous mixture, an extruder with a counter-rotating screw configuration was used. A twin screw extruder unit with a diameter of 18 mm was used in the production of the compound. Pre-drying was carried out at 80°C for 24 hours.

The same parameters as in the first step in compound production were used. The parameters are as follows; the feeding zone is 25°C, the melt retarding zone is 190°C, the mixing and conveying is 220°C and the die head temperature is 225°C.



Figure 3.28: Modified Short Fiber Reinforcement Composite Compounds

The prepared compounds were vacuumed and stored in their bags to protect them from moisture until the next process. It was then shipped to the University of Alberta.



### 3.3.3 Short Fiber Reinforced PA6 matrix Composites Filament Extrusion

Filament production processes of the compounds with twin-screw were carried out in the Multi-functional Composite Laboratory of the University of Alberta.

PurePA6, PA6CF10c, PA6CF20c, PA6GF10c, PA6GF20c, PA6HF10c, and PA6HF20c compounds were dried in a Thermo Fisher Scientific Lindberg/Blue M vacuum oven shown in figure 3.29 at  $80^{\circ}\text{C} \pm 0.1^{\circ}\text{C}$  for 24 hours before extrusion.



Figure 3.29: Vacuum Oven

All specimens were packed with vacuum packaging as seen in figure 3.30 to protect them from moisture after drying. This process was carried out so that the dried polymeric composite compounds do not encounter air during the waiting phase before production with a single-screw extruder.

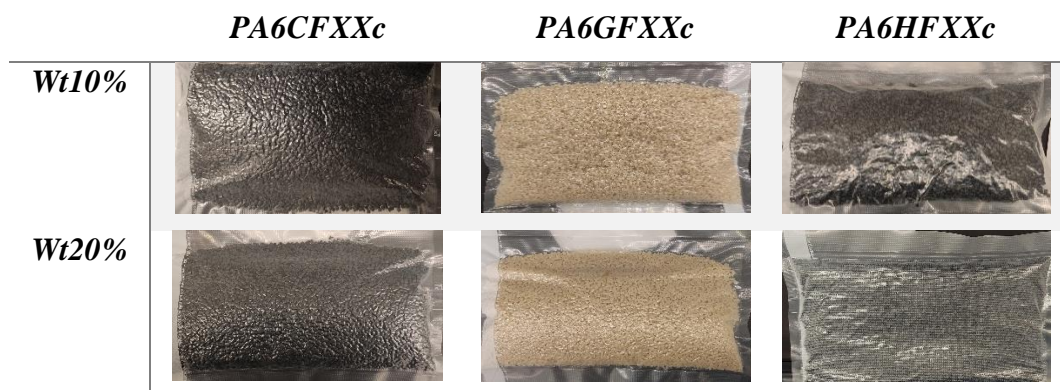


Figure 3.30: Vacuumed Compounds

All compounds were melt-extruded using a Brabender™ single screw extruder connected to the ATR Plasti-Corder drive system in figure 3.31 with a 3 mm circular

cross-section die feeding a filabot brand cooling and reel winding system seen in figure 3.32. Since a 2.85 mm diameter filament was desired to be produced, a 3mm circular cross-section die was used.



Figure 3.31: Single Screw Extruder

Cooling speed and reel speed settings are adjusted to provide a 2.85mm filament diameter in Filabot brand air-cooled system and reel winding system. Since the ultimaker3 device is used in the specimen production processes with the FFF method, a filament with a diameter of 2.85 mm suitable for the use of this device was produced and wound on spools.



Figure 3.32: filabot airpath for cooling and filament spool system

Filabot FB00073 filament spooler and Filabot FB00626 air path were used to adjust the produced filament's diameter. The schematic representation is as in figure 3.33.

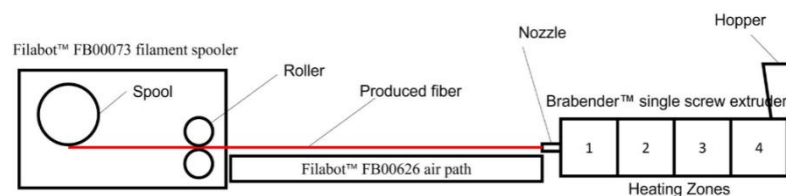


Figure 3.33: Schematic representation of the single screw extrusion line

Thermal properties (glass transition/melting/crystallization/decomposition temperatures) were analyzed by DSC to determine the extrusion parameters of the

composite compounds, which were turned into filaments for specimens' production in the FFF method. In addition, the torque value of the single-screw extruder was determined not to exceed 10Nm in the determination of the parameters. Single-screw extruder process parameters are given in table 3.9.

Table 3.9: Single-screw extruder barrel temperature

<i>Barrel1</i>	<i>Barrel2</i>	<i>Barrel3</i>	<i>Die</i>	<i>RPM</i>
210°C	215°C	225°C	220°C	6

Extruder temperature setting screen is as seen in figure 3.34.

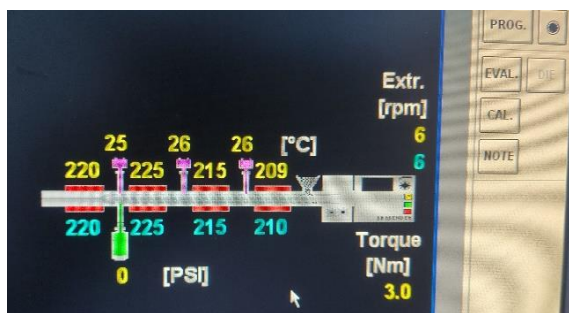


Figure 3.34: Single-screw extruder parameters adjusting screen

All filaments produced with a single-screw extruder were placed in a vacuum bag to protect them from moisture after production, as seen in figure 3.35.

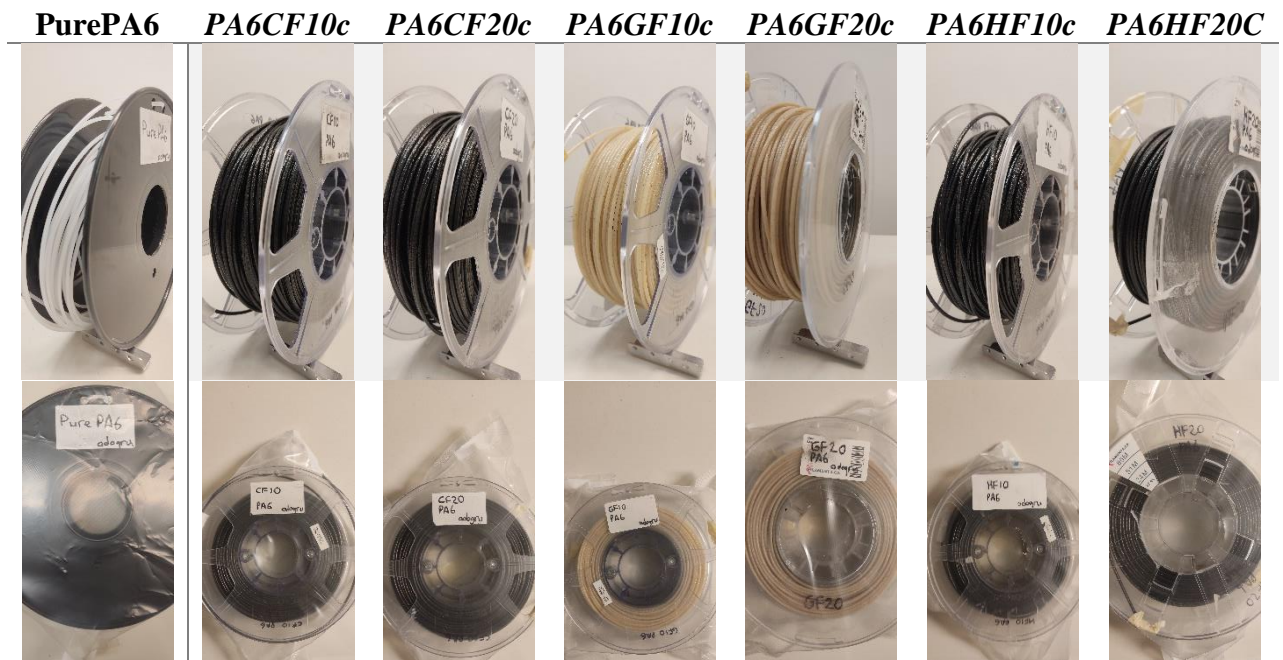


Figure 3.35: Filaments and Vacuumed filament spools

### 3.3.4 Modified Short Fiber Reinforced PA6 matrix Composites Production with FFF

Tensile, compression, and impact charpy test specimens were produced by FFF method using filaments produced with single screw. Drawing files of the standards in the first stage were used in all specimens' productions. Production parameters were not changed, and productions were carried out with the same gcode files. To accurately compare the results obtained by using carbon, glass, and hybrid (carbon/glass) fiber reinforced PA6 matrix filaments produced from the first stages of the doctoral thesis, all productions were carried out using the same brand model device and nozzle with the same characteristics. The Ultimaker 3 device in figure 3.36 was used in the production of hybrid composite specimens with the FFF method.

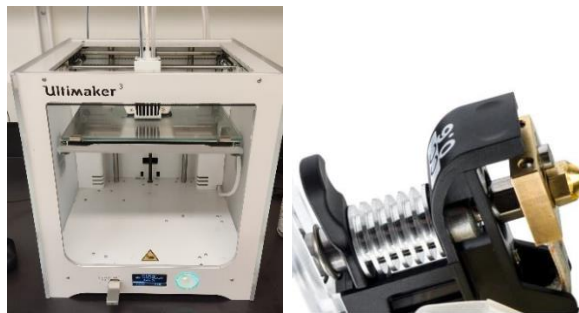


Figure 3.36: Ultimaker 3 FFF device and Ultimaker CC Printcore nozzle

All specimens were performed with the ultimaker CC printcore on the 0.6mm diameter sapphire-tipped figure 3.36, as in the first stage. A specially developed nozzle is used to produce short fiber reinforced composite filaments.

#### 3.3.4.1 Tensile Specimens

The nozzle temperature at which the highest tensile strength value was obtained among the specimens produced in the first stage of the thesis was used. Specimens with 3 different layer thicknesses (0.1-0.2-0.3 mm) were produced just to observe the effect of layer thicknesses. For this reason, the parameters numbered 13, 14 and 15 in the first stage were used. The FFF production parameters used in the second stage are given in table 3.10.

Table 3.10: FFF process parameters for Tensile Specimens

<b>Layer height</b>	0.1(13)-0.2(14)-0.3(15)mm
<b>Nozzle Temperature</b>	275°C
<b>Bed Temperature</b>	80°C
<b>Infill percentage</b>	100%
<b>Infill pattern</b>	-/+45 degrees
<b>Print Speed</b>	50mm/s
<b>Flow rate</b>	100%
<b>Nozzle Size</b>	0.6mm

To observe the standard deviation values, 5 specimens were produced from each material configuration and parameter. Images of hybrid composite samples containing 1% nanocellulose by weight are as in figure 3.37.

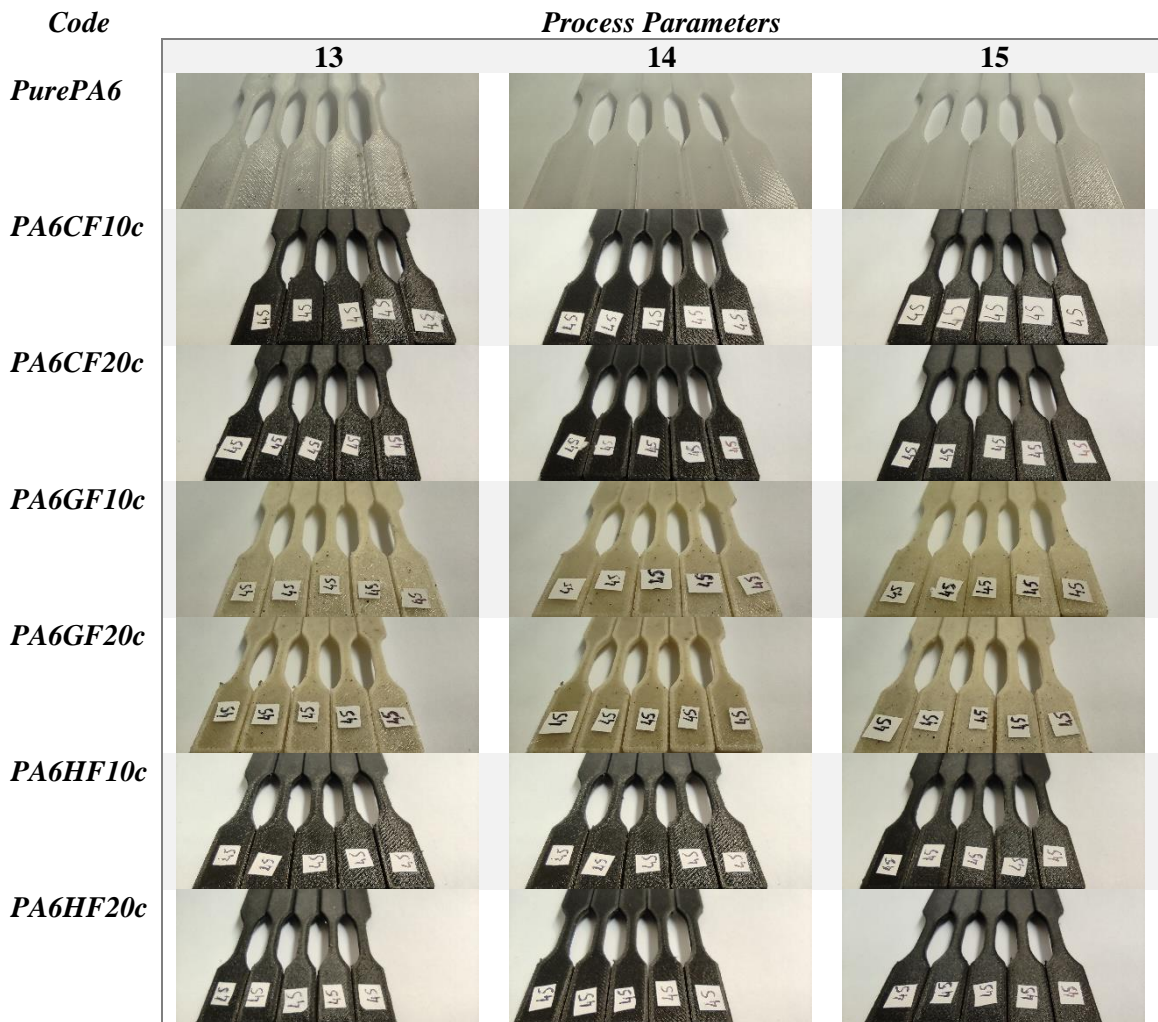


Figure 3.37: Tensile Test Specimens for second stage

Tensile test specimens of 6 different composite materials and one control group PurePA6 produced in 3 different parameters were tested in accordance with ASTM D638 standard. In the second stage's tensile strength tests of the control group are same

values were obtained in the first stage. The test results were shared in the Results and discussion chapter. In the microstructural analysis, these materials were expected to contain a maximum of 10% porosity and to have higher tensile strengths than specimens without nanocellulose modification.

### 3.3.4.2 Impact Specimens

As in the first stage, impact test specimens were produced to examine the effect of the infill pattern by considering the production parameters with the highest tensile strength. To compare the impact properties of the parts produced by the FFF method, production was carried out in the unnotched specimen geometry in the ISO 179 standard.

Impact test specimens were produced in two different infill patterns as before. The effect of nanocellulose modification on impact resistance was compared. Specimens' production was carried out at the nozzle temperature and layer thickness that called parameter 15, where the highest tensile strength was obtained.

Table 3.11: FFF Parameters for Impact Specimens

<i>PARAMETERS NO</i>	<i>LAYER HEIGHT (MM)</i>	<i>NOZZLE TEMPERATURE (°C)</i>
<i>15</i>	0.1	275

The effect of the infill pattern on the mechanical properties was discussed in the impact test. Two different impact specimens with 0/90 and +/- 45 orientations were produced from each composite specimen. To observe the standard deviation values, 5 specimens were produced for each material configuration and different infill patterns. One of each of the produced specimens is seen in figure 3.38. The specimens on the left are those with an orientation of +/-45, the specimens on the right are those with an orientation of 0/90.

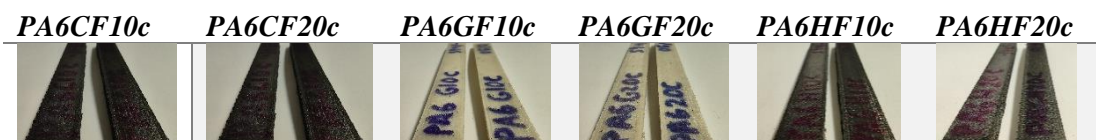


Figure 3.38: Impact Charpy Test Specimens

### 3.3.4.3 Compression Specimens

Comparing the compression properties of the parts produced by the FFF method, production was carried out in the specimen's geometry included in the ASTM D 695 standard.

Compression test specimens are produced in a single infill pattern as they have circular cross-sections. Specimens' production was carried out in different layer thicknesses at the nozzle temperature where the highest tensile strength was obtained.

Table 3.12: FFF Parameters for Compression Specimens

<i>PARAMETERS NO</i>	<i>LAYER HEIGHT (mm)</i>	<i>NOZZLE TEMPERATURE (°C)</i>
<i>13</i>	0.3	275
<i>14</i>	0.2	275
<i>15</i>	0.1	275

To observe the standard deviation values, 5 specimens were produced for each material configuration and different layer thicknesses. Produced specimens are shown in figure 3.39.

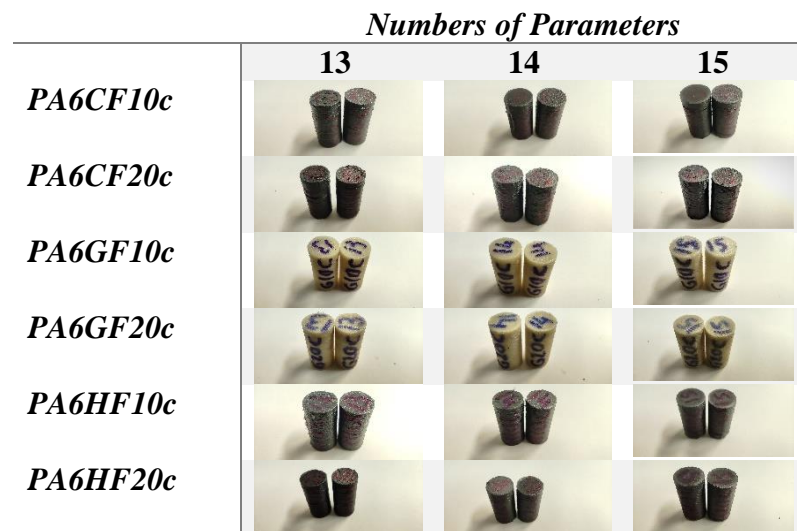


Figure 3.39: Compression Test Specimens

## 3.4 Mechanical Tests and Analysis

### 3.4.1 Thermal Analysis

#### 3.4.1.1 TGA

TGA of hybrid composite pellet specimens was performed using TGA Q50 (TA Instruments, USA) to measure their thermal stability (ie, their degradation temperature). A heating rate of 10°C/min was used and the temperature range was 25–800°C. Analysis was done in the air environment.



Figure 3.40: TA Instruments TGA Q50 Device

#### 3.4.1.2 DSC

DSC Q100 (TA Instruments, USA) device with modulated method was used to measure the transition temperatures of all composite pellets. Modulation,  $\pm 1.00^{\circ}\text{C}$  every 60 s. The heating rate was 10°C/min and the heating range was 25 to 260°C. Modulated DSC was performed to obtain the glass transition ( $T_g$ ) and melting ( $T_m$ ) temperatures of polymer composites.

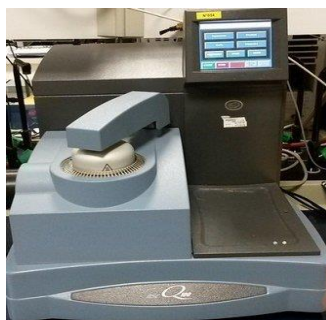


Figure 3.41: TA Instruments DSC Q100 Device



## 3.4.2 Mechanical Testing

### 3.4.2.1 Tensile

Tensile tests were carried out according to ASTM D638 standard with the ZwickRoell Z050 device at the first stage. All specimens are mounted on hand-tightened clamp-type handles. The tests were carried out at a constant displacement speed of 1 mm/min until the specimens failed. Load, displacement, time, and strain were recorded at 10 hz.



Figure 3.42: Zwick/Roell Z050 Tensile Testing Device

Tensile tests according to ASTM D638 standard were performed on Instron 5966 device with a 10 kN load sensor at the second stage. All specimens are mounted on hand-tightened clamp-type handles. The tests were carried out at a constant displacement speed of 1 mm/min until the specimens failed. Load, displacement, time, and strain were recorded at 10 hz.



Figure 3.43: Instron 5966 Tensile Testing Device

### 3.4.2.2 Impact Test

Impact Charpy tests were performed with the CEAST Resil Impactor device, the Instron model in Figure 3.44, according to the ISO 179 standard. The specimens were produced and tested without notches. It was struck at a kinetic energy of 2 J and an impact velocity of 2.9 m/s, taking into account an aperture length of 62 mm. Force-displacement curves and dynamic parameters of the material in terms of absorbed energy were recorded. The impact energy absorbed at the moment of fracture was calculated as the area under the impact force-displacement curve from the peak of the impact load to the first occurrence of zero loads after the maximum peak.



Figure 3.44: CEAST Resil Impactor Device

### 3.4.2.3 Compression Test

Compression tests according to ASTM D695 standards were performed with a 100 kN load sensor in Instron 5966 device. The tests were carried out at a constant displacement speed of 1.3 mm/min up to 2 mm of deformation, then at a constant displacement speed of 5 mm/min. The samples were tested up to a load of 90 kN. Load, displacement, time, and strain were recorded at 5hz.

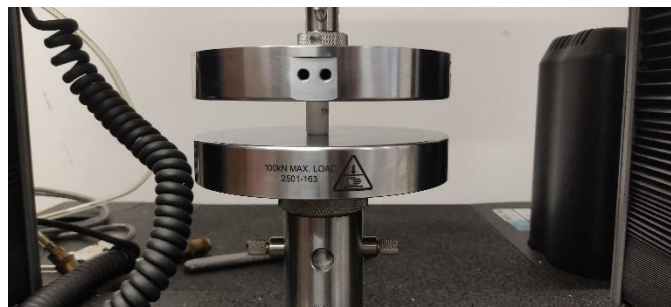


Figure 3.45: Instron 5966 Compression Testing Device

### 3.4.3 SEM

In the first stage of the thesis study, the unmodified nanocellulose composite samples were examined under the scanning electron microscope (SEM). Microstructure were performed with the SEM device at Dokuz Eylul University Izmir International Biomedicine and Genome Institute. Microstructural analyzes were performed with a Zeiss Sigma500 FESEM using the SE2 detector. Imaging of damaged surfaces after the tensile test was performed at different magnifications under 1.5-3.0 kV EHT. Before being placed in the microscope chamber, specimens were fixed on stubs with double-sided carbon tape and sputter-coated with 5 nm gold.



Figure 3.46: Zeiss Sigma500 FESEM Device

In the second stage, SEM analyzes were carried out to observe the interfacial improvements in the specimens modified with nanocellulose. Microstructure analyzes were performed with the SEM device at the University of Alberta, NanoFab Department. Microstructure analyzes of the specimens were performed with the Zeiss EVO MA10 microscope using the SE1 detector. The damaged areas of the nanocellulose-modified specimens were examined after the tensile test. Specimens imaging was performed at different magnifications under 15kV EHT. Before being placed in the microscope chamber, specimens were fixed on stubs with double-sided carbon tape and spray-coated with gold for 120 seconds in the Gold Sputtering Unit DESK II.



Figure 3.47: Zeiss EVO MA10

# Chapter 4

## 4 Results and Discussion

This section shares the thermal analysis results of prepared compounds, filaments, and produced specimens with FFF. The effects of thermal analysis results on filament production and part production with FFF and the control of additive ratios are mentioned.

The results of the mechanical tests and morphological analysis of the produced specimens were shared, interpreted, and evaluated. The hybrid structures in which carbon fiber, glass fiber, and carbon/glass fibers are used together were compared and the effect of fiber proportions on mechanical properties was investigated. In addition, the importance of fiber interfacial bonding and the benefits of interfacial improvement with nanocellulose added are stated.

### 4.1 Results

The use of unreinforced polymer filaments limits the wide application area of parts produced by this method in industry and research environments (65). Providing superior mechanical properties in the parts produced by the FFF method will increase the number of final products produced by this method. In the production of fiber-reinforced thermoplastic matrix composite, it is critical to determine the values such as the orientation of the fibers in the matrix, not exceeding the decomposition temperature of the polymer, the glass transition temperature ( $T_g$ ) and melting temperature ( $T_m$ ) required in the forming processes. In this context, thermal analyzes were carried out to control the correct fiber reinforcement by weight in the PA6 matrix in the determined ratios, to maintain the homogeneity of the distribution of the fibers in the matrix, to determine the appropriate temperature values in the twin-screw,

single-screw, and FFF processes. Tensile, impact, and compression strengths of the produced specimens were measured and the effects of fiber type, the difference in fiber proportions, and surface modification on mechanical properties were investigated. Finally, fiber distributions in the matrix and matrix-fiber interface bonding were examined by morphological analysis, and microstructure images were obtained. In addition, the diameter and length measurements of the fibers were carried out with SEM.

#### 4.1.1 Thermal Analysis

Thermal analysis is a branch of materials science that studies the changes in material properties with temperature. With thermal analysis methods, changes in the properties of a substance or its derivatives under a certain temperature program are examined, mass changes can be measured, or the heat absorbed or released in the reaction is measured. In this thesis, TGA and DSC analyzes were performed on the compounds, filaments and specimens produced by the FFF method.

##### 4.1.1.1 TGA Results

TGA is a technique in which the mass of a specimen is monitored as a function of temperature (thermal) or time (equilibrium) under a controlled temperature program in a controlled atmosphere. With TGA analysis, the fiber proportion in each compound was verified and the decomposition temperatures of the compounds were examined. In the thesis study, two different fiber reinforcements, 10% and 20% by weight were applied to the PA6 matrix. By TGA analysis, the weight ratios were controlled, and the decomposition temperatures were determined. TGA analysis was carried out separately for PurePA6 and all other fiber-reinforced materials used in the study in the form of compounds, specimens in filament form, and specimens produced by the FFF method. The differences in the decomposition temperatures of the materials that enter the thermal cycle during the compound preparation, filament production, and FFF and production stages were investigated.

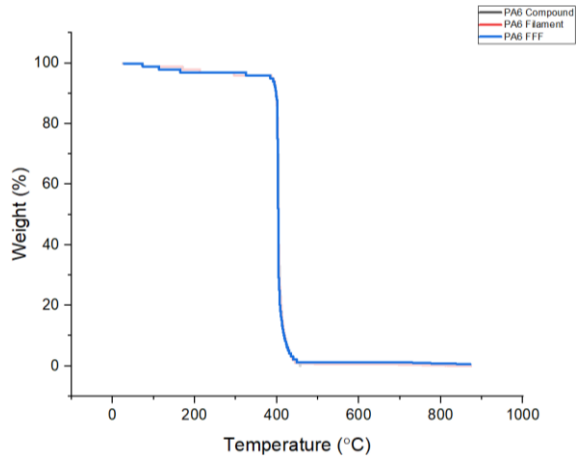


Figure 4.1: Pure PA6 Materials TGA Result

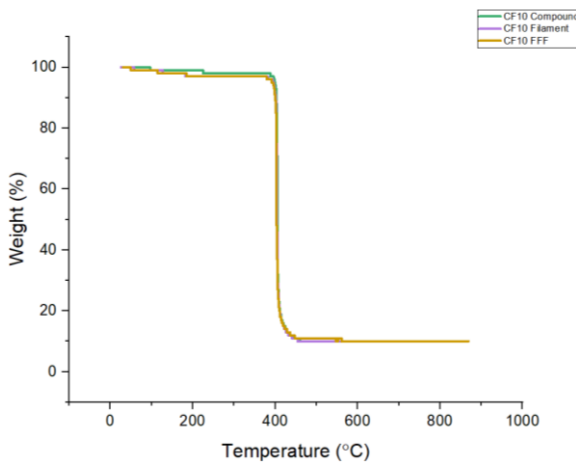


Figure 4.2: PA6CF10 Materials TGA Result

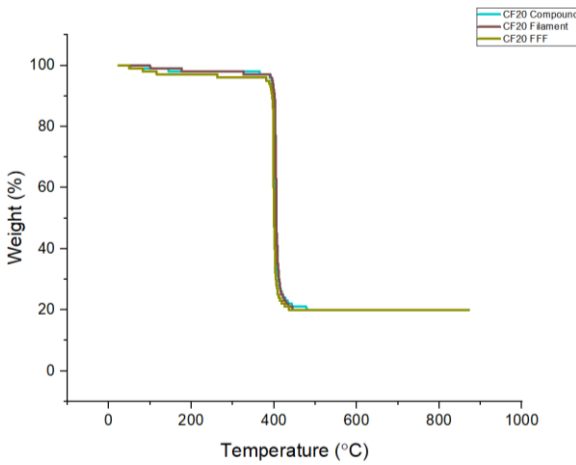


Figure 4.3: PA6CF20 Materials TGA Result

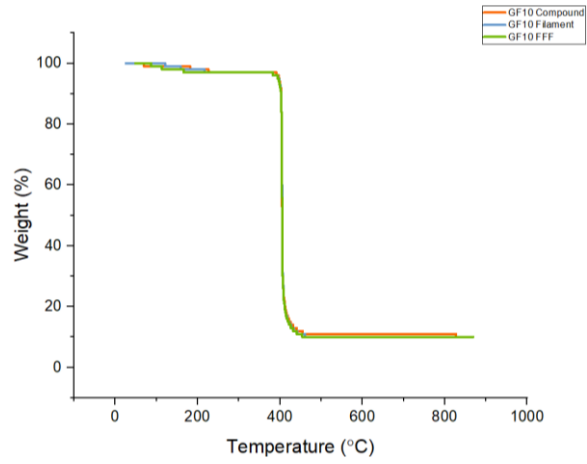


Figure 4.4: PA6GF10 Materials TGA Result

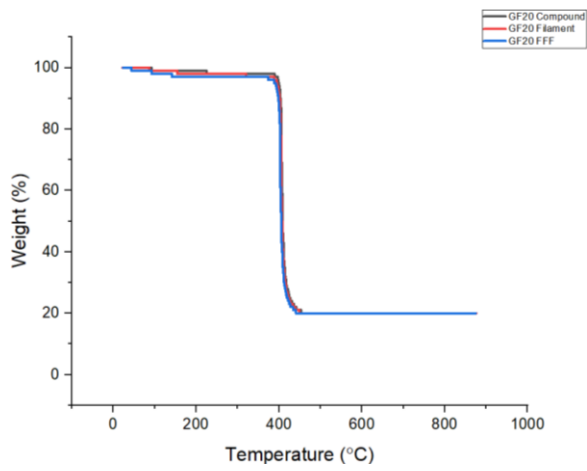


Figure 4.5: PA6GF20Materials TGA Result

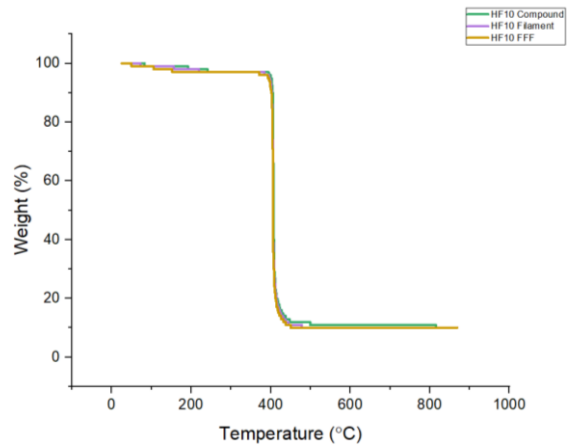


Figure 4.6: PA6HF10 Materials TGA Result



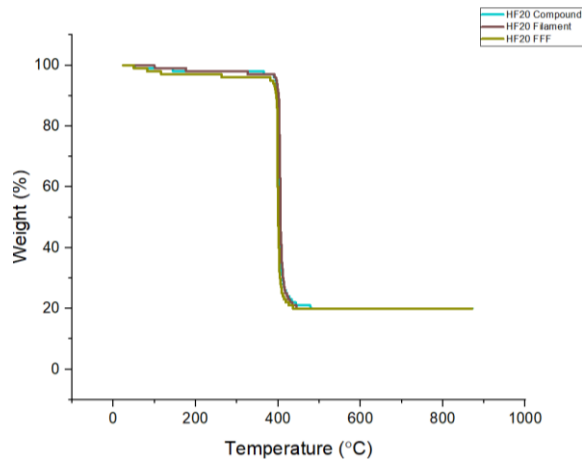


Figure 4.7: PA6HF20 Materials TGA Result

#### 4.1.1.2 DSC results

DSC analyzes were performed to determine thermal properties (Glass transition/melting/crystallization/decomposition temperatures). The term differential in the method is used because the examination of the changes in the specimen with respect to the reference material (thermal change does not occur in the reference material) takes place. DSC was performed to obtain the glass transition temperature ( $T_g$ ), crystallization temperature ( $T_c$ ), and melting temperatures ( $T_m$ ) of hybrid polymer composites. The variation of the heat flow with respect to the temperature and the measured  $T_g$ ,  $T_c$ , and  $T_m$  values are shown in table 4.1.

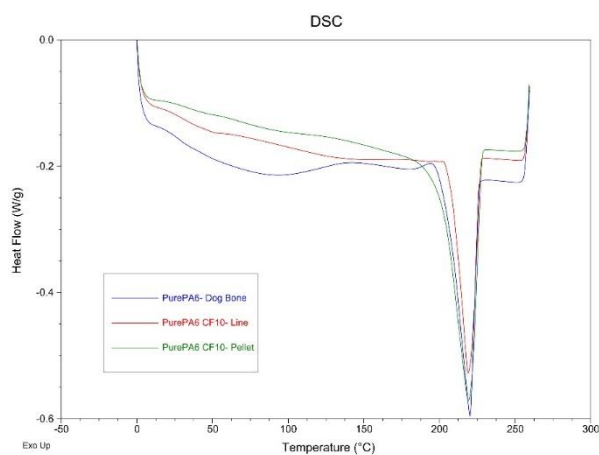


Figure 4.8: PurePA6 Specimens DSC Results

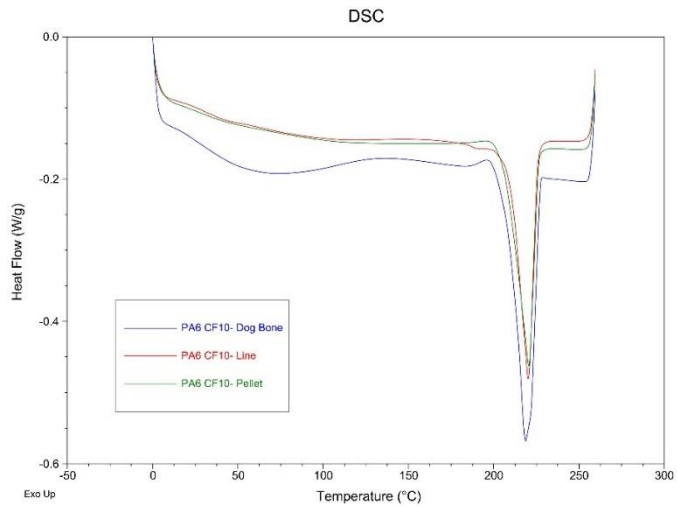


Figure 4.9: PA6CF10 Specimens DSC Results

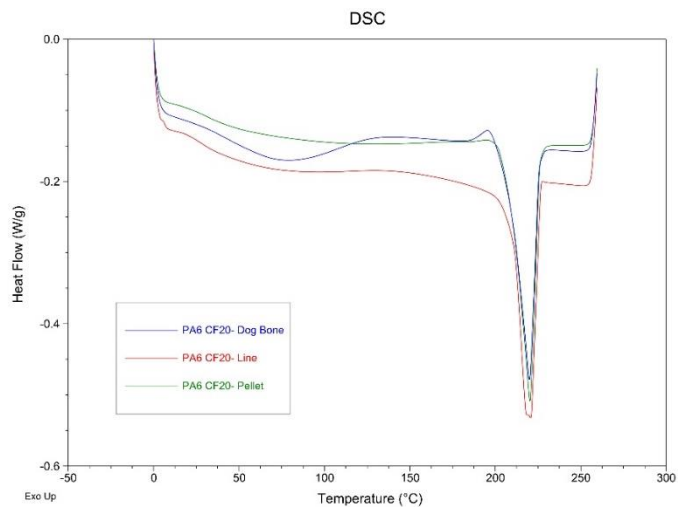


Figure 4.10: PA6CF20 Specimens DSC Results

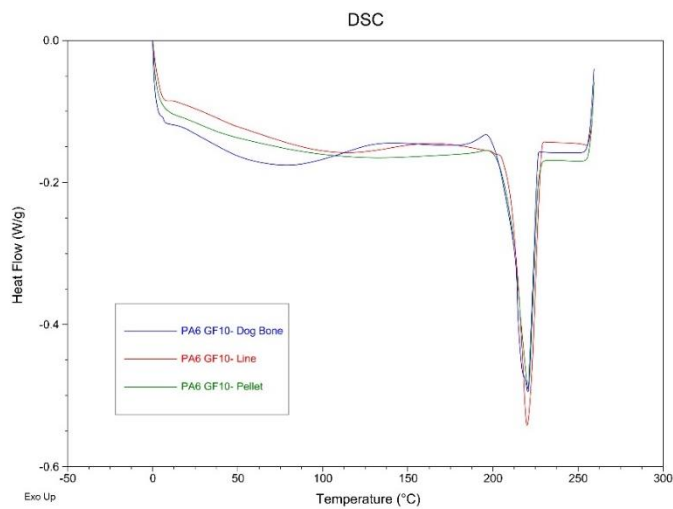


Figure 4.11: PA6GF10 Specimens DSC Results

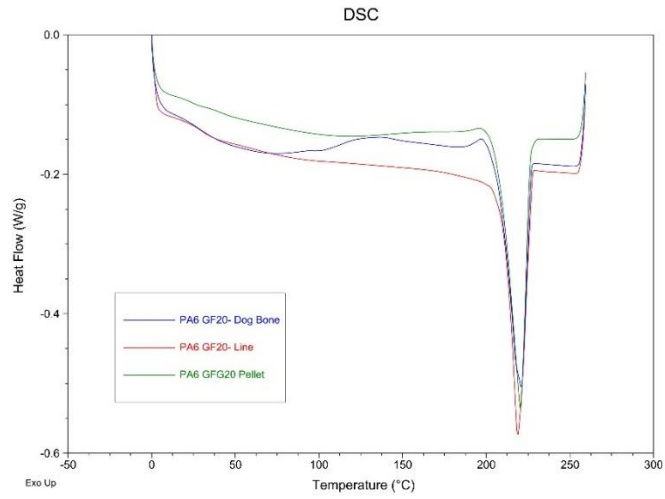


Figure 4.12: PA6GF20 Specimens DSC Results

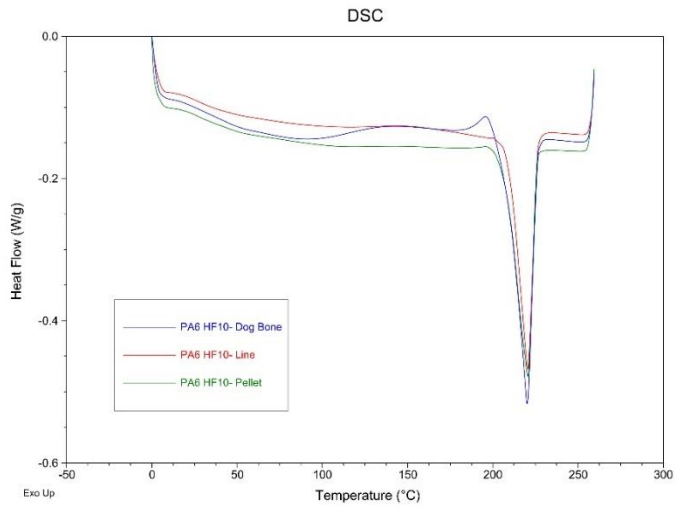


Figure 4.13: PA6HF10 Specimens DSC Results

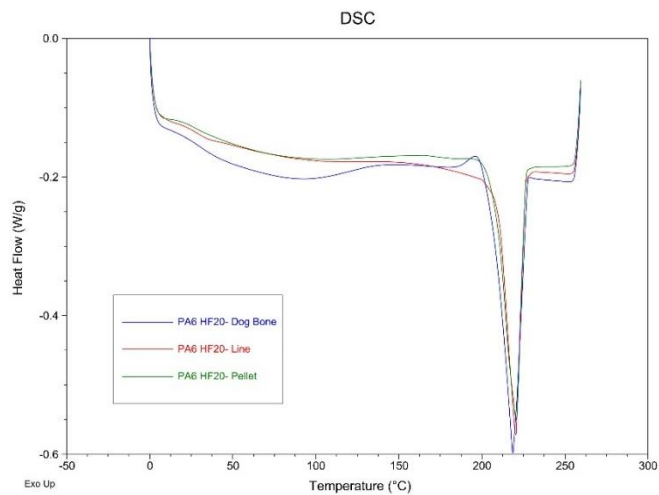


Figure 4.14: PA6HF20 Specimens DSC Results

Table 4.1: DSC results

	PA6 Pure	PA6 CF10		PA6 CF20		PA6 GF10		PA6 GF20		PA6 HF10		PA6 HF20	
Nanocellulose Ratio (%)	-	-	1	-	1	-	1	-	1	-	1	-	1
T <sub>g</sub> (°C) (pellet)	45.98	36.54	36.96	36.45	36.52	30.74	32.67	28.54	28.93	28.54	28.91	28.94	28.8
T <sub>g</sub> (°C) (filament)	35.5	34.91	33.94	33.98	34.79	27.78	28.06	25.42	29.94	25.42	30.23	26.78	29.67
T <sub>g</sub> (°C) (3D printed)	33.06	30.08	28.4	29.12	28.81	26.96	29.44	24.26	29.07	24.26	26.9	26.66	31.75
T <sub>c</sub> (°C) (pellet)	202.11	208.78	207.77	208.54	208.87	207.24	208.29	207.02	207.89	207.02	208.03	207.88	208.65
T <sub>c</sub> (°C) (filament)	209.12	210.3	209.86	210.28	210.35	209.91	211.32	210.87	211.1	210.87	209.92	208.78	209.52
T <sub>c</sub> (°C) (3D printed)	206.12	209.84	208.83	210.22	208.19	210.4	207.17	211.54	208.3	209.54	208.93	208.61	209.02
T <sub>m</sub> (°C) (pellet)	219.11	219.78	220.55	220.48	220.25	220.02	220.69	220.11	220.51	219.29	220.55	220.1	220.66
T <sub>m</sub> (°C) (filament)	218.8	220.3	220.23	220.23	220.77	219.87	220.08	219.88	218.9	220.17	220.52	220.08	220.32
T <sub>m</sub> (°C) (3D printed)	220.11	219.84	218.53	220.04	219.94	220.54	220.54	220.14	220.95	220.04	220.14	219.7	218.51

## 4.1.2 Mechanical Testing

### 4.1.2.1 Tensile Test

In the first stage of the thesis study, tests of tensile test specimens produced in 15 different parameters were carried out with the FFF method. Tensile test specimens for 7 different material configurations were performed in accordance with ASTM D638. The first stage specimens were tested with the ZwickRoell Z050 device.

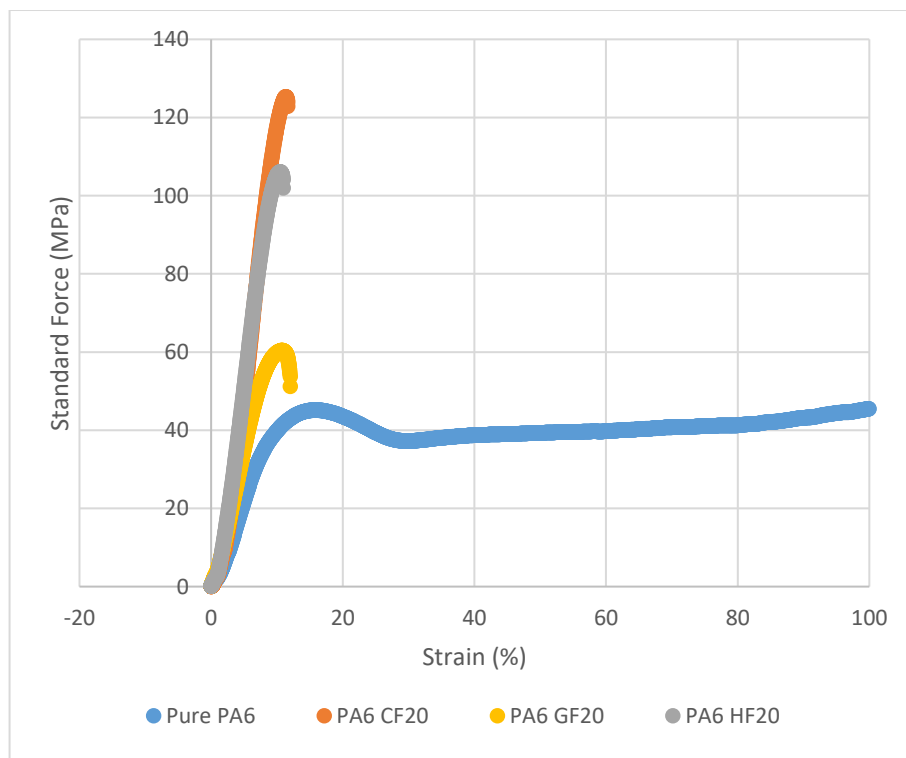


Figure 4.15: Non-modified Specimens Tensile Test Results (Parameter 15)

Tensile test results for PA6 matrix specimens produced in different parameters were used for parameter optimization. In the production of parts with the FFF method, there are many different parameters that affect the mechanical properties, geometric tolerances, production speed, weight, and the parts. Among these parameters, the layer height, nozzle temperature, and infill pattern most affect the mechanical properties. The effect of the infill pattern was examined with impact Charpy tests, and the effect of nozzle temperature and layer thickness, and tensile strength data were analyzed.

Table 4.2: PurePA6 Specimens Tensile Test Results

<i>Parameters</i>	<i>Unit</i>	<i>Specimens</i>							
		1	2	3	4	5	Avr.	Max.	Min.
<b>1</b>	MPa	27.64	24.61	30.68	24.75	30.06	<b>27.55</b>	3.13	2.94
<b>2</b>		30.16	28.41	31.91	29.66	33.20	<b>30.67</b>	2.53	2.25
<b>3</b>		31.60	28.35	34.85	30.33	33.35	<b>31.69</b>	3.16	3.35
<b>4</b>		31.27	28.38	34.16	30.57	34.53	<b>31.78</b>	2.74	3.40
<b>5</b>		32.44	31.94	32.95	30.90	35.33	<b>32.71</b>	2.62	1.81
<b>6</b>		38.72	37.45	39.99	35.12	39.22	<b>38.10</b>	1.89	2.98
<b>7</b>		33.58	32.87	34.28	29.77	34.85	<b>33.07</b>	1.78	3.30
<b>8</b>		35.20	33.65	36.74	31.86	35.90	<b>34.67</b>	2.07	2.81
<b>9</b>		39.39	35.79	42.99	38.94	40.94	<b>39.61</b>	3.38	3.82
<b>10</b>		34.20	30.40	38.01	31.33	37.80	<b>34.35</b>	3.66	3.95
<b>11</b>		38.20	34.86	41.54	34.78	42.01	<b>38.28</b>	3.73	3.49
<b>12</b>		41.59	41.14	42.04	40.05	44.93	<b>41.95</b>	2.98	1.90
<b>13</b>		34.31	31.43	37.19	31.24	34.76	<b>33.79</b>	3.40	2.55
<b>14</b>		38.88	35.47	42.30	38.58	41.76	<b>39.40</b>	2.90	3.93
<b>15</b>		44.54	43.00	46.09	43.73	47.96	<b>45.06</b>	2.89	2.07

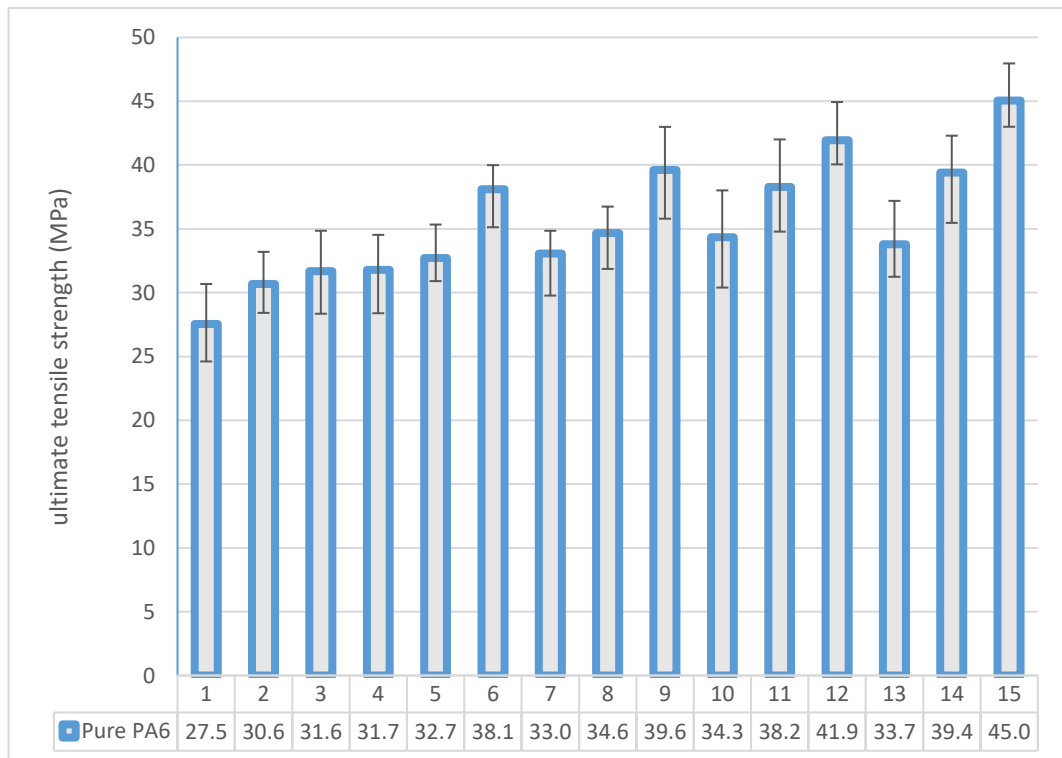


Figure 4.16: PurePA6 Specimens Tensile Test Results

Table 4.3: PA6CF10 Specimens Tensile Test Results

<i>Parameters</i>	<i>Unit</i>	<i>Specimens</i>							
		1	2	3	4	5	Avr.	Max.	Min.
<b>1</b>	MPa	35.03	31.30	38.77	35.00	37.44	<b>35.51</b>	3.26	4.21
<b>2</b>		36.50	32.96	40.04	35.67	40.23	<b>37.08</b>	3.15	4.12
<b>3</b>		37.95	34.04	41.86	36.41	41.49	<b>38.35</b>	3.51	4.31
<b>4</b>		36.29	33.70	38.89	32.66	36.46	<b>35.60</b>	3.29	2.94
<b>5</b>		39.69	38.86	40.52	38.33	39.72	<b>39.42</b>	1.09	1.10
<b>6</b>		40.01	38.47	41.55	39.50	40.84	<b>40.07</b>	1.48	1.61
<b>7</b>		40.30	38.92	41.67	36.26	41.84	<b>39.80</b>	2.04	3.54
<b>8</b>		40.79	39.42	42.15	40.54	42.17	<b>41.01</b>	1.15	1.59
<b>9</b>		42.43	41.92	42.95	40.68	43.80	<b>42.35</b>	1.44	1.68
<b>10</b>		40.67	36.64	44.71	39.71	41.19	<b>40.58</b>	4.13	3.95
<b>11</b>		40.97	40.72	41.21	38.50	45.00	<b>41.28</b>	3.72	2.78
<b>12</b>		42.83	41.07	44.58	42.06	43.07	<b>42.72</b>	1.86	1.65
<b>13</b>		41.99	41.03	42.96	37.92	43.75	<b>41.53</b>	2.22	3.61
<b>14</b>		43.66	41.19	46.13	42.02	44.62	<b>43.52</b>	2.60	2.33
<b>15</b>		45.15	44.38	45.91	44.79	47.62	<b>45.57</b>	2.05	1.19

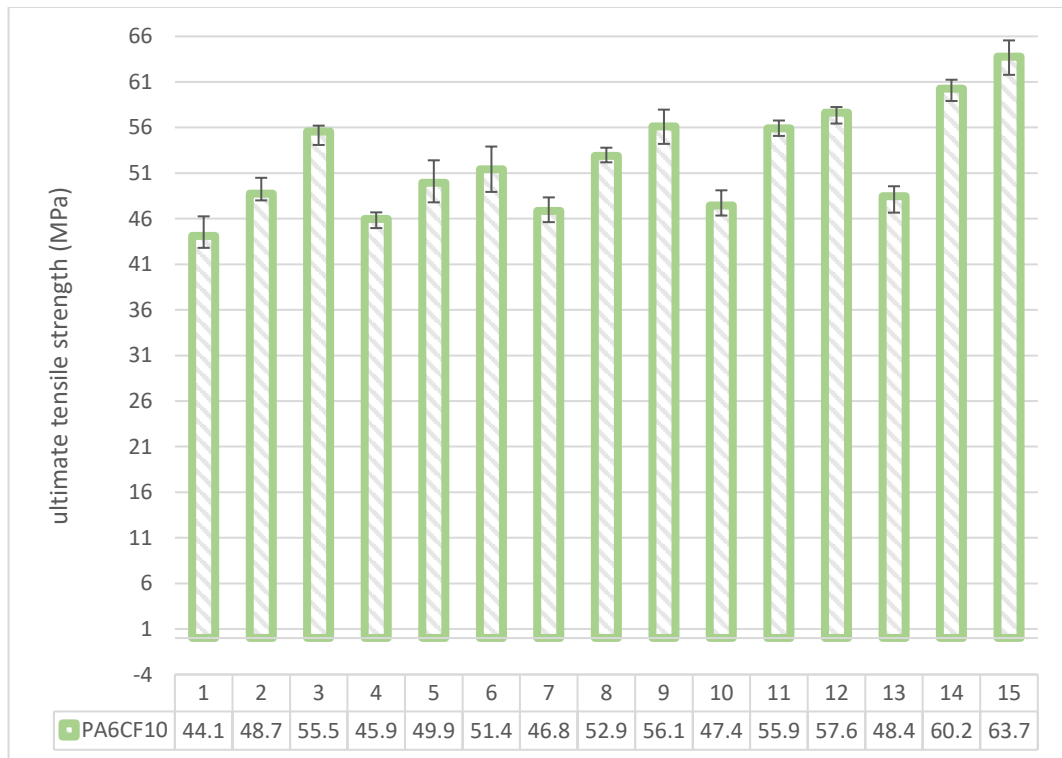


Figure 4.17: PA6CF10 Specimens Tensile Test Results

Table 4.4: PA6CF20 Specimens Tensile Test Results

<i>Parameters</i>	<i>Unit</i>	<i>Specimens</i>							
		1	2	3	4	5	Avr.	Max.	Min.
<i>1</i>	MPa	60.47	57.34	63.59	59.33	61.24	<b>60.39</b>	3.20	3.05
<i>2</i>		62.97	60.49	64.46	59.94	64.10	<b>62.39</b>	3.46	3.50
<i>3</i>		77.86	75.81	79.91	77.38	81.09	<b>78.41</b>	2.68	2.60
<i>4</i>		66.47	62.67	70.28	64.96	68.52	<b>66.58</b>	3.69	3.91
<i>5</i>		79.30	76.94	81.67	78.91	83.10	<b>79.98</b>	3.12	3.05
<i>6</i>		89.17	88.68	89.65	87.94	91.53	<b>89.39</b>	2.14	1.45
<i>7</i>		69.47	67.96	70.98	66.97	69.96	<b>69.07</b>	1.91	2.10
<i>8</i>		87.61	87.22	88.00	83.71	89.12	<b>87.13</b>	1.99	3.43
<i>9</i>		110.67	109.45	111.90	108.90	111.06	<b>110.40</b>	1:50	1.49
<i>10</i>		70.37	67.86	72.87	67.38	71.59	<b>70.01</b>	2.86	2.64
<i>11</i>		92.48	88.57	96.39	89.57	94.99	<b>92.40</b>	3.99	3.83
<i>12</i>		120.16	118.39	121.93	119.40	124.07	<b>120.79</b>	3.28	2.40
<i>13</i>		82.72	79.73	85.71	81.86	84.49	<b>82.90</b>	2.81	3.17
<i>14</i>		95.93	93.02	98.84	92.45	98.92	<b>95.83</b>	3.09	3.39
<i>15</i>		125.29	124.53	126.06	122.38	128.20	<b>125.29</b>	2.91	2.91

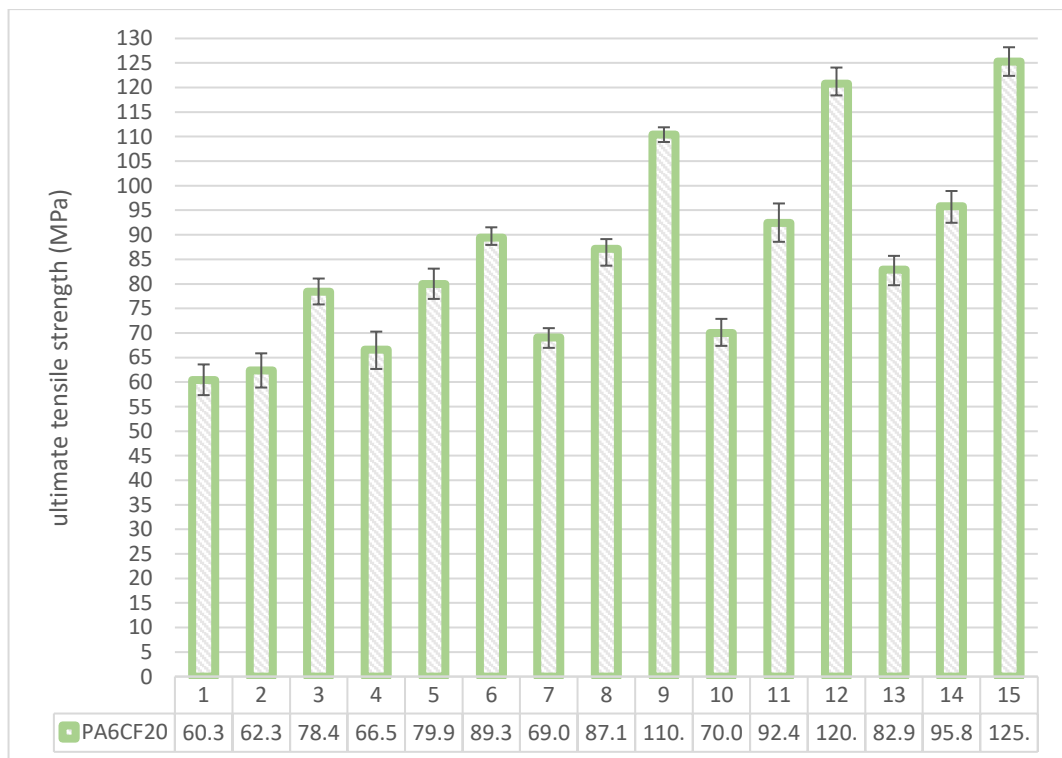


Figure 4.18: PA6CF20 Specimens Tensile Test Results



Table 4.5: PA6GF10 Specimens Tensile Test Results

<i>Parameters</i>	<i>Unit</i>	<i>Specimens</i>							
		1	2	3	4	5	Avr.	Max.	Min.
<b>1</b>	MPa	35.03	31.30	38.77	35.00	37.44	<b>35.51</b>	3.26	4.21
<b>2</b>		36.50	32.96	40.04	35.67	40.23	<b>37.08</b>	3.15	4.12
<b>3</b>		37.95	34.04	41.86	36.41	41.49	<b>38.35</b>	3.51	4.31
<b>4</b>		36.29	33.70	38.89	32.66	36.46	<b>35.60</b>	3.29	2.94
<b>5</b>		39.69	38.86	40.52	38.33	39.72	<b>39.42</b>	1.09	1.10
<b>6</b>		40.01	38.47	41.55	39.50	40.84	<b>40.07</b>	1.48	1.61
<b>7</b>		40.30	38.92	41.67	36.26	41.84	<b>39.80</b>	2.04	3.54
<b>8</b>		40.79	39.42	42.15	40.54	42.17	<b>41.01</b>	1.15	1.59
<b>9</b>		42.43	41.92	42.95	40.68	43.80	<b>42.35</b>	1.44	1.68
<b>10</b>		40.67	36.64	44.71	39.71	41.19	<b>40.58</b>	4.13	3.95
<b>11</b>		40.97	40.72	41.21	38.50	45.00	<b>41.28</b>	3.72	2.78
<b>12</b>		42.83	41.07	44.58	42.06	43.07	<b>42.72</b>	1.86	1.65
<b>13</b>		41.99	41.03	42.96	37.92	43.75	<b>41.53</b>	2.22	3.61
<b>14</b>		43.66	41.19	46.13	42.02	44.62	<b>43.52</b>	2.60	2.33
<b>15</b>		45.15	44.38	45.91	44.79	47.62	<b>45.57</b>	2.05	1.19

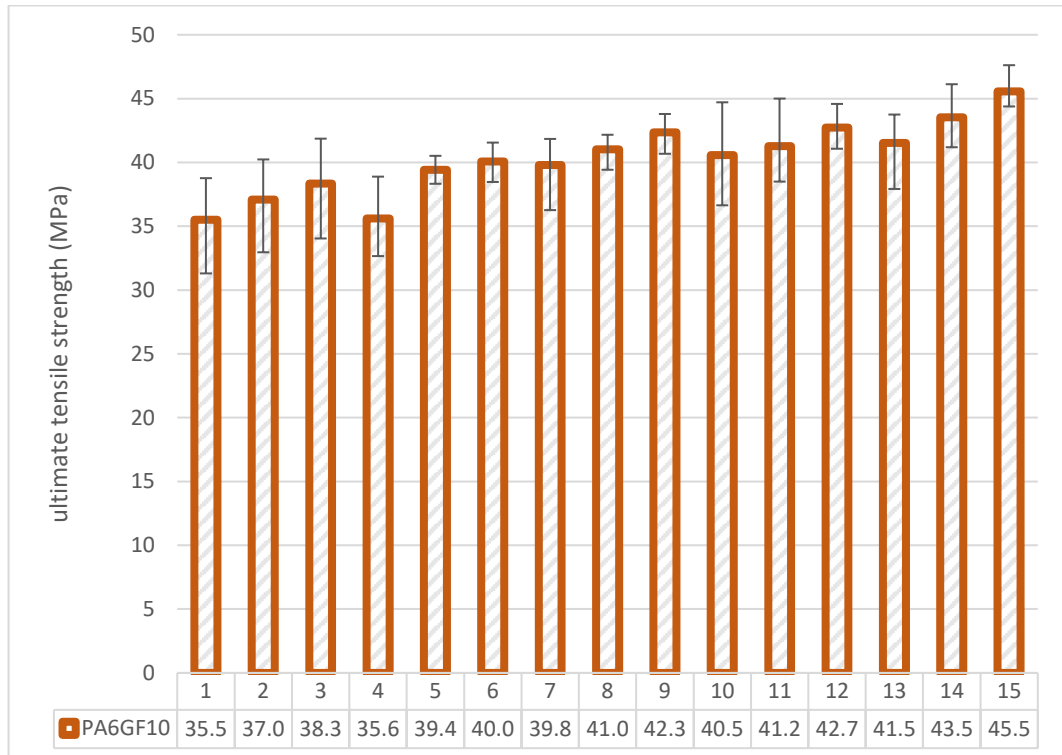


Figure 4.19: PA6GF10 Specimens Tensile Test Results

Table 4.6: PA6GF20 Specimens Tensile Test Results

<i>Parameters</i>	<i>Unit</i>	<i>Specimens</i>							
		1	2	3	4	5	Avr.	Mak.	Min.
<b>1</b>	MPa	49.79	49.41	50.16	49.47	50.97	<b>49.96</b>	1.01	0.55
<b>2</b>		54.25	54.21	54.29	51.80	54.63	<b>53.84</b>	0.79	2.04
<b>3</b>		56.44	54.74	58.15	54.85	56.48	<b>56.13</b>	2.02	1.40
<b>4</b>		50.99	50.67	51.30	49.26	52.69	<b>50.98</b>	1.71	1.72
<b>5</b>		57.09	54.64	59.54	54.68	57.40	<b>56.67</b>	2.87	2.03
<b>6</b>		59.18	57.59	60.78	57.50	61.64	<b>59.34</b>	2.30	1.83
<b>7</b>		51.36	49.64	53.09	50.82	52.95	<b>51.57</b>	1.52	1.93
<b>8</b>		57.45	55.04	59.86	56.96	59.18	<b>57.70</b>	2.16	2.66
<b>9</b>		61.19	59.51	62.87	60.30	63.60	<b>61.50</b>	2.11	1.98
<b>10</b>		52.30	51.76	52.85	51.18	53.98	<b>52.41</b>	1.57	1.24
<b>11</b>		58.90	58.41	59.39	57.19	59.45	<b>58.67</b>	0.78	1.48
<b>12</b>		64.16	63.26	65.06	61.74	64.65	<b>63.77</b>	1.28	2.03
<b>13</b>		59.34	58.22	60.47	59.06	60.24	<b>59.47</b>	1.00	1.25
<b>14</b>		60.39	58.68	62.10	58.90	61.52	<b>60.32</b>	1.78	1.64
<b>15</b>		64.88	62.47	67.30	64.36	66.59	<b>65.12</b>	2.18	2.65

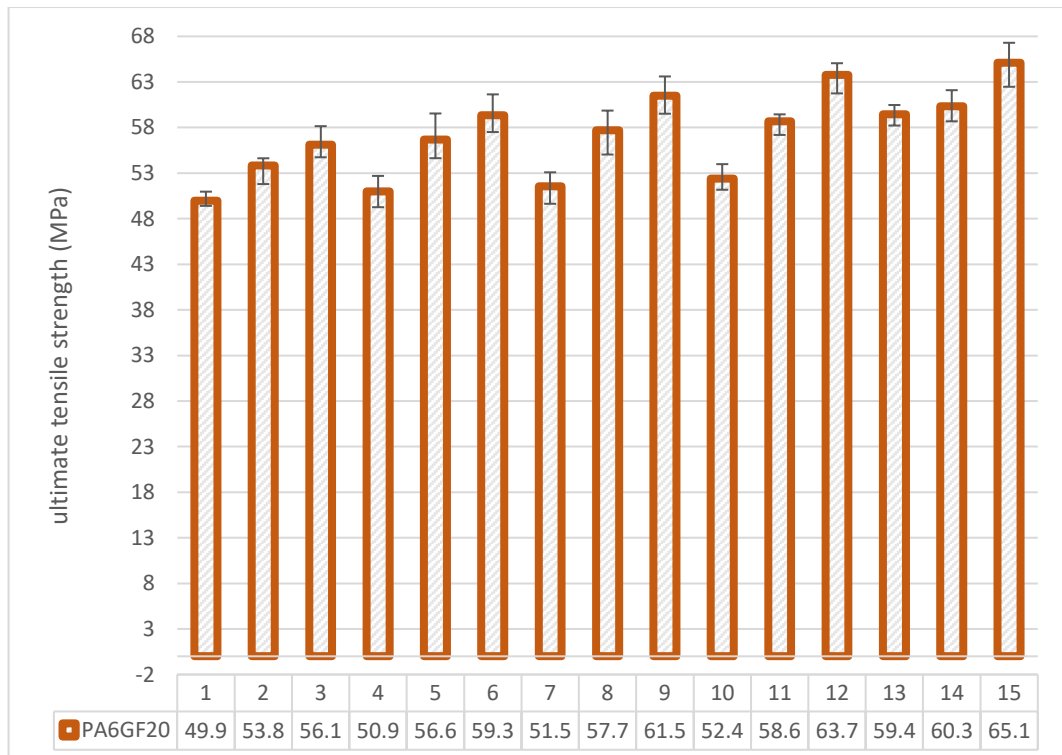


Figure 4.20: PA6GF20 Specimens Tensile Test Results

Table 4.7: PA6HF10 Specimens Tensile Test Results

<i>Parameters</i>	<i>Unit</i>	<i>Specimens</i>							
		1	2	3	4	5	Avr.	Mak.	Min.
<b>1</b>	MPa	35.69	33.56	37.81	33.09	38.89	<b>35.81</b>	3.08	2.71
<b>2</b>		46.07	45.49	46.64	43.58	46.99	<b>45.75</b>	1.23	2.18
<b>3</b>		47.48	46.82	48.13	45.83	48.06	<b>47.27</b>	0.87	1.43
<b>4</b>		39.05	39.02	39.09	37.68	42.96	<b>39.56</b>	3.40	1.88
<b>5</b>		47.78	46.14	49.43	45.91	50.27	<b>47.91</b>	2.37	2.00
<b>6</b>		50.75	48.98	52.52	48.84	51.02	<b>50.42</b>	2.10	1.58
<b>7</b>		44.61	40.98	48.24	44.36	46.38	<b>44.91</b>	3.33	3.94
<b>8</b>		50.06	48.05	52.08	48.38	53.70	<b>50.45</b>	3.24	2.41
<b>9</b>		52.12	50.20	54.03	49.81	54.13	<b>52.06</b>	2.07	2.25
<b>10</b>		47.32	47.07	47.57	45.67	49.24	<b>47.37</b>	1.86	1.71
<b>11</b>		52.23	50.54	53.91	50.62	52.48	<b>51.95</b>	1.95	1.41
<b>12</b>		55.01	52.71	57.32	51.96	56.70	<b>54.74</b>	2.58	2.78
<b>13</b>		48.01	46.36	49.66	44.89	50.32	<b>47.85</b>	2.47	2.96
<b>14</b>		53.60	51.99	55.21	50.12	55.25	<b>53.23</b>	2.02	3.12
<b>15</b>		59.06	56.01	62.11	58.06	60.66	<b>59.18</b>	2.93	3.17

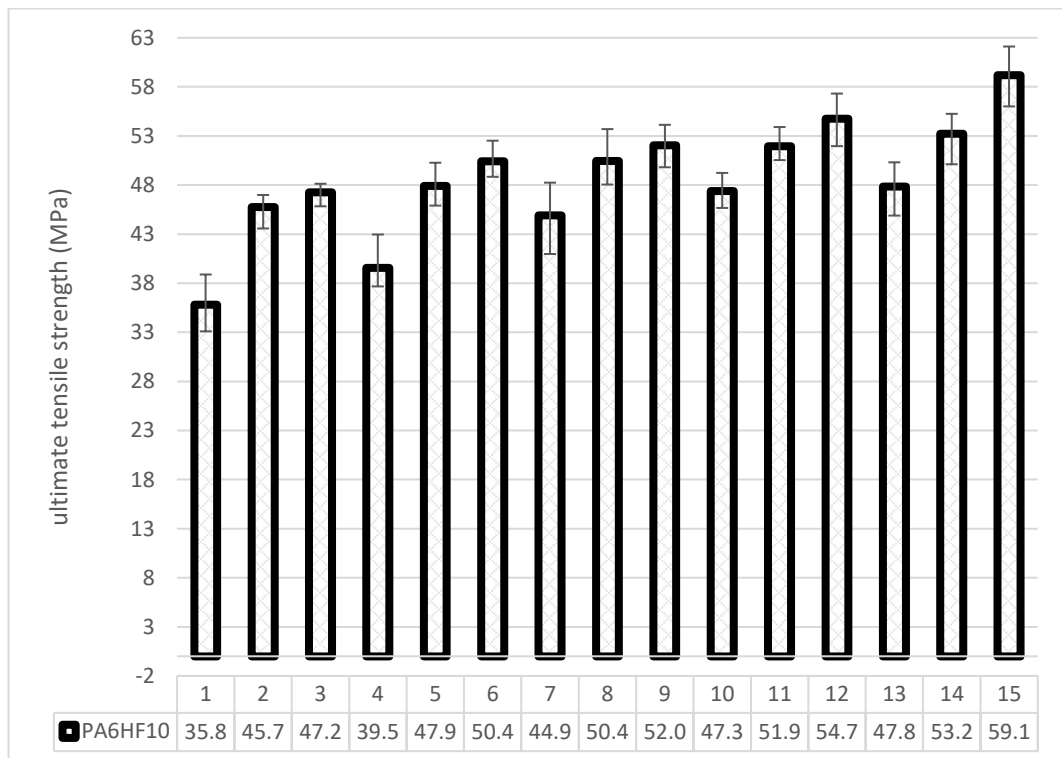


Figure 4.21: PA6HF10 Specimens Tensile Test Results

Table 4.8: PA6HF20 Specimens Tensile Test Results

<i>Parameters</i>	<i>Unit</i>	<i>Specimens</i>							
		1	2	3	4	5	Avr.	Max.	Min.
<b>1</b>	MPa	52.74	49.38	56.11	48.94	53.66	<b>52.17</b>	3.94	3.23
<b>2</b>		59.09	55.86	62.32	56.72	62.45	<b>59.29</b>	3.17	3.43
<b>3</b>		77.60	74.43	80.76	73.65	81.08	<b>77.50</b>	3.58	3.85
<b>4</b>		63.75	62.62	64.88	63.50	66.91	<b>64.33</b>	2.58	1.71
<b>5</b>		67.84	64.81	70.88	66.38	68.98	<b>67.78</b>	3.10	2.96
<b>6</b>		77.89	73.94	81.84	77.12	80.92	<b>78.34</b>	3.49	4.40
<b>7</b>		65.48	65.23	65.73	62.96	69.43	<b>65.77</b>	3.66	2.81
<b>8</b>		75.85	74.38	77.31	74.37	76.10	<b>75.60</b>	1.71	1.23
<b>9</b>		96.99	96.22	97.76	93.56	98.45	<b>96.60</b>	1.86	3.03
<b>10</b>		68.95	66.42	71.47	67.84	69.72	<b>68.88</b>	2.59	2.46
<b>11</b>		76.22	74.75	77.70	72.28	78.75	<b>75.94</b>	2.81	3.66
<b>12</b>		100.18	96.76	103.60	99.52	101.66	<b>100.34</b>	3.26	3.59
<b>13</b>		72.15	71.05	73.25	70.03	75.57	<b>72.41</b>	3.16	2.38
<b>14</b>		90.03	86.08	93.98	88.80	91.13	<b>90.00</b>	3.97	3.92
<b>15</b>		106.10	105.44	106.76	105.12	110.05	<b>106.69</b>	3.35	1.58

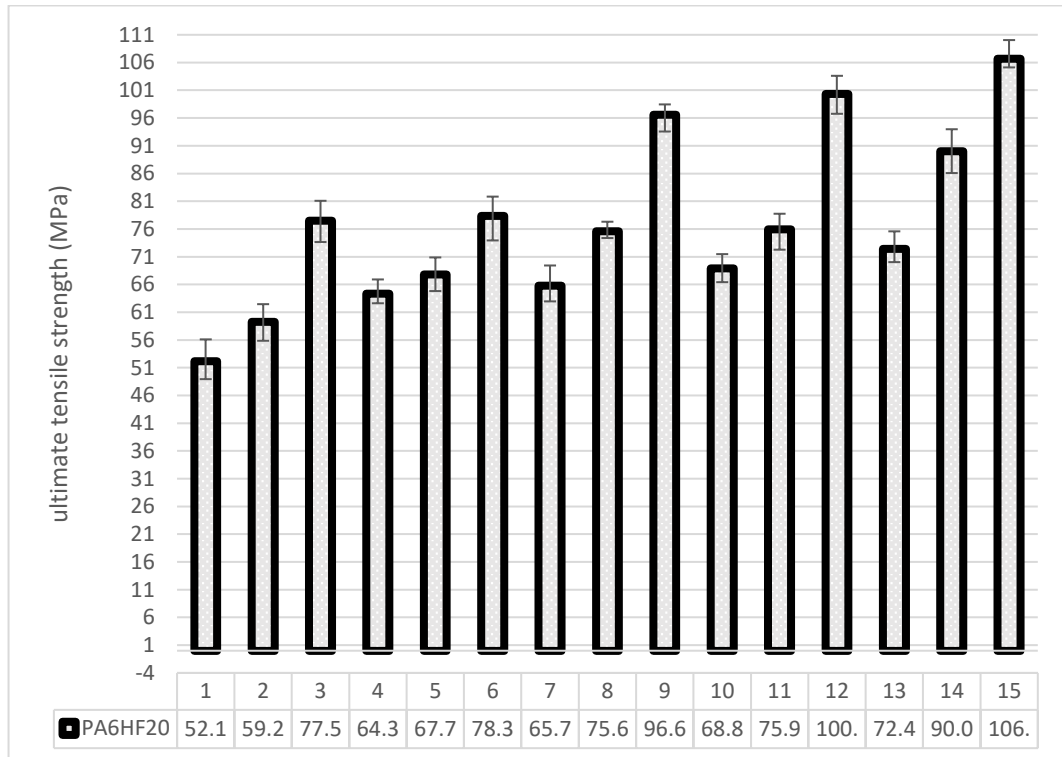
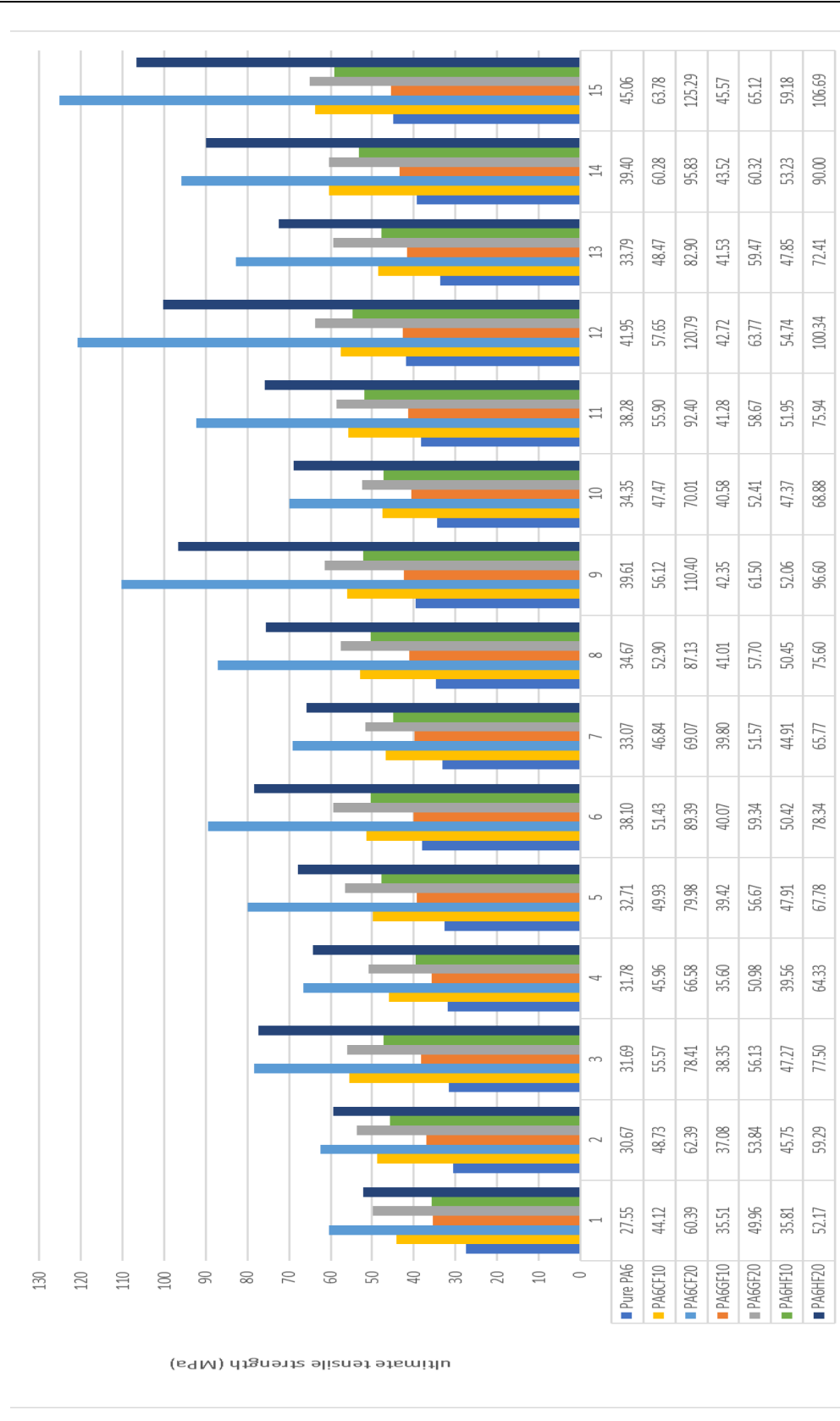


Figure 4.22: PA6HF20 Specimens Tensile Test Results

Table 4.9: Non-modified Specimens Tensile test results



The tensile tests at the second stage of the thesis study were also carried out according to the ASTM D638 standard. Tensile tests were performed on Instron 5966 device with a 10 kN load sensor. Tensile test specimens with 3 different layer thicknesses were produced at the nozzle temperature at which the highest tensile strength was obtained at the first stage. The tests of the specimens produced in parameters 13, 14, and 15 were carried out.

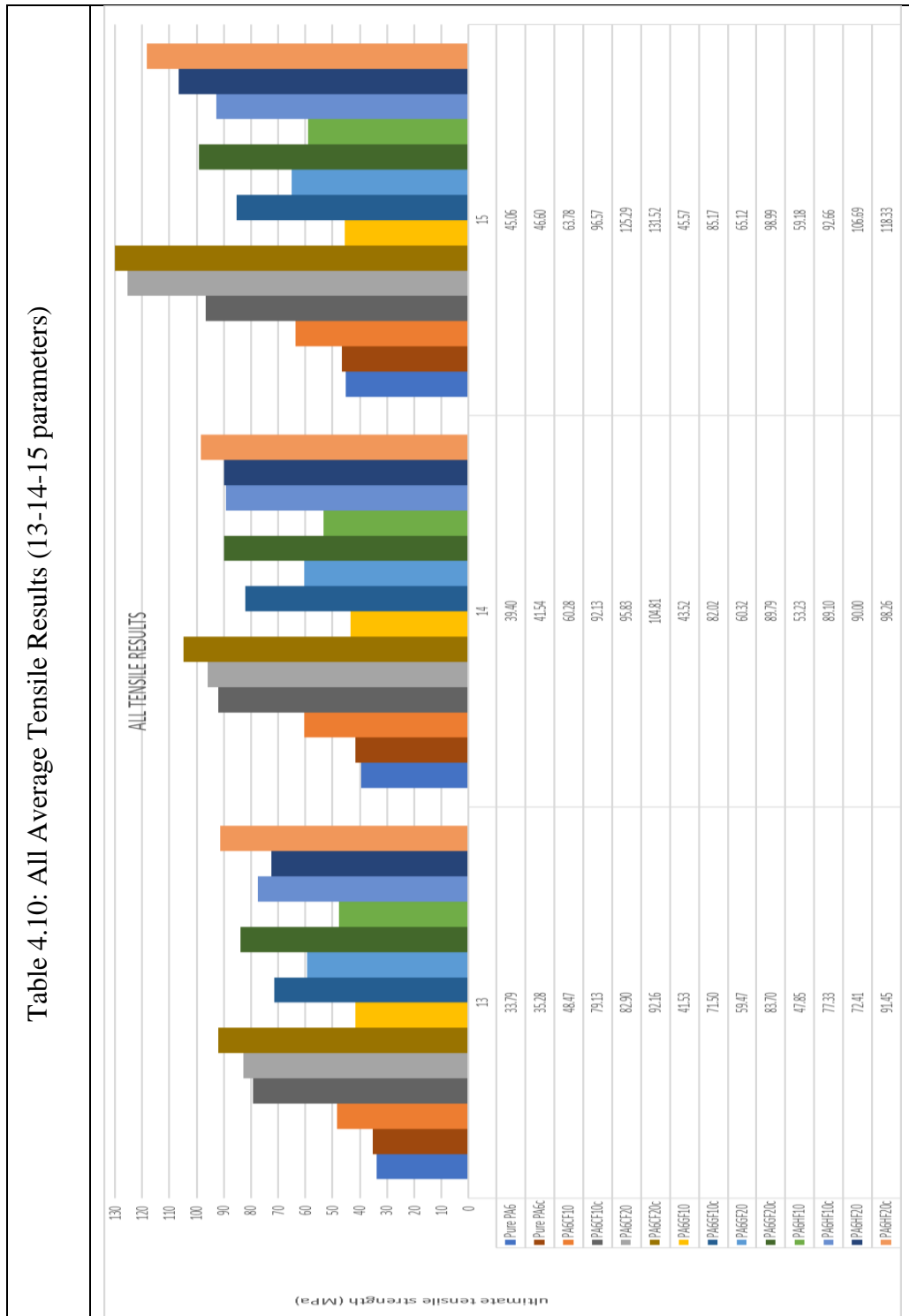


Table 4.11: PA6CF10c Specimens Tensile Test Results

<i>Parameters</i>	<i>Unit</i>	<i>Specimens</i>							
		1	2	3	4	5	Avr.	Max.	Min.
<b>13</b>	MPa	79.71	78.65	78.15	80.00	79.13	<b>79.13</b>	0.87	0.98
<b>14</b>		91.00	93.78	92.10	91.62	92.13	<b>92.13</b>	1.65	1.12
<b>15</b>		96.04	95.81	97.94	96.47	96.57	<b>96.57</b>	1.38	0.76

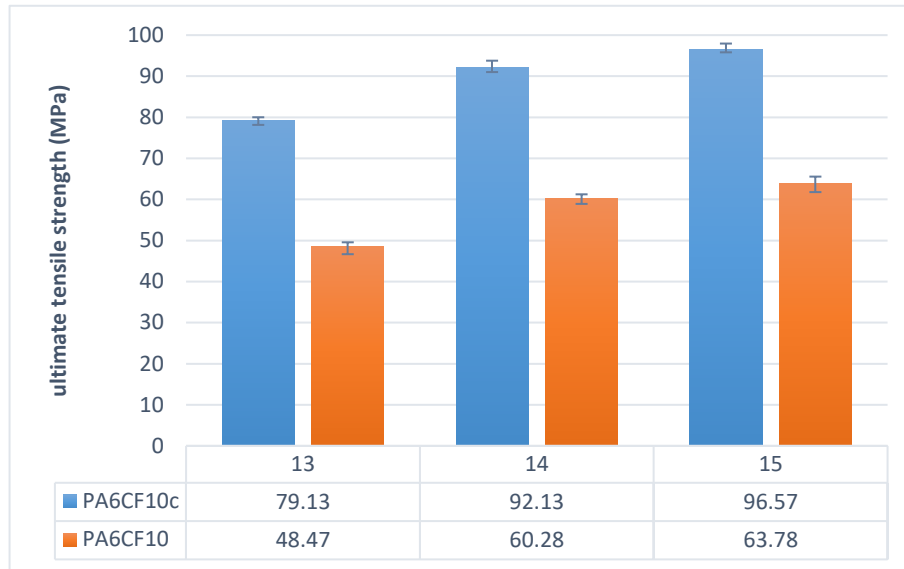


Figure 4.23: PA6CF10c and PA6CF10 Specimens Tensile Test Results

Table 4.12: PA6CF20c Specimens Tensile Test Results

<i>Parameters</i>	<i>Unit</i>	<i>Specimens</i>							
		1	2	3	4	5	Avr.	Max.	Min.
<b>13</b>	MPa	91.96	92.28	92.41	91.99	92.16	<b>92.16</b>	0.25	0.20
<b>14</b>		104.02	104.77	105.23	105.21	104.81	<b>104.81</b>	0.42	0.79
<b>15</b>		132.31	131.03	131.99	130.74	131.52	<b>131.52</b>	0.79	0.77

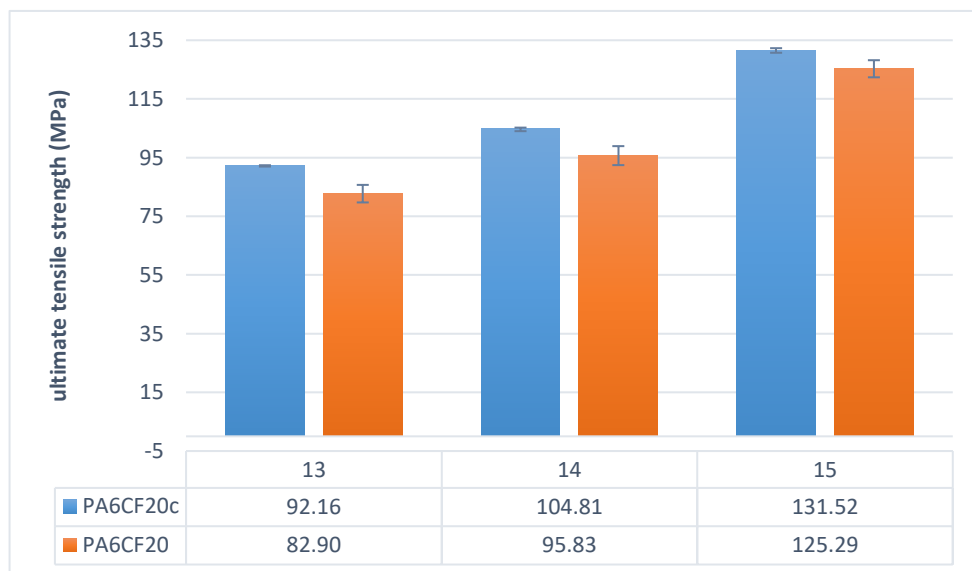


Figure 4.24: PA6CF20c and PA6CF20 Specimens Tensile Test Results

Table 4.13: PA6GF10c Specimens Tensile Test Results

Parameters	Unit	Specimens							
		1	2	3	4	5	Avr.	Max.	Min.
13	MPa	71.86	72.42	70.83	70.87	71.50	<b>71.50</b>	0.92	0.66
14		83.74	80.70	82.68	80.95	82.02	<b>82.02</b>	1.72	1.31
15		85.35	85.27	85.22	84.84	85.17	<b>85.17</b>	0.18	0.33

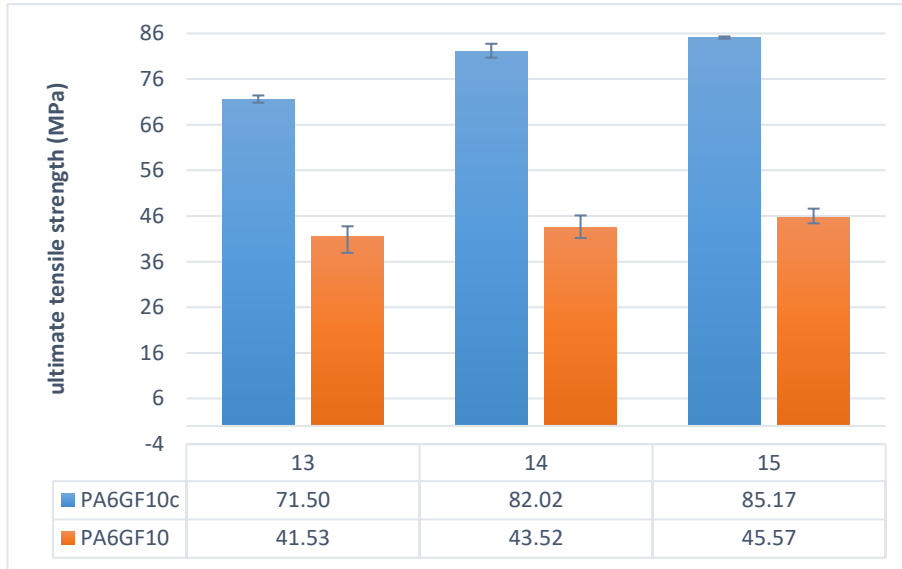


Figure 4.25: PA6GF10c and PA6GF10 Specimens Tensile Test Results

Table 4.14: PA6GF20c Specimens Tensile Test Results

Parameters	Unit	Specimens							
		1	2	3	4	5	Avr.	Max.	Min.
13	MPa	84.07	83.65	84.73	82.33	83.70	<b>83.70</b>	1.04	1.37
14		89.96	89.89	89.57	89.72	89.79	<b>89.79</b>	0.17	0.21
15		99.86	98.03	98.95	99.11	98.99	<b>98.99</b>	0.87	0.96

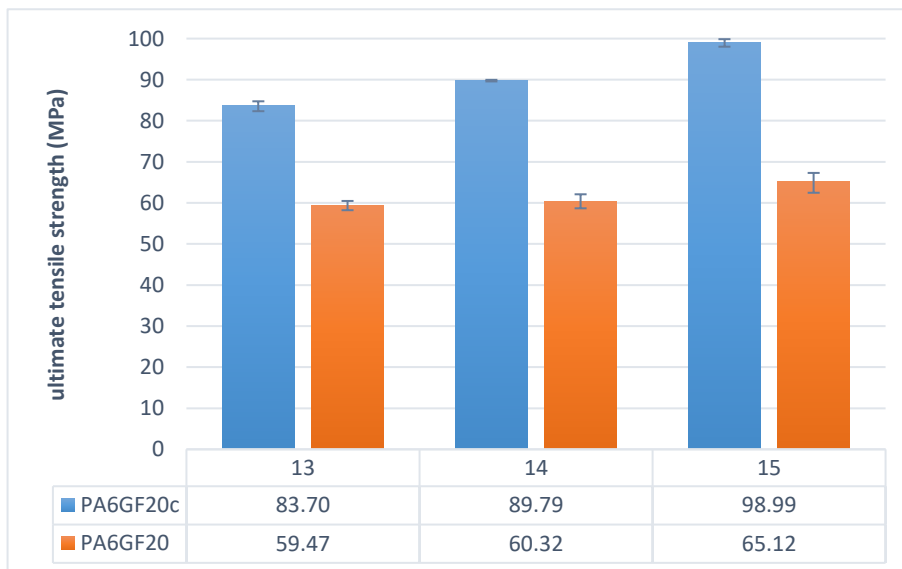


Figure 4.26: PA6GF20c and PA6GF20 Specimens Tensile Test Results



Table 4.15: PA6HF10c Specimens Tensile Test Results

Parameters	Unit	Specimens							
		1	2	3	4	5	Avr.	Max.	Min.
13	MPa	77.63	76.88	77.58	77.24	77.33	<b>77.33</b>	0.30	0.45
14		88.83	89.49	89.25	88.85	89.10	<b>89.10</b>	0.39	0.28
15		94.33	91.85	92.01	92.45	92.66	<b>92.66</b>	1.67	0.81

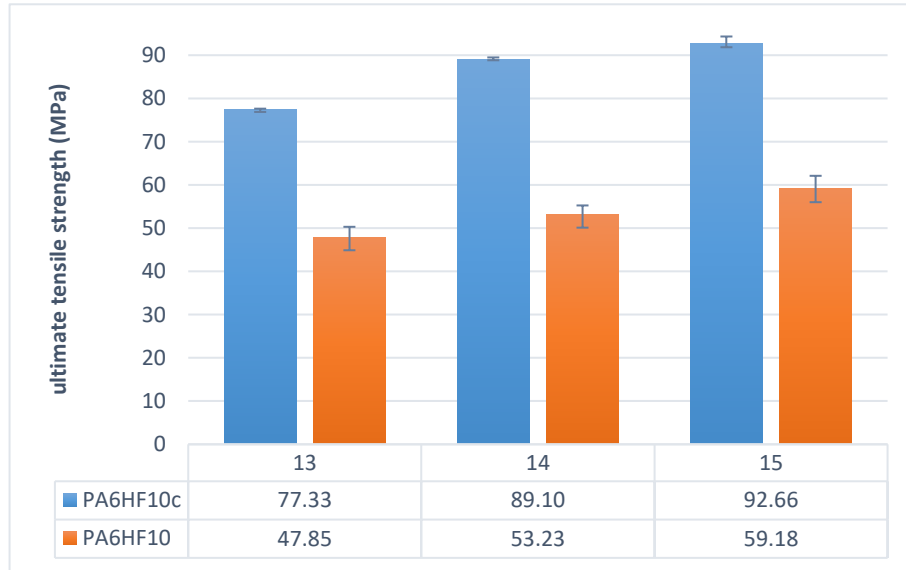


Figure 4.27: PA6HF10c and PA6HF10 Specimens Tensile Test Results

Table 4.16: PA6HF20c Specimens Tensile Test Results

Parameters	Unit	Specimens							
		1	2	3	4	5	Avr.	Max	min.
13	MPa	92.14	91.45	91.51	90.69	91.45	<b>91.45</b>	0.69	0.75
14		96.74	98.18	98.90	99.23	98.26	<b>98.26</b>	0.97	1.52
15		116.54	118.27	119.13	119.39	118.33	<b>118.33</b>	1.06	1.79

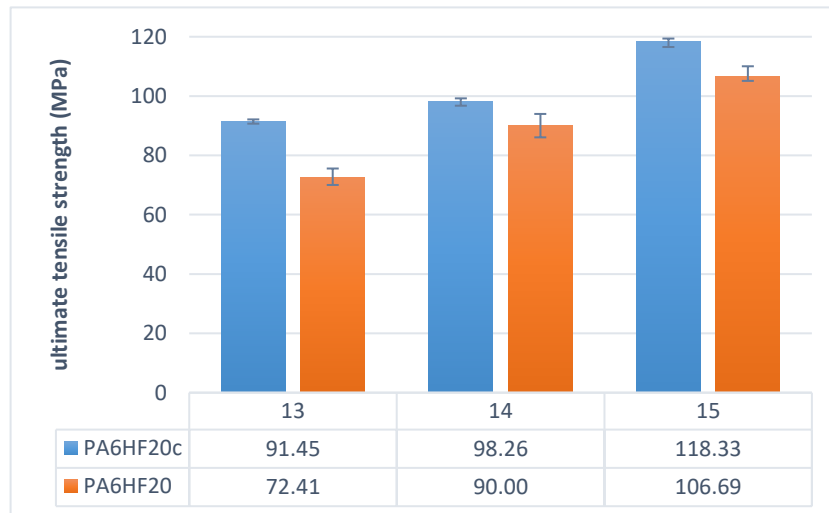


Figure 4.28: PA6HF20c and PA6HF20 Specimens Tensile Test Results

#### 4.1.2.2 Impact Test

Impact test on unnotched Charpy test specimens was performed according to ISO179 standard. The tests were carried out with the Instron model CEAST Resil Impactor device. Impact Charpy test specimens produced in two different infilled patterns were tested in parameter 15, where the highest tensile strength was obtained at the first stage.

Table 4.17: Non-modified Specimens Impact Charpy Test Results

Code	Infill Pattern	Units	Specimens					Avr.	Min.	Max.
			one	2	3	4	5			
<b>Pure PA6</b>	-/+45	kJ/m <sup>2</sup>	63.93	68.02	58.50	60.11	61.68	<b>62.45</b>	58.50	68.02
	0/90		54.55	53.47	50.88	48.60	48.10	<b>51.12</b>	48.10	54.55
<b>PA6CF10</b>	-/+45		30.12	30.83	27.56	27.79	28.77	<b>29.01</b>	27.56	30.83
	0/90		30.41	32.73	27.11	26.42	22.40	<b>27.81</b>	22.40	32.73
<b>PA6CF20</b>	-/+45		26.86	31.05	23.67	24.73	24.55	<b>26.17</b>	23.67	31.05
	0/90		26.90	25.18	23.30	23.55	25.03	<b>24.79</b>	23.30	26.90
<b>PA6GF10</b>	-/+45		48.60	49.71	44.34	43.42	50.77	<b>47.37</b>	43.42	50.77
	0/90		44.55	44.97	41.92	43.00	43.43	<b>43.57</b>	41.92	44.97
<b>PA6GF20</b>	-/+45		36.28	38.92	30.93	34.22	34.11	<b>34.89</b>	30.93	38.92
	0/90		32.89	34.33	31.31	30.74	30.57	<b>31.97</b>	30.57	34.33
<b>PA6HF10</b>	-/+45		37.81	42.11	34.51	35.40	33.41	<b>36.65</b>	33.41	42.11
	0/90		35.88	35.63	32.64	32.89	32.30	<b>33.87</b>	32.30	35.88
<b>PA6HF20</b>	-/+45		32.62	38.57	31.28	30.69	28.22	<b>32.28</b>	28.22	38.57
	0/90		31.35	31.14	27.98	28.46	27.91	<b>29.37</b>	27.91	31.35

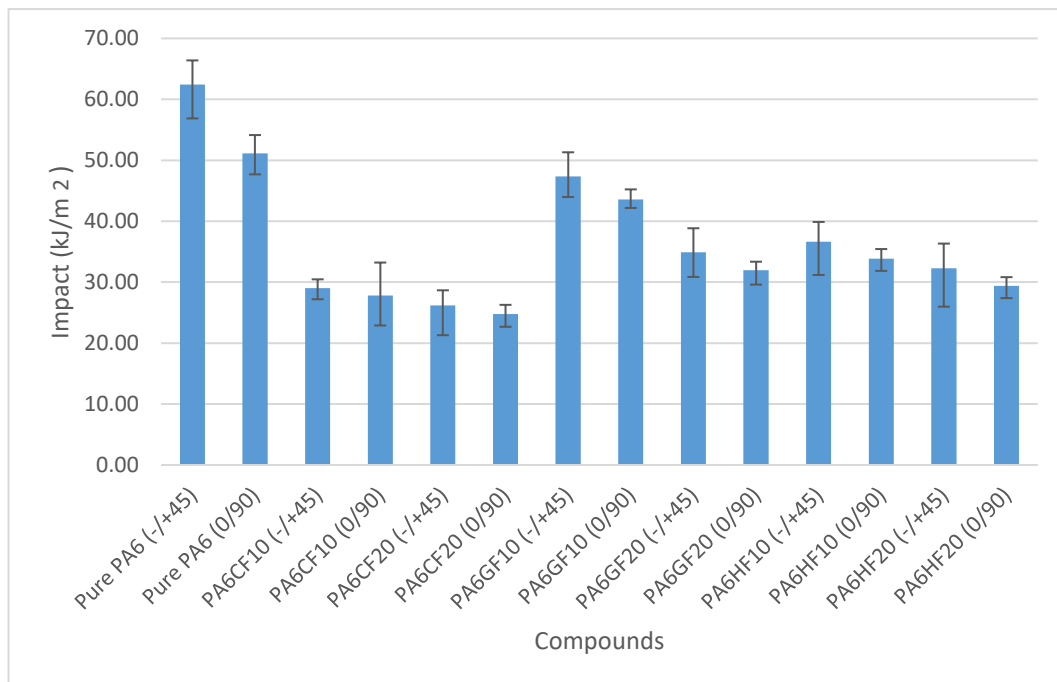


Figure 4.29: Non-modified Specimens Impact Charpy Test Results

Table 4.18: Modified Specimens Impact Charpy Test Results

Code	Infill Pattern	Units	Specimens					Avr.	Min.	Max.
			one	2	3	4	5			
PA6CF10c	-/+45	kJ/m2	32.45	34.20	29.88	28.91	29.40	<b>30.97</b>	28.91	34.20
	0/90		30.89	30.85	27.70	27.96	25.73	<b>28.63</b>	25.73	30.89
PA6CF20c	-/+45		27.82	29.65	25.67	26.21	26.03	<b>27.08</b>	25.67	29.65
	0/90		28.26	27.66	25.06	23.53	26.82	<b>26.26</b>	23.53	28.26
PA6GF10c	-/+45		51.99	50.45	47.75	48.00	53.52	<b>50.34</b>	47.75	53.52
	0/90		48.52	48.94	45.89	46.97	47.40	<b>47.54</b>	45.89	48.94
PA6GF20c	-/+45		40.29	42.11	35.86	38.75	37.71	<b>38.94</b>	35.86	42.11
	0/90		37.00	36.65	35.94	33.07	34.68	<b>35.47</b>	33.07	37.00
PA6HF10c	-/+45		41.70	43.67	37.68	37.51	37.30	<b>39.57</b>	37.30	43.67
	0/90		39.13	39.76	34.11	36.14	35.55	<b>36.94</b>	34.11	39.76
PA6HF20c	-/+45		36.19	40.68	34.85	34.26	32.61	<b>35.72</b>	32.61	40.68
	0/90		36.11	36.78	32.74	33.22	32.67	<b>34.30</b>	32.67	36.78

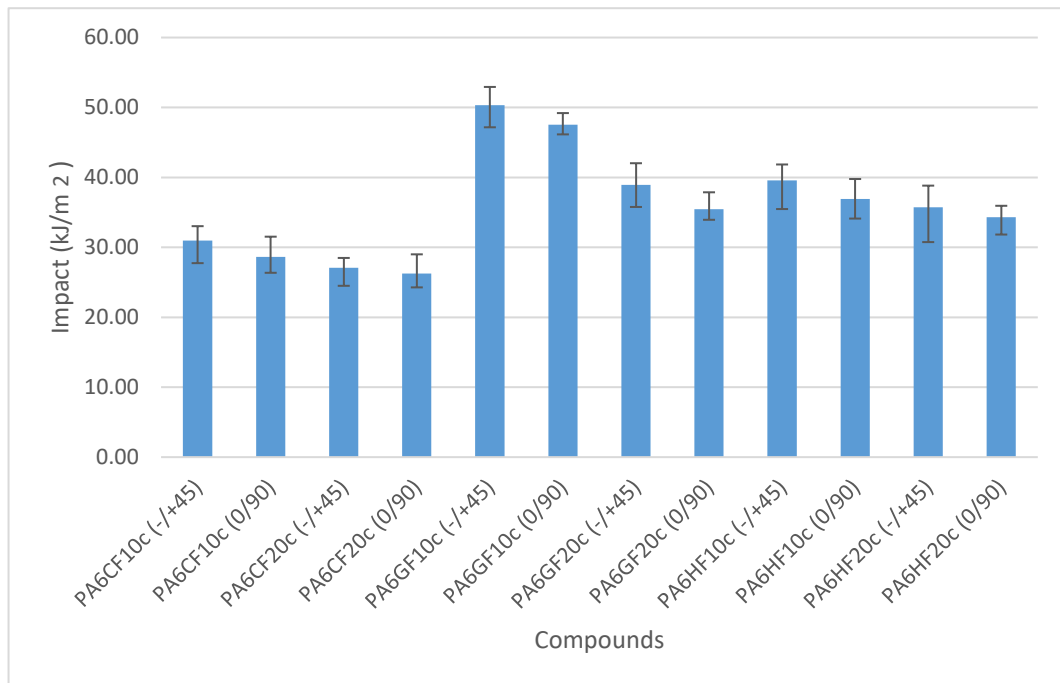


Figure 4.30: Modified Specimens Impact Charpy Test Results

#### 4.1.2.3 Compression Test

Compression tests according to ASTM D695 standards were performed in Instron 5966 device. All specimens were produced according to this standard and the specimens' dimensions were proper to ASTM D695. All composites were tested with compression force under 9000N and their properties about strain under compression were compared. All composites were produced with 13,14, and 15 parameters by AM.

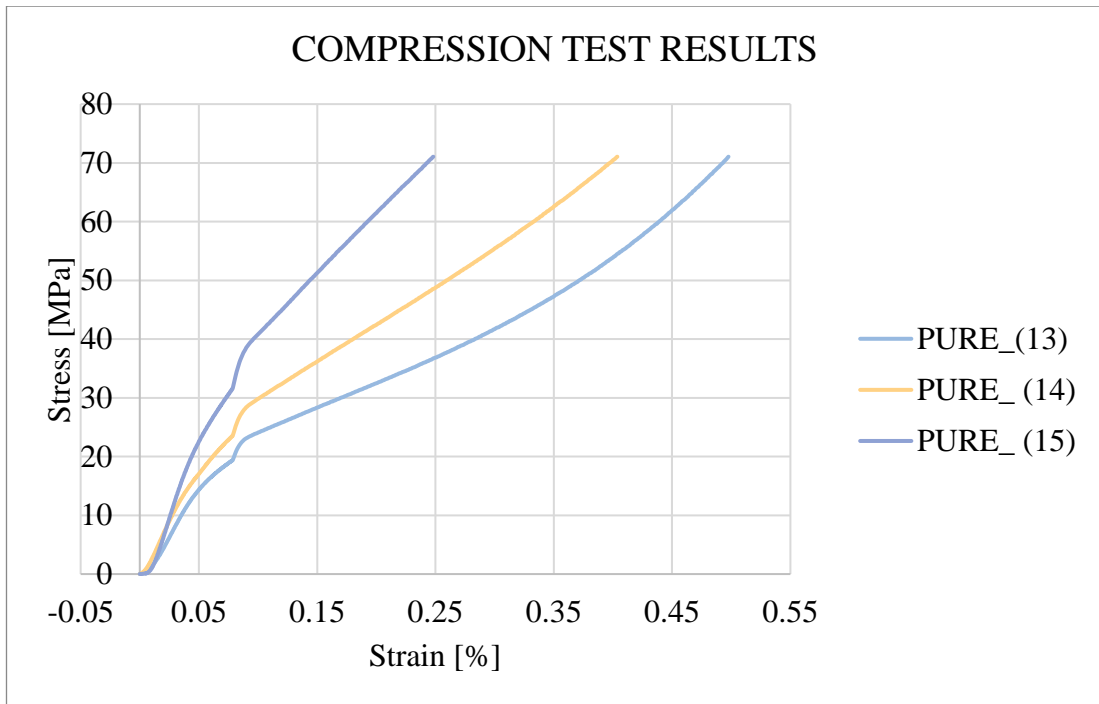


Figure 4.31: Pure PA6 Compression Test Results

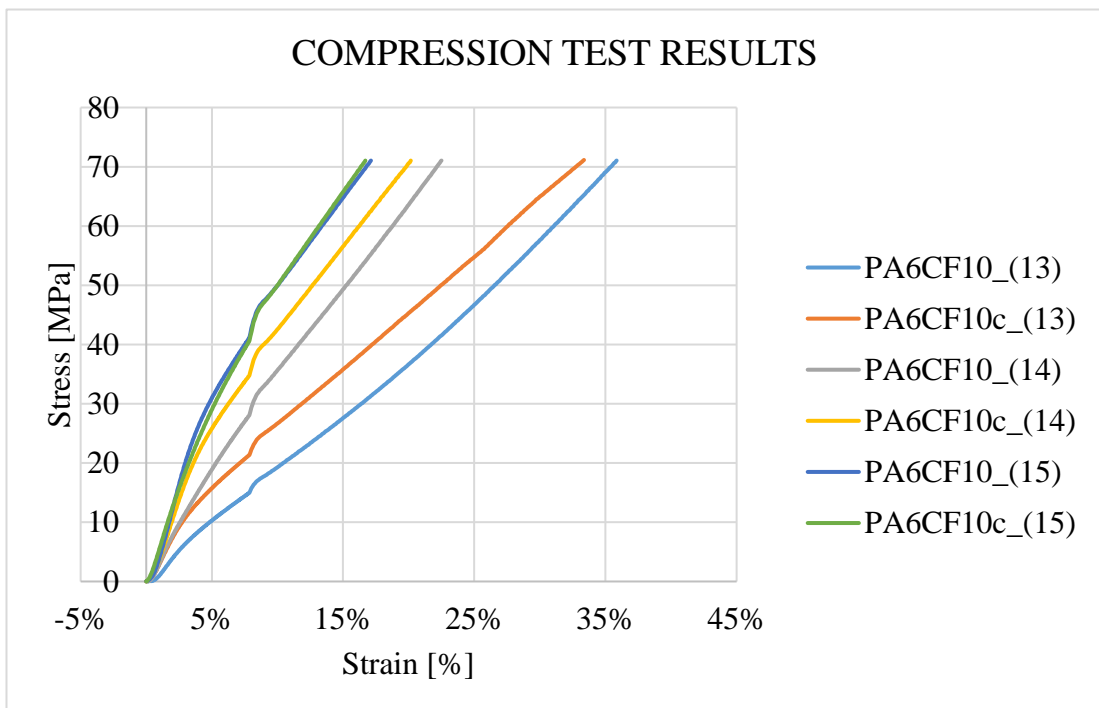


Figure 4.32: PA6 wt10% CF reinforcement Specimens Compression Test Results

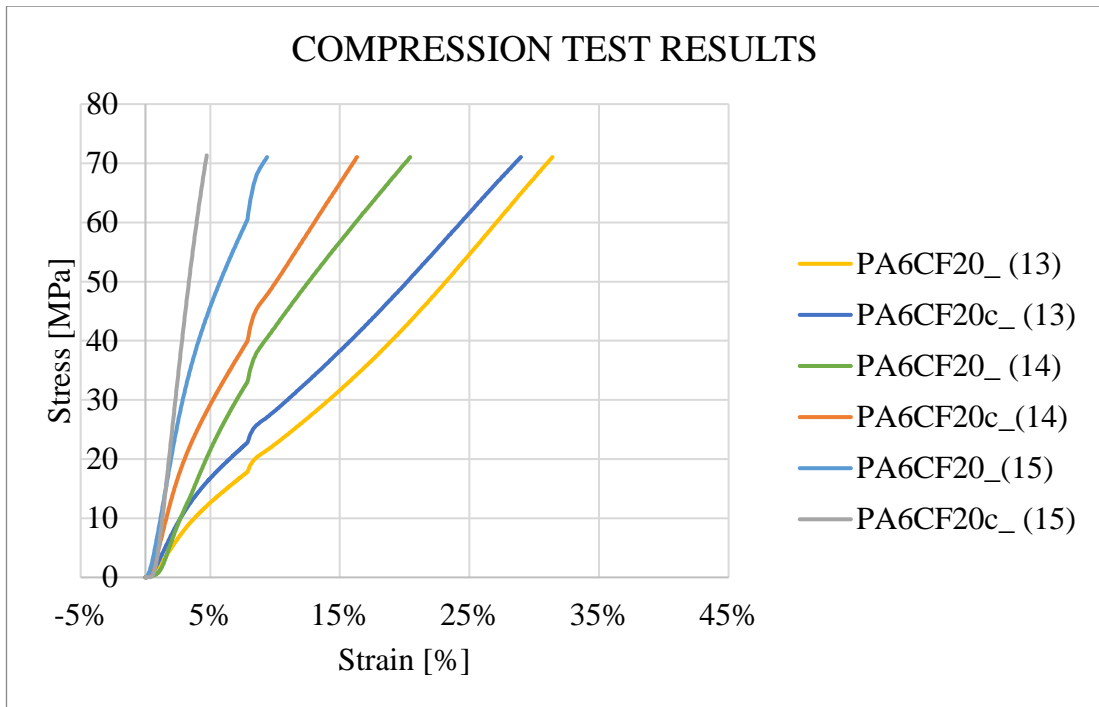


Figure 4.33: PA6 wt20% CF reinforcement Specimens Compression Test Results

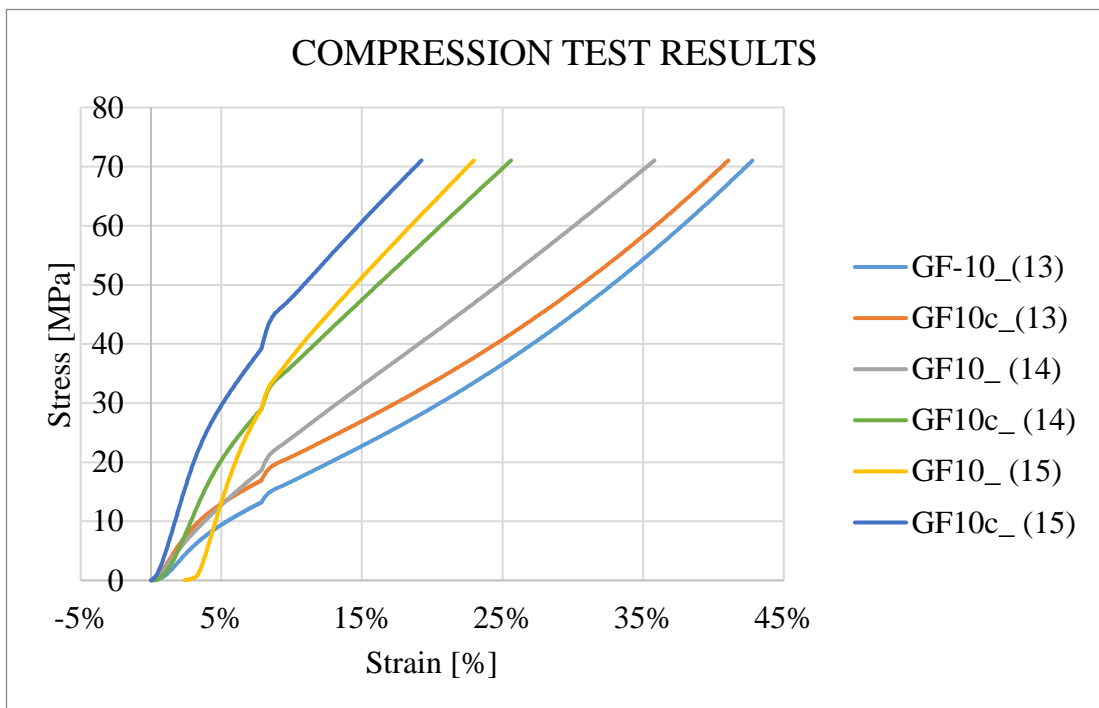


Figure 4.34: PA6 wt10% GF reinforcement Specimens Compression Test Results

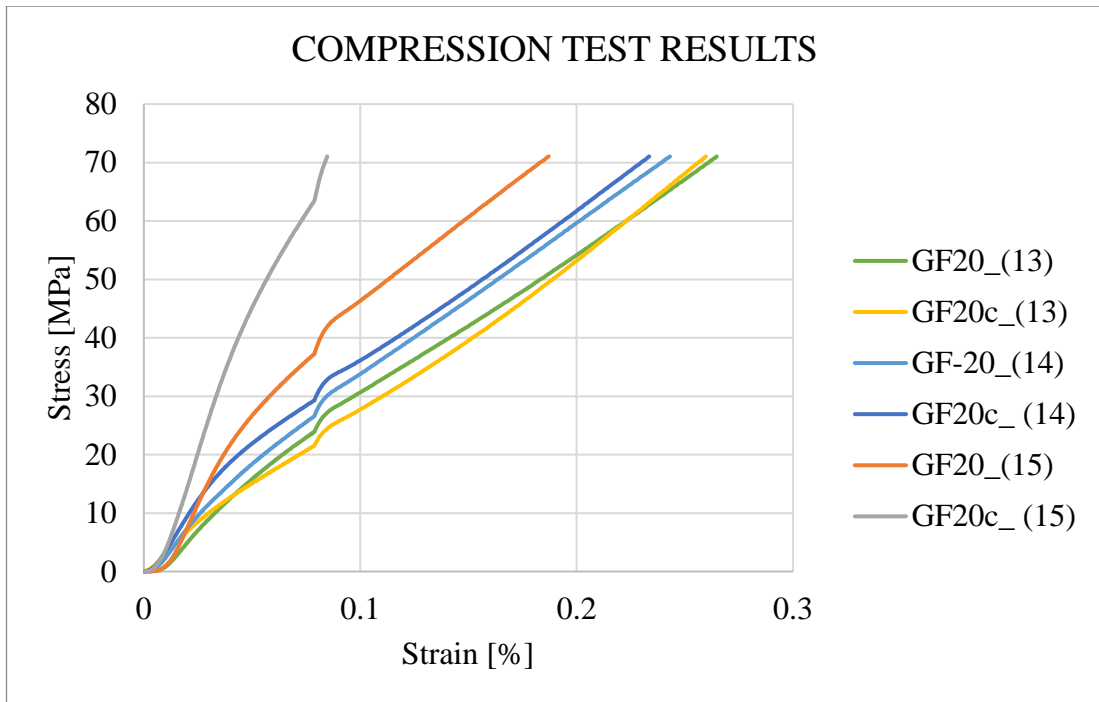


Figure 4.35: PA6 wt20% GF reinforcement Specimens Compression Test Results

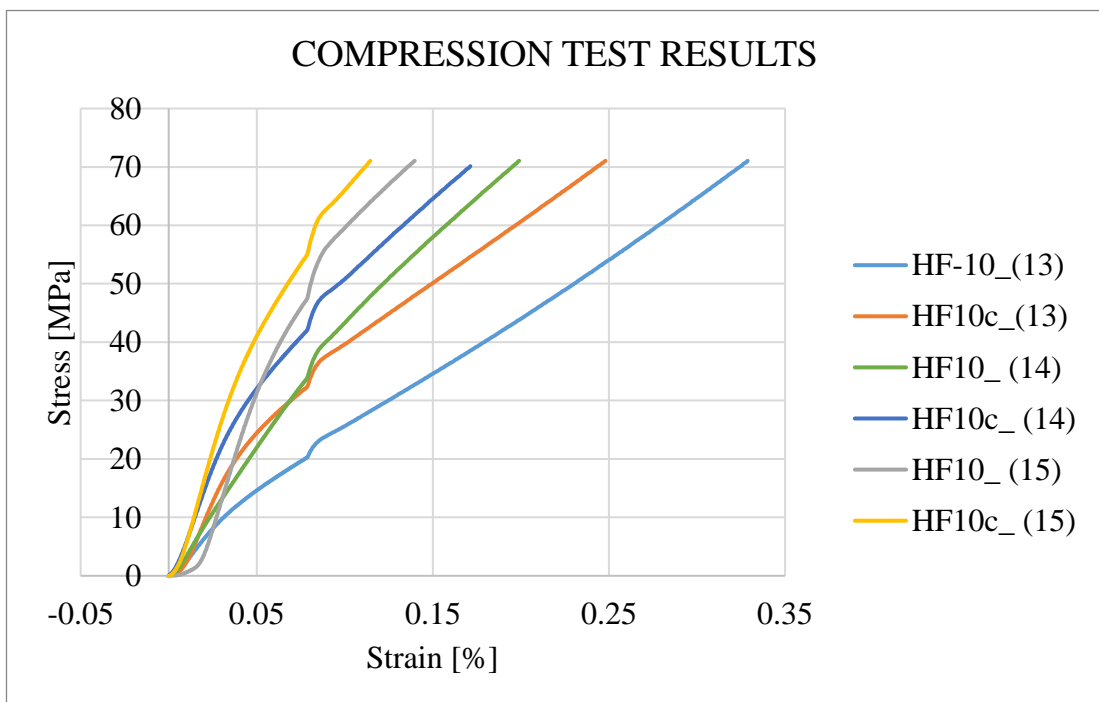


Figure 4.36: PA6 wt10% HF reinforcement Specimens Compression Test Results

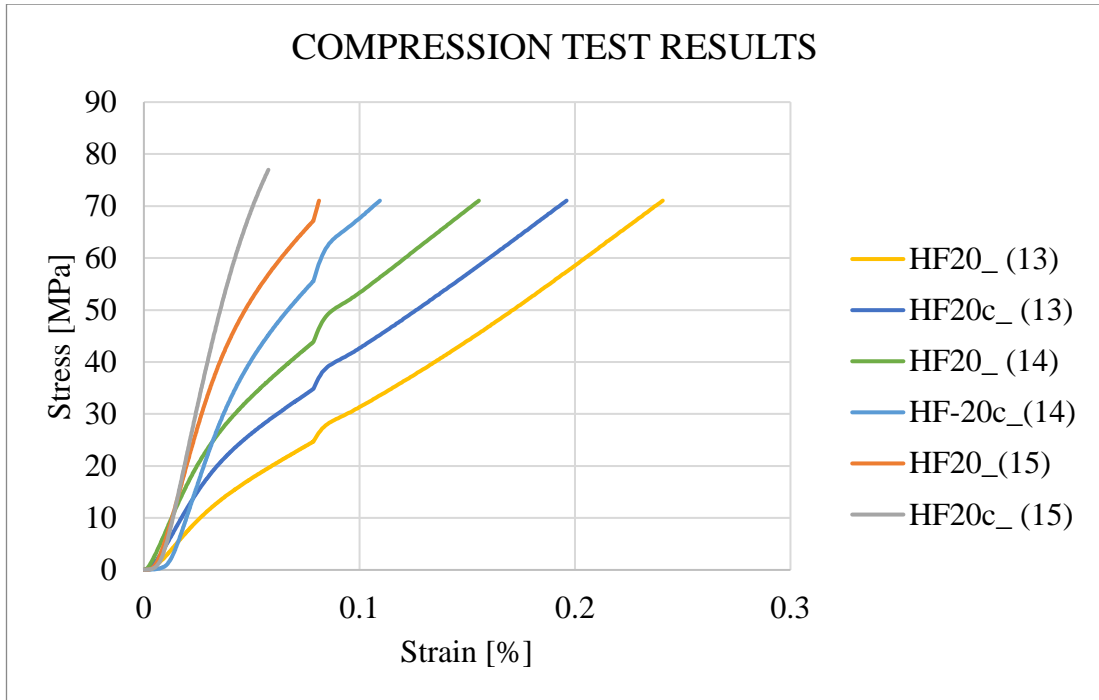


Figure 4.37: PA6 wt20% HF reinforcement Specimens Compression Test Results

The mechanical behavior of all specimens modified and unmodified with nanocellulose under compression testing was observed. The force values of the specimens produced in 3 different production parameters are converted to stress units and the displacement under force is given in the graphics as strains.

### 4.1.3 Morphology

Microstructure analyzes of the specimens non-modified with nanocellulose were performed with the SEM device at Dokuz Eylul University Izmir International Biomedicine and Genome Institute. Damaged surfaces formed after tensile tests at different magnifications under 1.5-3.0 kV EHT on the Zeiss Sigma500 SEM device were examined.

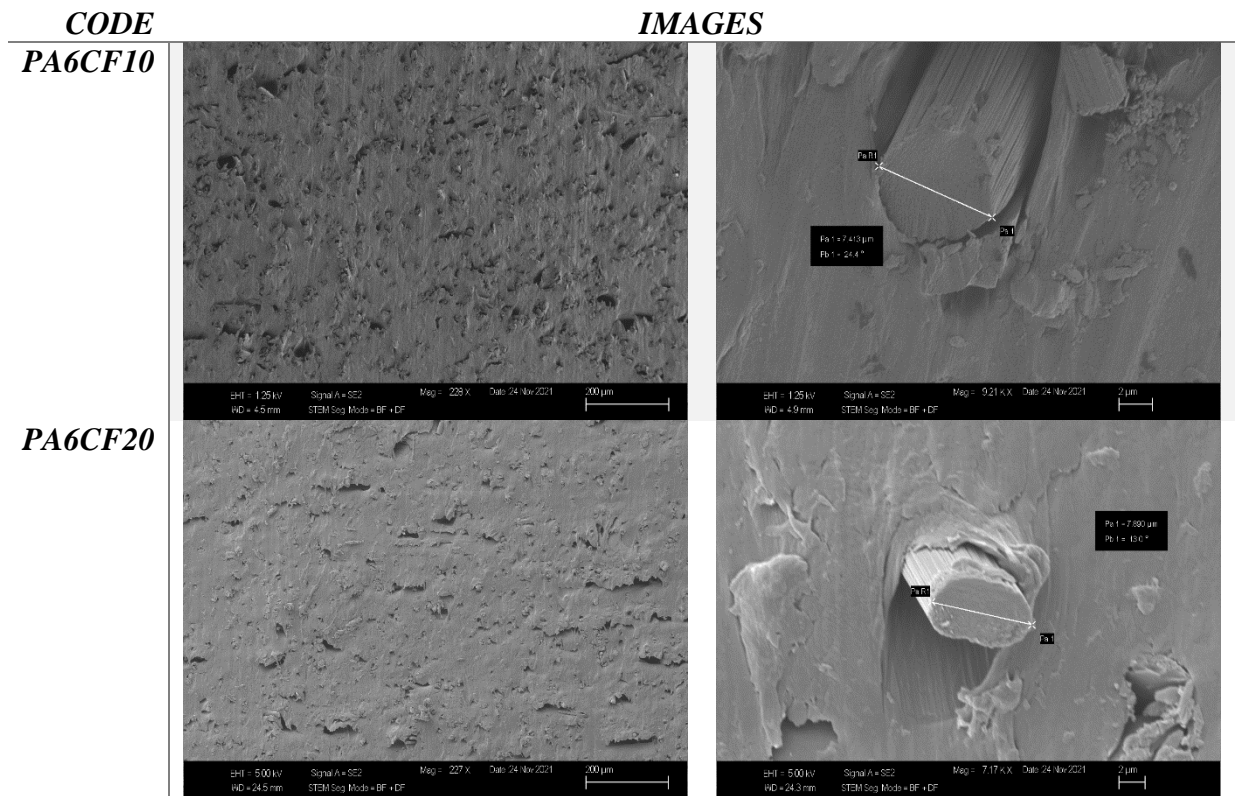


Figure 4.38: Non-modified Carbon Reinforcement Specimens SEM Images

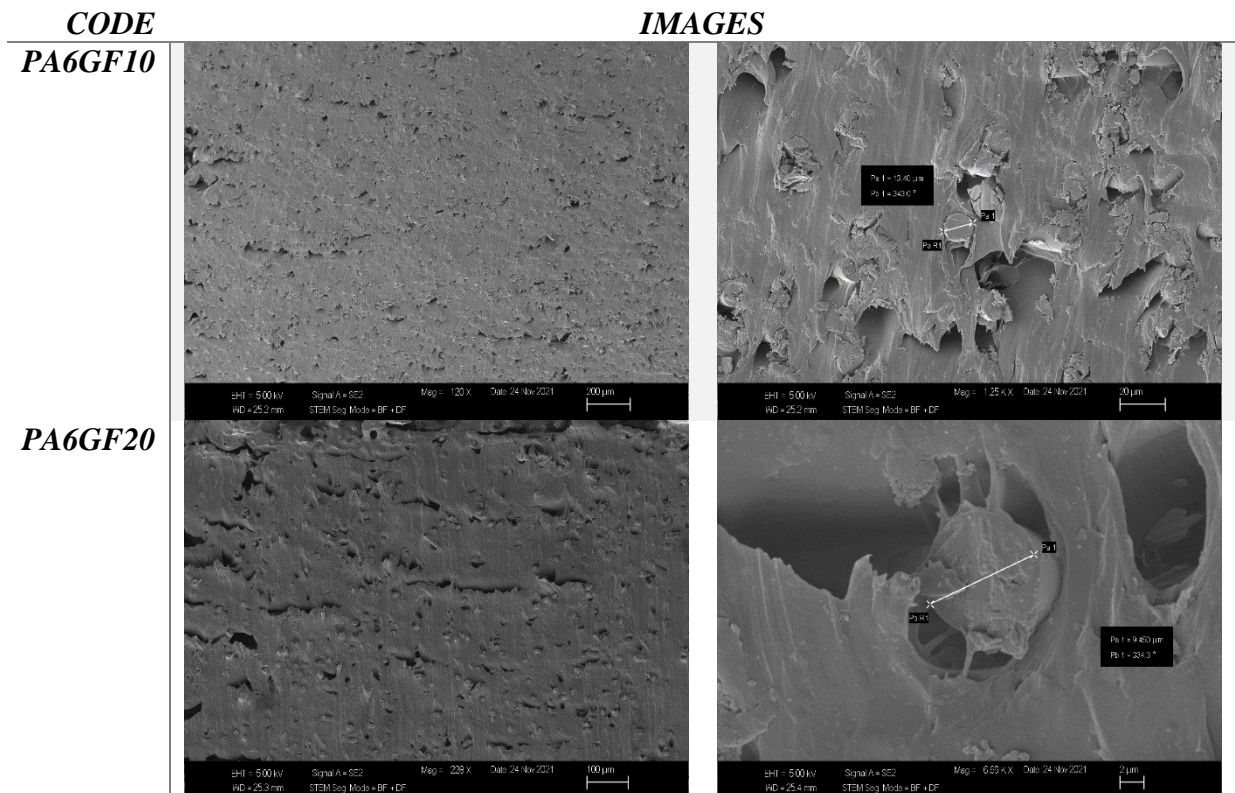


Figure 4.39: Non-modified Glass Reinforcement Specimens SEM Images



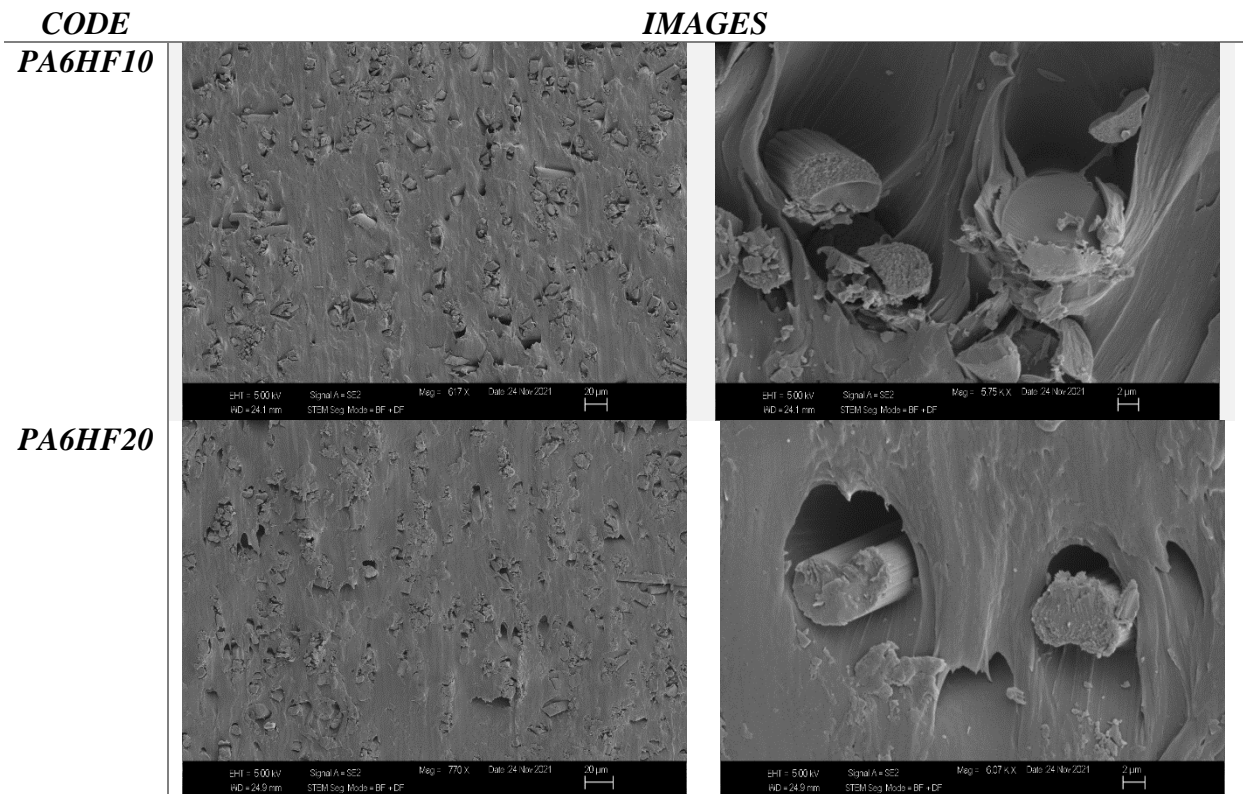


Figure 4.40: Non-modified Hybrid (Carbon/glass) Reinforcement Specimens SEM Images

Microstructure analyzes of the specimens that were modified with nanocellulose produced in the second stage of the thesis study were performed with the SEM device at the University of Alberta, NanoFab Department. Microstructure analyzes were carried out with the Zeiss EVO MA10 brand model SEM device.

The damaged areas of the nanocellulose-modified specimens were examined after the tensile test. Damaged surfaces are gold-plated for inspection in the SEM device. Specimens imaging was performed at different magnifications under 15kV EHT.

The interface region of the fibers modified with nanocellulose with PA6 matrix was visualized by SEM. The effect of the interaction of nanocellulose modification with carbon and glass fibers on mechanical properties was compared.

The distribution of carbon and glass fiber reinforcements in different weight ratios in the matrix was examined. Specimens were analyzed by imaging made in different parts of the pieces at different magnifications.

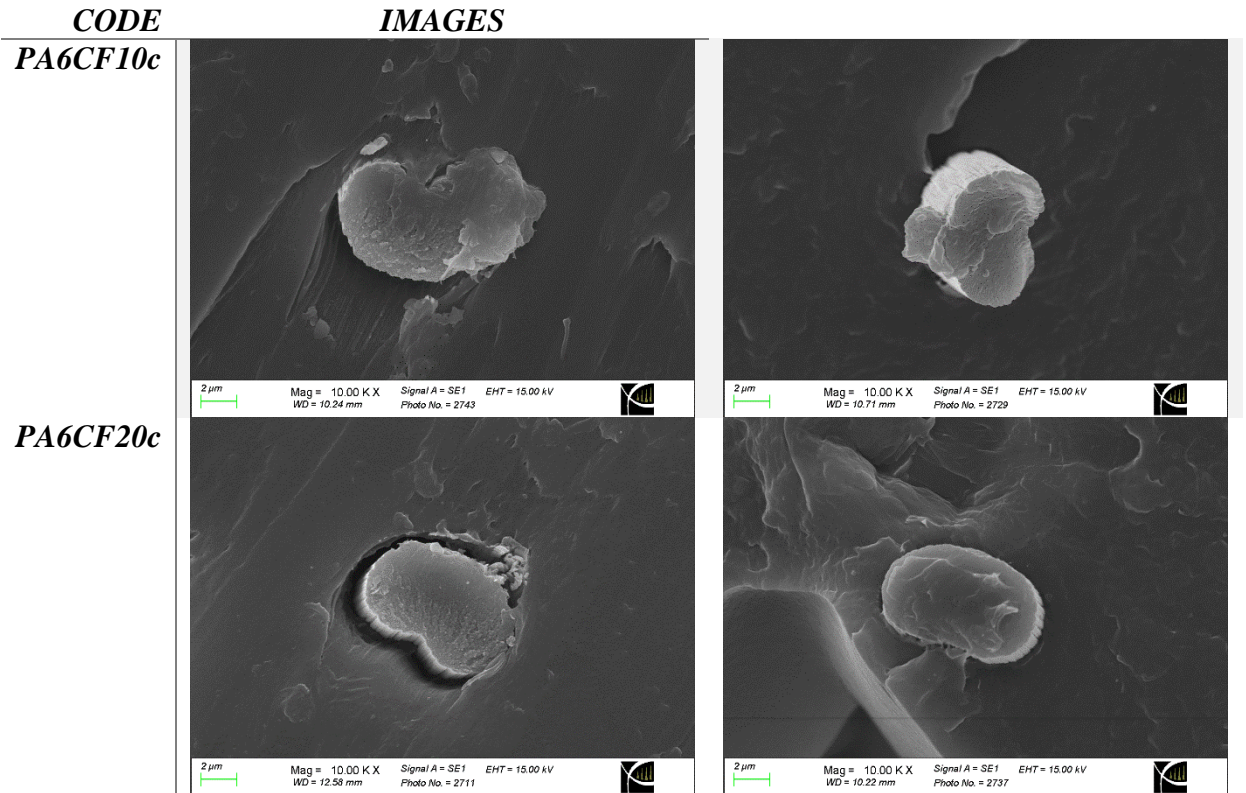


Figure 4.41: Modified Carbon Reinforcement Specimens SEM Images

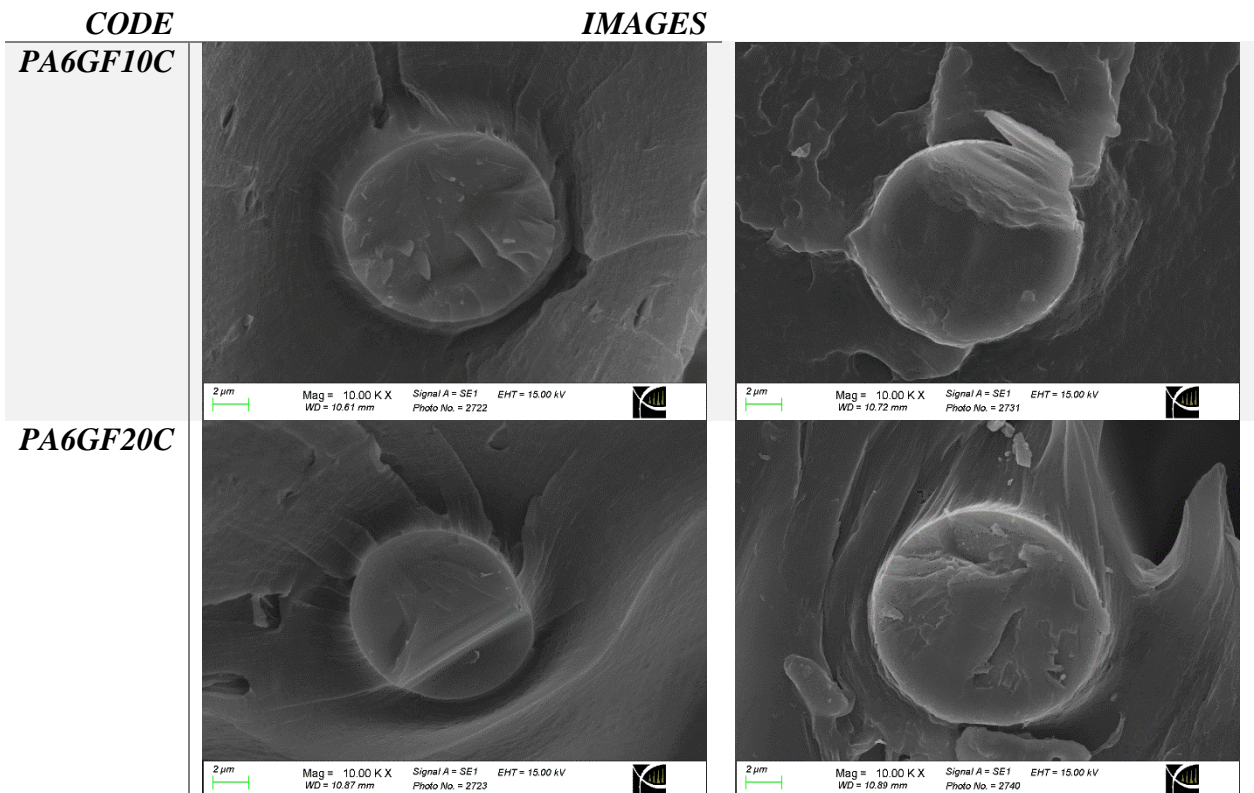


Figure 4.42: Modified Glass Reinforcement Specimens SEM Images

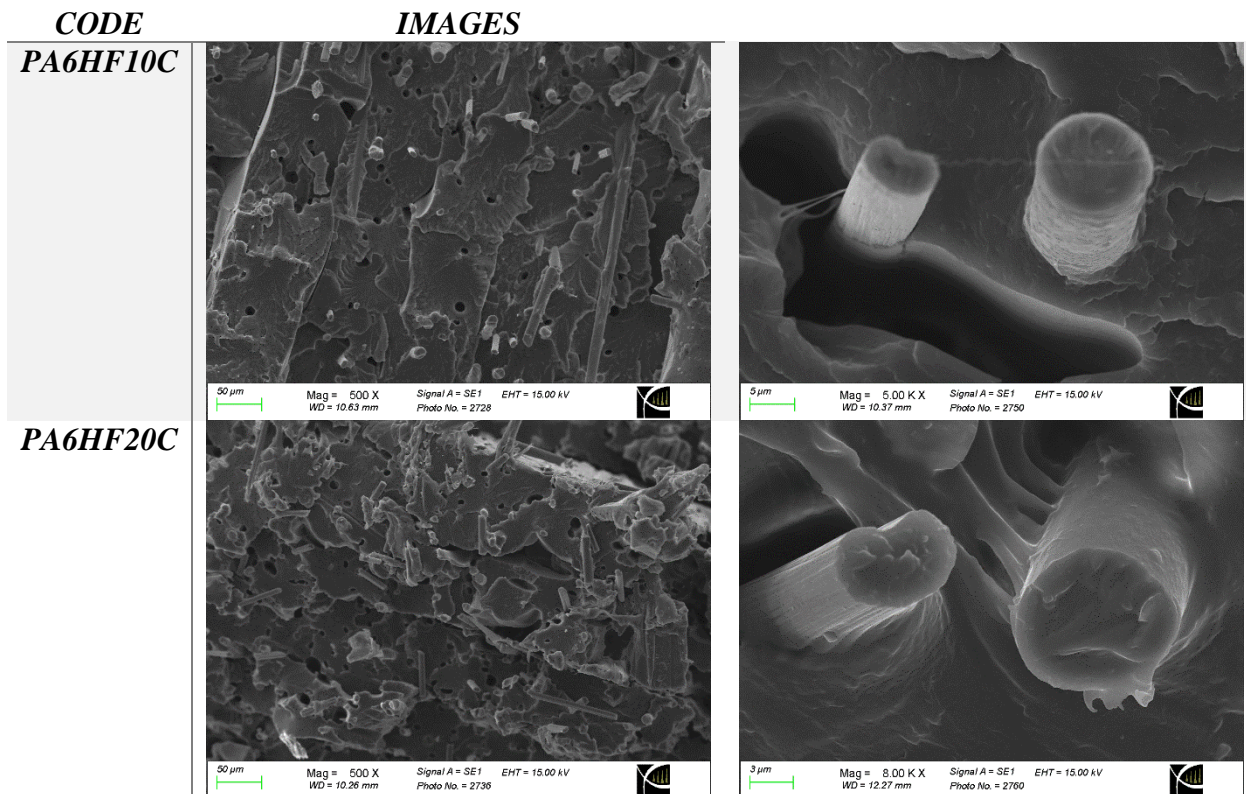


Figure 4.43: Modified Hybrid (Carbon/Glass) Reinforcement Specimens SEM Images

## 4.2 Discussion

### 4.2.1 TGA

Although the recycling feature of the types of polymer materials in the thermoplastic class provides a great advantage, the recycled forms of these polymer materials exhibit lower mechanical properties than their original forms (142). Although the molecular bonds of polymer materials and thermoplastic polymers are recycled and reused, each heating process negatively affects the chemical and physical properties of thermoplastics. Shaping the polymer granule raw material into filament with a single screw extruder and then melting it again with a FFF device is an example of this situation. In addition, adding a reinforcement element to the pellet polymer means applying an extra heat treatment to the existing heat process with a twin screw extruder. When the decomposition temperatures of different forms of all specimens were compared, it was observed that the decomposition temperatures decreased slightly after each heat treatment, that is, the decomposition started earlier.

No significant degradation of the mass at elevated temperatures up to 380°C, indicating that the pellets are stable below 380°C. In addition, the fact that no degradation was observed up to 380°C in the TGA analysis results showed that the barrel temperatures used in filament production were appropriate. All specimens started to decompose at a temperature of about 380°C and it was observed that the fiber proportions and type did not affect the degradation temperature. This indicates that the nozzle temperature determined in the FFF printing parameters is lower than the distortion temperatures measured in TGA and ensures the integrity of the materials.

As a result of degradation in fiber-reinforced specimens, mass accumulation was observed as much as fiber reinforcement ratios. The ratios of the fibers in the specimens to the remaining masses after degradation indicate that the specimens were prepared in accordance with the ratios determined for reinforcement. It has also been confirmed that fiber reinforcement is made in the correct proportions by weight.

#### 4.2.2 DSC

When the DSC results are examined, it is seen that the T<sub>g</sub> of all specimens decreases in general. The reason for this is that the thermoplastic matrix deteriorates in each extrusion process. The value of 45.98°C in PurePA6 pellets decreased to 35.5°C in filament form and 33.06°C after FFF production. T<sub>g</sub> decreased after each heating process. When the effect of fiber reinforcement on T<sub>g</sub> is examined, it can be said that glass fiber additive reduces T<sub>g</sub> value more. The value, which was 45.98°C in PurePA6 pellets, decreased to an average of 36°C in carbon fiber-reinforced specimens and 30°C in glass fiber-reinforced specimens. Modification of the fibers with nanocellulose did not cause a significant change in T<sub>g</sub> values. The reason why glass fibers lower the T<sub>g</sub> value more may be because they have different thermal conductivity coefficients.

When the crystallization temperatures (T<sub>c</sub>) of the specimens are examined, it is seen that there is a slight temperature increase in the filament form of all specimens. After FFF production, crystallization temperatures decreased. This temperature change may have occurred due to the porous structure of FFF production.

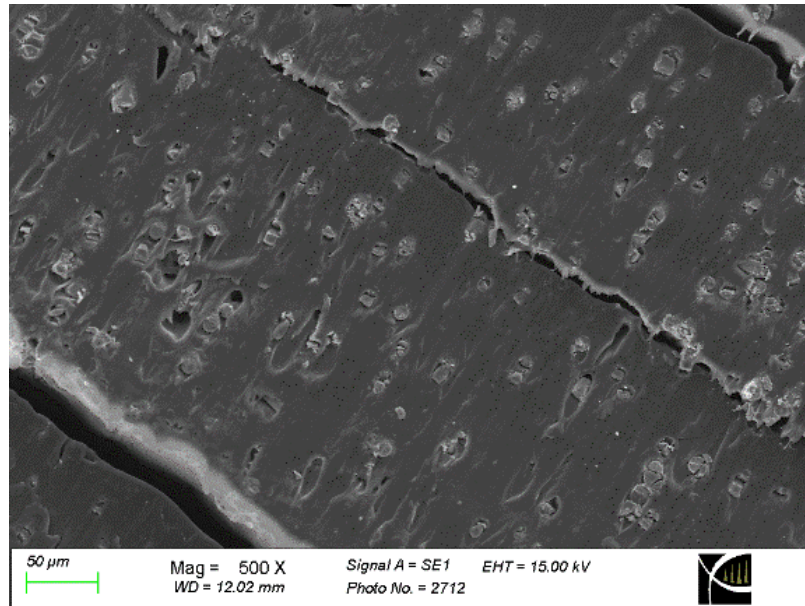


Figure 4.44: Spaces Between Layers in FFF Printed Specimen

It is seen that the melting temperature of PurePA6 is on average 219°C.  $T_m$  value did not change after thermal processes or depending on fiber additive ratios. The determination of twin-screw and single-screw parameters was based on 220°C.

Although the melting initiation temperatures of nanocellulose-doped PA6 GF20 and PA6 CF20 specimens were slightly higher than pure PA6, the same parameters were used in filament production from all pellets. Only the cooling and filament drawing cycles were changed in order to meet the diameter tolerance.

Changes in  $T_g$  and  $T_c$  temperatures indicate that the thermoplastic matrix decomposes depending on temperature. Although thermoplastic materials are recyclable, this change in their thermal properties will also affect their mechanical properties.

It was observed that the nanocellulose modification process did not show a significant change in  $T_g$ ,  $T_c$ , and  $T_m$  values. Similar results have been reported previously (143). The decrease in the  $T_g$  value means that fiber addition can improve the recovery performance of the material (144).

### 4.2.3 Tensile Testing

When the effects of production parameters, different fibers, and different fiber ratios on tensile strength in the specimens produced in the first stage of the thesis study;

It was observed that the decrease in layer thickness in all specimens increased the tensile strength. In addition, the increase in nozzle temperature also increased the tensile strength values. The highest tensile strength was observed in all specimens at 0.1 mm layer thickness and at a nozzle temperature of 275°C.

With a 0.1 mm layer thickness nozzle temperature increase, PurePA6 specimens increased by 42% from 31.69 MPa to 45.06 MPa, PA6CF10 specimens increased by 15% from 55.57 MPa to 63.78 MPa, PA6CF20 specimens increased by 60% from 78.41 MPa to 125.29 MPa, PA6GF10 specimens increased by 19% from 38.44 MPa to 45.57 MPa, PA6GF20 specimens increased by 16% from 56.13 MPa to 65.12 MPa, PA6HF10 specimens increased by 25% from 47.27 MPa to 59.18 MPa, and PA6HF20 specimens increased by 38% from 77.50 MPa to 106.69 MPa. The increase in nozzle temperature creates advantages for the z-axis joining of the layers. In high-temperature prints, the bonding between the layers is better since the amount of cooling is low. Polymer bonds become stronger with increasing temperature.

With the change of layer thickness at a nozzle temperature of 275°C, PurePA6 specimens increased by 14% from 33.79 MPa to 45.06 MPa, PA6CF10 specimens increased by 32% from 48.47 MPa to 63.78 MPa, PA6CF20 specimens increased by 51% from 82.90 MPa to 125.29 MPa, PA6GF10 specimens increased by 10% from 41.53 MPa to 45.57 MPa, PA6GF20 specimens increased by 10% from 59.47 MPa to 65.12 MPa, PA6HF10 specimens increased by 24% from 47.85 MPa to 59.18 MPa, and PA6HF20 specimens reached 106.69 MPa with an increase of 47% from 72.41 MPa. The reduction in layer thickness increases the production time. At the same time, more material is extruded per unit volume in the z-axis. This situation reduces the hollow structure in the parts produced with FFF. SEM images confirm this. In addition, there is a similar situation for different materials in the literature

PA6HF20 specimens reached 106.69 MPa with an increase of 47% from 72.41 MPa.

Tensile strength 0.1mm layer thickness and 275°C nozzle temperature, which was 45.06 MPa in PurePA6 specimens, increased by 42% to 63.78 MPa in PA6CF10 specimens, increased by 178% to 125 MPa in PA6CF20 specimens, increased by 1% to 45.57 MPa in PA6GF10 specimens, increased by 45% to 65.12 MPa in PA6GF20 specimens, increased by 31% to 59.18 MPa in PA6HF10 specimens, and PA6HF20

specimens increased by 137% to 106.60 MPa. When the tensile strength effect of fiber reinforcements applied to PurePA6 specimens was examined, it was observed that carbon fiber reinforcement was more effective than glass fiber. In addition, the increase in the additive ratio for each fiber type increased the tensile strength.

In the first stage of the doctoral thesis, when the mechanical properties of the produced specimens were compared with the mechanical properties of the nanocellulose-modified specimens;

The tensile strength value was 41.53 MPa in the PA6GF10 specimen without nanocellulose modification produced by the FFF method with parameter 13, 71.50 MPa was observed with an increase of 72% in the PA6GF10c specimen.

The tensile strength value was 43.23 MPa in the PA6GF10 specimen without nanocellulose modification produced by the FFF method with parameter 14, 82.02 MPa with an increase of 88% was observed in the PA6GF10c specimen.

The tensile strength value was 45.57 MPa in the PA6GF10 specimen without nanocellulose modification produced by the FFF method with parameter 15, 85.17 MPa was observed with an increase of 87% in the PA6GF10c specimen.

While a 10% change was observed in PA6GF10 specimens depending on the layer thickness at 275°C, an increase of 19% was observed in PA6GF10c specimens.

The tensile strength value was 59.47 MPa in the PA6GF20 specimen without nanocellulose modification produced by the FFF method with parameter 13, it was observed at 83.70 MPa with an increase of 41% in the PA6GF20c specimen.

The tensile strength value was 60.32 MPa in the PA6GF20 specimen without nanocellulose modification produced by the FFF method with parameter 14, it was observed 89.79 MPa with an increase of 49% in the PA6GF20c specimen.

The tensile strength value was 65.12 MPa in the PA6GF20 specimen without nanocellulose modification produced by the FFF method with parameter 15, it was observed 98.99 MPa with an increase of 52% in the PA6GF20c specimen.

While a 10% change was observed in PA6GF20 specimens depending on the layer thickness at 275°C, an 18% increase was observed in PA6GF20c specimens.

Nanocellulose modification showed very successful results in glass fiber reinforced PA6 specimens. Compared to the PA6GF10 specimens without nanocellulose, the tensile strength values increased by 72 to 88% in the PA6GF10c specimens, which were produced with nanocellulose modified and produced in different parameters. It can be said that a very high tensile strength increase was achieved when compared with PA6GF10 specimens that did not contain nanocellulose. Compared with the PA6GF20 specimens without nanocellulose, the tensile strength values increased by 41 to 52% in the PA6GF20c specimens, which were produced with nanocellulose additives and produced in different parameters. It can be said that a very high tensile strength increase was achieved when compared with PA6GF20 specimens that did not contain nanocellulose. It has been observed that the nanocellulose modification creates a significant mechanical property difference. It can be thought that the amorphous structure of the glass fiber increased the effect of the modification made with nanocellulose.

The tensile strength value was 48.47 MPa in the PA6CF10 specimen without nanocellulose modification produced by the FFF method with parameter 13, 79.13 MPa with an increase of 63% was observed in the PA6CF10c specimen.

The tensile strength value was 60.28 MPa in the PA6CF10 specimen without nanocellulose modification produced by the FFF method with parameter 14, 92.13 MPa with an increase of 53% was observed in the PA6CF10c specimen.

The tensile strength value was 63.78 MPa in the PA6CF10 specimen without nanocellulose modification produced by the FFF method with parameter 15, 96.57 MPa with an increase of 51% was observed in the PA6CF10c specimen.

While a 32% change was observed in PA6CF10 specimens, an increase of 22% was observed in PA6CF10c specimens depending on the layer thickness at 275°C.

The tensile strength value was 82.90 MPa in the PA6CF20 specimen without nanocellulose modification produced by the FFF method with parameter 13, 92.16 MPa with an increase of 11% was observed in the PA6CF20c specimen.



The tensile strength value was 95.83 MPa in the PA6CF20 specimen without nanocellulose modification produced by the FFF method with parameter 14, 104.81 MPa with an increase of 9% was observed in the PA6CF20c specimen.

The tensile strength value was 125.29 MPa in the PA6CF20 specimen without nanocellulose modification produced by the FFF method with parameter 15, 131.52 MPa with an increase of 5% was observed in the PA6CF20c specimen.

While a 51% change was observed in PA6CF20 specimens, an increase of 43% was observed in PA6CF20c specimens depending on the layer thickness at 275°C.

Nanocellulose modification showed successful results in carbon fiber reinforced PA6 specimens. Compared with the PA6CF10 specimens without nanocellulose, the tensile strength values increased by 51 to 63% in the PA6CF10c specimens, which were produced with nanocellulose modification and produced in different parameters. It can be said that a very high tensile strength increase was achieved when compared with PA6CF10 specimens that did not contain nanocellulose. Compared to the PA6CF20 specimens without nanocellulose, the tensile strength values increased by 5 to 11% in the PA6CF20c specimens modified with nanocellulose and produced in different parameters. It can be said that a very low tensile strength increase was achieved when compared with PA6CF20 specimens that did not contain nanocellulose. Compared to the 10% by-weight carbon fiber reinforced specimens, the increase in the specimens with 20% carbon fiber reinforcement was very low. Considering the amount of increase in tensile strength caused by nanocellulose additive made to glass fiber reinforced PA6 specimens, it can be said that there is a small increase in carbon fiber reinforced PA6 matrix specimens. In addition, although nanocellulose modification increased the tensile strength value and change rates in each parameter, the amount of increase depending on the layer thickness decreased. Although the highest tensile strength value was observed in the PA6CF20c specimen produced with parameter 15, the highest tensile strength change rate was observed in the PA6GF20c specimen. This may have the effect of increasing the use of low-cost fibers such as glass fiber instead of expensive additives such as carbon fiber. The nanocellulose surface modification made to the glass fiber, which is low cost even from the PA6 matrix material and reduces the costs in proportion to its addition, has created a great change in tensile strength.

It was observed that the decrease in the layer thickness of nanocellulose modification in glass fiber-reinforced specimens had a positive effect on the increase in tensile strength. In this case, it can be said that the nanocellulose additive with a large surface area provides higher bonding in the production of the material in dense layers and positively affects the interface bonds between the layers. It has been observed that higher mechanical properties are obtained by choosing low-layer thickness in nanocellulose-doped PA6 specimens.

In the carbon fiber reinforced PA6 matrix specimens, the nanocellulose additive caused a significant increase in mechanical properties independent of the weight ratio, while the effect of the nanocellulose modifier was low depending on the layer thickness. This shows that the nanocellulose modification applied to the carbon fiber material reaches saturation and the interface improvement that increases the tensile strength is close to the optimum points.

The tensile strength value was 47.85 MPa in the PA6HF10 specimen without nanocellulose modification produced by the FFF method with parameter 13, 77.33 MPa with an increase of 62% was observed in the PA6HF10c specimen.

The tensile strength value was 53.23 MPa in the PA6HF10 specimen without nanocellulose modification produced by the FFF method with parameter 14, 89.10 MPa with an increase of 67% was observed in the PA6HF10c specimen.

The tensile strength value was 59.18 MPa in the PA6HF10 specimen without nanocellulose modification produced by the FFF method with parameter 15, 92.66 MPa with an increase of 57% was observed in the PA6HF10c specimen.

While a 24% change was observed in PA6HF10 specimens, a 20% increase was observed in PA6HF10c specimens depending on the layer thickness at 275°C.

The tensile strength value was 72.41 MPa in the PA6HF20 specimen without nanocellulose modification produced by the FFF method with parameter 13, 91.45 MPa with an increase of 26% was observed in the PA6HF20c specimen.

The tensile strength value was 90 MPa in the PA6HF20 specimen without nanocellulose modification produced by the FFF method with parameter 14, 98.26 MPa with an increase of 9% was observed in the PA6HF20c specimen.

The tensile strength value was 106.69 MPa in the PA6HF20 specimen without nanocellulose modification produced by the FFF method with parameter 15, 118.33 MPa with an increase of 11% was observed in the PA6HF20c specimen.

While a 47% change was observed in PA6HF20 specimens, a 29% increase was observed in PA6HF20c specimens depending on the layer thickness at 275°C.

The effect of surface modification with nanocellulose on carbon fibers on mechanical properties was not as effective as the increase in glass fiber-reinforced specimens. This may be the crystal structure of the carbon fiber and the surface modification made for PA6 compatibility with the carbon fibers used. Although the highest tensile strength value was observed in the PA6CF20C specimen produced with parameter 15, the observed change was not as high as in the PA6GF20 specimen when compared to the PA6CF20 specimen value without nanocellulose. Depending on the layer thickness, the change in tensile strength decreased with nanocellulose modification. This shows that the nanocellulose additive reaches saturation and the interface improvement, which increases the tensile strength, is close to the optimum points. It has been observed that the production parameters are quite effective on the mechanical properties.

The variation in layer thickness is quite high in carbon fiber-reinforced specimens, it is lower in glass fiber-reinforced specimens. The high thermal capacity of the carbon during the bonding of the layers of the carbon fiber reinforced PA6 matrix may have caused this. It can be thought that the low thermal capacity of the glass fiber causes rapid cooling during the production of the layers and a lower effect on the joints between the layers.

#### 4.2.4 Impact Testing

When a sudden load is applied to a material, the maximum force that the material can resist is defined as impact resistance. The effect of the high force applied to the

material in a short time is greater than the low force applied for a long time. In the first stage of the thesis study, it is parameter number 15 where the highest tensile strength values are obtained among the tensile test specimens produced in 15 different parameters. The highest tensile strength was obtained in parameter 15 for all specimens. All tensile test specimens were produced in  $-/+45$  orientation as standard. Anisotropic material production is possible with the FFF method (Parandoush and Lin, 2017). Direction-related features can be changed with production parameters. For this reason, the effect of the change in the infill pattern on the mechanical properties was investigated with the Charpy test. In this context, two different specimen groups were produced in  $-/+45$  and  $0/90$  orientation with the FFF method using 7 different compounds. The specimens were produced and tested in accordance with the ISO179 standard.

It has been observed that the impact resistance of pure PA6 is higher than the fiber-reinforcement ones. Although the fiber reinforcement increases the tensile strength, it decreased the impact resistance. It also caused a decrease in ductility and a brittle structure. The increase in fiber proportion decreased the impact resistance. In ISO 179 Charpy specimens produced from both glass fiber, carbon fiber, and hybrid form compounds, the impact strength of those with both orientations decreased with the increase in fiber proportion. In all compounds, the impact resistance of the specimens with the  $-/+45$  orientation is higher than the ones with the  $0/90$  orientation. Similar results were obtained with studies in the literature on the impact of resistance change due to infill patterns (Galeja et al., 2020) .

When carbon and glass fiber reinforcements are compared, although carbon fiber-reinforced compounds have higher tensile strength, their impact resistance is lower than glass fiber-reinforced ones. This situation was observed similarly for the ones with 10% and 20% fiber additive ratios and for the specimens produced in both directions. It has been observed that the impact strength of hybrid additive compounds is between glass fiber and carbon fiber. This is an indication that hybrid structures can be used to optimize impact resistance.

The reason why glass fibers have higher impact resistance can be said to be more flexible than carbon fiber. The reason why the increase in the fiber ratio causes a

decrease in the impact strength is the decrease in the matrix material ratio and the poor bonding under sudden load.

Table 4.19: Non-Modified and Modified Specimens Average Charpy Results

	<i>Non-Modified Fiber</i>	<i>Modified Fiber</i>	<i>Percent Increase</i>
<b><i>PA6CF10 (-/+45)</i></b>	29.01	30.97	6.8%
<b><i>PA6CF10 (0/90)</i></b>	27.81	28.63	2.9%
<b><i>PA6CF20 (-/+45)</i></b>	26.17	27.08	3.5%
<b><i>PA6CF20 (0/90)</i></b>	24.79	26.26	5.9%
<b><i>PA6GF10 (-/+45)</i></b>	47.37	50.34	6.3%
<b><i>PA6GF10 (0/90)</i></b>	43.57	47.54	9.1%
<b><i>PA6GF20 (-/+45)</i></b>	34.89	38.94	11.6%
<b><i>PA6GF20 (0/90)</i></b>	31.97	35.47	10.9%
<b><i>PA6HF10 (-/+45)</i></b>	36.65	39.57	8.0%
<b><i>PA6HF10 (0/90)</i></b>	33.87	36.94	9.1%
<b><i>PA6HF20 (-/+45)</i></b>	32.28	35.72	10.7%
<b><i>PA6HF20 (0/90)</i></b>	29.37	34.3	16.8%

When the Charpy results of the specimens containing nanocellulose-modified fiber were examined, it was observed that the impact strengths increased slightly as an indicator of interface improvement. The impact strength increase in glass fiber-reinforced specimens is higher than in carbon fiber-reinforced specimens. It can be said that nanocellulose surface modification is more effective on glass fibers.

#### 4.2.5 Compression Testing

In the first stage of the thesis, compression test specimens were produced by using the parameters that produced the specimens with the highest tensile strength. The effect of the change in layer thickness under the compression force was investigated. In this context, 3 different layer thickness specimens were produced at constant nozzle temperature.

Table 4.20: Specimens Average Compression Results

Specimens	Dis.	Strain	Specimens	Dis.	Strain	Specimens	Dis.	Strain
	mm	%		mm	%		mm	%
Pure PA6 (13)	12.64	49.77	Pure PA6 (14)	10.25	40.37	Pure PA6 (15)	6.3	24.81
PA6CF10c (13)	8.48	33.37	PA6GF10c (13)	10.43	41.07	PA6HF10c (13)	6.3	24.8
PA6CF10 (13)	9.11	35.86	PA6GF10 (13)	10.86	42.77	PA6HF10 (13)	8.35	32.87
PA6CF10c (14)	5.12	20.16	PA6GF10c (14)	6.5	26.6	PA6HF10c (14)	4.44	17.48
PA6CF10 (14)	5.72	22.5	PA6GF10 (14)	9.09	35.8	PA6HF10 (14)	5.05	19.9
PA6CF10c (15)	4.24	16.7	PA6GF10c (15)	4.89	19.24	PA6HF10c (15)	2.91	11.45
PA6CF10 (15)	4.35	17.13	PA6GF10 (15)	5.83	22.96	PA6HF10 (15)	3.55	13.97
PA6CF20c (13)	7.36	28.98	PA6GF20c (13)	6.6	25.97	PA6HF20c (13)	4.98	19.61
PA6CF20 (13)	7.98	31.4	PA6GF20 (13)	6.72	26.47	PA6HF20 (13)	6.12	24.07
PA6CF20c (14)	4.15	16.34	PA6GF20c (14)	5.93	23.35	PA6HF20c (14)	2.78	10.95
PA6CF20 (14)	5.19	20.43	PA6GF20 (14)	6.17	24.31	PA6HF20 (14)	3.95	15.43
PA6CF20c (15)	1.32	5.2	PA6GF20c (15)	2.15	8.47	PA6HF20c (15)	1.31	5.16
PA6CF20 (15)	2.38	9.38	PA6GF20 (15)	4.75	18.47	PA6HF20 (15)	2.06	8.13

By using all the filaments modified and unmodified with nanocellulose, specimens were produced with the FFF method in parameters 13, 14, and 15. Compression tests were performed on Instron 5966 device according to ASTM D695 standards. All composites were studied under load up to 9000N.

A change in strain was observed in all specimens depending on the layer thickness changing. The reduction in layer thickness reduced the amount of displacement under compression load. The lowest strain values were observed at 0.1mm layer thickness.

Fiber surface modification with nanocellulose showed a positive effect in compression tests as well as in tensile tests. Lower strain values were exhibited in the specimens that were modified for each layer thickness.

The increase in fiber additive ratios had a positive effect for each fiber type and the strain value decreased. Carbon fiber-reinforced specimens produced lower strain than glass-reinforced specimens. The higher tensile and impact properties of carbon fibers may be the reason for this. Hybrid fiber-reinforced specimens produced better results under compression compared to carbon-reinforced specimens. It has been observed that different fibers used together give more effective results in the compression direction. The fact that the fibers have different lengths and diameters may have increased the compressive strength.

Fiber-reinforced specimens showed superior compressive strength compared to pure PA6 specimens. Fiber reinforcement increased the mechanical properties of the specimens in the compression direction as well as in the tensile direction. The fiber matrix interface improvement has also resulted in a positive result in the compression direction. It has been observed that the fiber reinforcements in the pure polymer exhibit a more rigid structure under force compared to the specimens without fiber reinforcement.

#### 4.2.6 SEM Analysis

In the thesis study, the weight ratios of fiber reinforcement determined for each compound were verified by TGA analysis. On the other hand, it is critical that the fiber distribution in the matrix is homogeneous in composite structures. In fiber-reinforced composite materials, homogeneity in fiber distribution is required to provide consistent properties over the entire area of the part (Goh et al., 2019). Thanks to the screw configuration of the twin-screw extruder used, the successful homogeneous distribution of the fibers was controlled by microstructure analysis. It was observed that the fibers reinforced into the PA6 matrix in all compounds were homogeneously dispersed. An example image is shared in Figure 4.45.

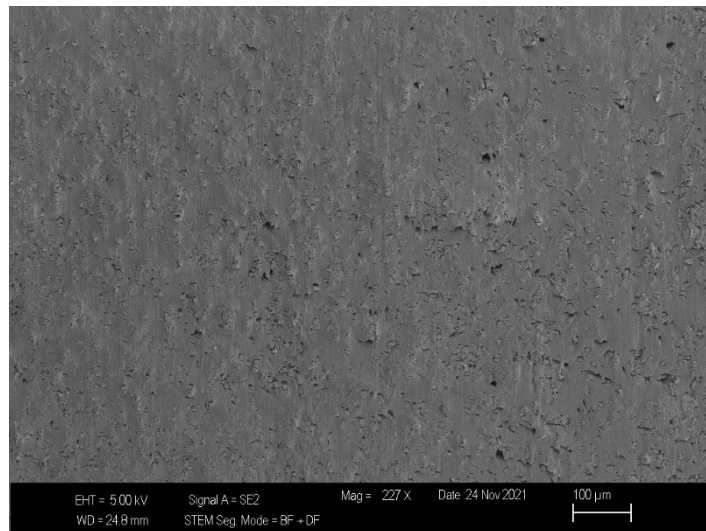


Figure 4.45: PA6HF20 Specimen SEM Image

Diameter controls of the fiber reinforcements added to the PA6 matrix were carried out with SEM images. In the production of parts with the FFF method, the polymer is extruded from the heated nozzle head. Tips of different diameters are used in the nozzle

head, where polymer or polymeric composites are extruded. Nozzle tips with diameters of 0.4-0.6-0.8-1mm are commonly used in the FFF method. In the thesis study, specimen productions were carried out with a 0.6mm diameter special sapphire nozzle tip. Fiber diameters are important to prevent nozzle clogging. In this context, fiber products of Dowaksa and Şişecam were used in compound production. In microstructural analysis, glass fiber diameters were measured as  $\sim 10\mu$  and carbon fiber diameters were measured as  $\sim 8\mu$ .

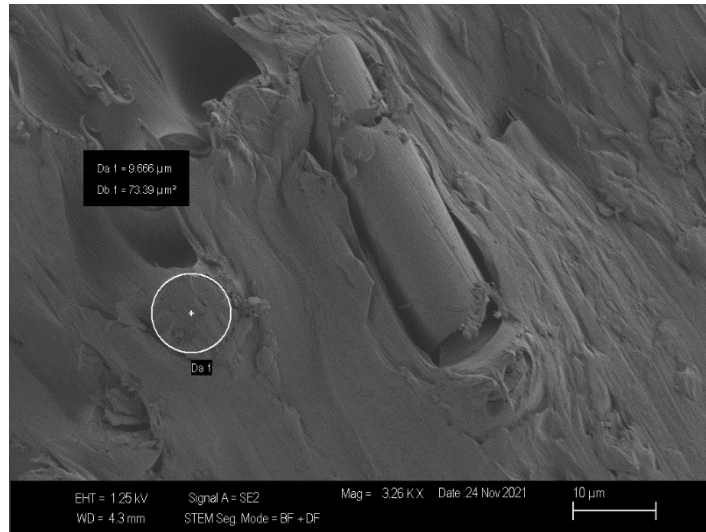


Figure 4.46: PA6GF10 Specimen SEM Image

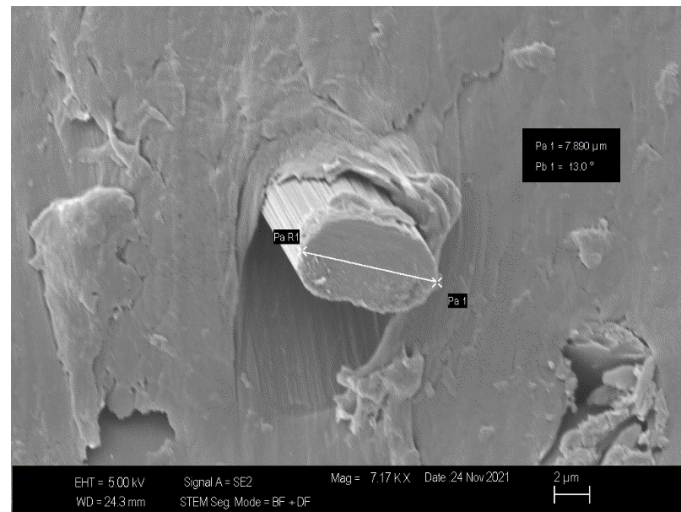


Figure 4.47: PA6CF20 Specimen SEM Image

In the first stage of the thesis study, a nanocellulose modification was applied for interfacial improvement in order to increase the mechanical properties of the tested specimens. When the mechanical properties of all specimens are examined, it is seen that the modification of the fiber surfaces with nanocellulose has a positive effect. It



has been observed by microstructure analyses that these processes are effective in their adhesion in the matrix and fiber junction areas. 4.1.3. In the images shared in the section titled, the effect of nanocellulose on interfacial bonding is seen in detail.

Fiber-reinforced composites, filament production with a single-screw extruder, and FFF method production have a positive effect on the orientation of the fibers. Fiber orientation has given anisotropic properties in the produced specimens. In the SEM images, it was observed that the fibers were oriented in the tensile direction.

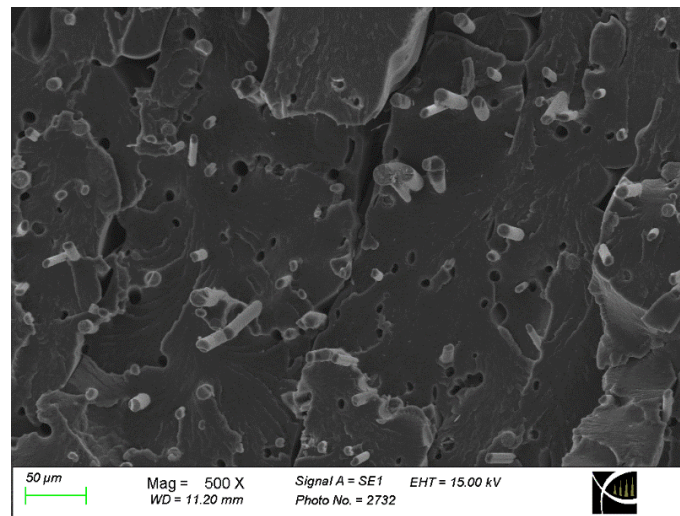


Figure 4.48: PA6HF10c Specimen SEM Image

To produce load-bearing parts with the FFF method, high-performance composite filaments must be developed. The main reason why polymer products produced with FFF do not show high mechanical properties is the interface defects in the internal structure that occur during production. In the thesis study, it was aimed and achieved to produce hybrid composite structures with high performance in complex geometry by the FFF method, without the disadvantages of traditional methods and by improving the interface. When the SEM images were examined, it was observed that the fiber-matrix interfacial bonds were quite good and the nanocellulose additive improved this. The obtained tensile strength values are also the biggest indicator of this.

# Chapter 5

## 5 Conclusion

Thermoplastic composites are the focus of new-generation research and development studies on sustainable materials, green composites, and circular economy concepts. Thermoplastic materials have the advantage that they can be recycled up to a certain cycle time. Heat and pressure are applied to produce and shape composites with a thermoplastic matrix. The disadvantages of thermoplastics are that they have very high expansion and contain high viscosity.

The most innovative forming method of thermoplastics is additive manufacturing technologies. The most common among them is FFF technology. The main advantage of the FFF method is the ability to directly transform a computerized 3D model into a finished product without using any auxiliary tools. This facilitates the production of complex geometric parts that are difficult to manufacture with conventional manufacturing processes. Additive manufacturing devices will play an important role in the transformation of industry 4.0 in terms of producing products in one piece without the need for assembly, not producing any residual material, and containing many new generation technologies.

Studies are carried out on the production of high-performance polymer products with the additive manufacturing method. In addition, commercial products are coming to the market in this area. Currently, pure polymers are used in the FFF method. In addition to pure polymers, fiber-reinforced polymer filaments are also being developed. The increase in the variety of materials used in this area will increase the industrial use of the products produced by the FFF method. In addition, composite structures will be manufactured without plastic injection, vacuum infusion, or pressure molding. With fiber-reinforced polymer filaments, it will allow the production of

complex geometry products, especially in the aerospace, defense, automotive and medical sectors, at low cost.

Being able to produce fiber-reinforced materials by additive manufacturing is the main goal of a number of research in the 3D printing industry. Fiber-reinforced polymer composites have been used for many years, but in recent years, their use has increased, especially in the aerospace, defense, automotive, and medical industries. Conventional composite manufacturing processes such as hand-lay out, resin transfer molding, and automatic laying have many practical and financial problems that limit their use. Processes such as manual laying and vacuum infusion are inexpensive, and easy to set up, but labor intensive. There are variations in the properties of the parts depending on the skills of the operators. Processes such as automated laying require the use of expensive and short shelf-life pre-preg materials. Composite part production processes with the FFF method will remove some barriers to traditional composite production methods. Additive manufacturing methods do not require any molds or autoclaves required by conventional processes. There is also the freedom to choose polymer and fiber layers, and composite parts with complex geometries can be produced. Additive manufacturing processes offer greater design and material freedom than traditional composite manufacturing processes.

Existing filaments used in the FFF method have low elastic modulus and mechanical properties. The use of unreinforced polymer filaments limits the wide application of parts produced by this method in industry and research environments. In this context, fiber reinforced PA6 matrix composites developed in the thesis study may offer opportunities. The industrial usage area of the products produced by the FFF method will increase thanks to the fiber reinforcement and the filaments reinforced with nanocellulose modification. In addition, the low mechanical properties observed in the specimens produced by the fiber-reinforced polymer matrix FFF method were improved to a certain extent by modifying the fibers with nanocellulose. Moreover, it has been observed that the production parameters of the FFF method are quite effective on the tensile strength values. In addition, it has been seen that nanocellulose additive can be used for interface modification and improves mechanical properties. Among the material configurations developed in the thesis study, tensile strength values reaching 130 MPa can be an alternative for many areas.

The most significant disadvantage of the FFF method is that the layer mergers are weak. For this reason, they exhibit lower mechanical properties under tensile force when compared to the specimens produced by injection molding, etc. polymer production methods. For this reason, their behavior under compression load and the effect of the change in layer thickness on the strain value in the compression direction were investigated. The values obtained in the compression test results constitute meaningful data for comparing similar composites with different production methods. In addition, it was observed that nanocellulose surface modification produced positive results under compression force. One of the critical criteria of the design is the forces under which the parts will work in the working environment. It can be thought that the products that can use under compression load produced by additive manufacturing will have good results and create new application areas.

# References

- [1] Gouzman I, Grossman E, Verker R, Atar N, Bolker A, Eliaz N. Advances In Polyimide-Based Materials For Space Applications. *Adv Mater.* 2019;31(18):1–15.
- [2] Vendan SA, Natesh M, Garg A, Gao L. Confluence Of Multidisciplinary Sciences For Polymer Joining. *Confluence Of Multidisciplinary Sciences For Polymer Joining.* 2019.
- [3] Chawla K. *Composite Materials Science And Engineering.* Springer; 2012.
- [4] Batten SR, Champness NR, Chen XM, Garcia-Martinez J, Kitagawa S, Öhrström L, Et Al. Coordination Polymers, Metal–Organic Frameworks And The Need For Terminology Guidelines, 2012;14(9):3001–4.
- [5] Callister WD, Rethwisch DG. *Materials Science And Engineering : An Introduction.*
- [6] Brinson HF, Brinson LC. *Polymer Engineering Science And Viscoelasticity: An Introduction, Second Edition. Polymer Engineering Science And Viscoelasticity: An Introduction.* Springer US; 2015. 1–482 P.
- [7] Utekar S, V K S, More N, Rao A. Comprehensive Study Of Recycling Of Thermosetting Polymer Composites – Driving Force, Challenges And Methods. *Compos Part B Eng.* 2021; 207 : 108596.
- [8] Abali BE, Yardımcı MY, Zecchini M, Daissè G, Marchesini FH, De Schutter G, Et Al. Experimental Investigation For Modeling The Hardening Of Thermosetting Polymers During Curing. *Polym Test.* 2021; 102 : 107310.
- [9] Zhao P, Rao C, Gu F, Sharmin N, Fu J. Close-Looped Recycling Of Polylactic Acid Used In 3D Printing: An Experimental Investigation And Life Cycle Assessment. *J Clean Prod.* 2018; 197 : 1046–55.
- [10] Ebewele RO, Raton B, York N. *Polymer Science And Technology [Internet].*

CRC Press; 2000 [Cited 2022 Mar 24]. Available From: <https://www.taylorfrancis.com/books/mono/10.1201/9781420057805/polymer-science-technology-robert-ebewe>

- [11] Grigore ME. Methods Of Recycling, Properties And Applications Of Recycled Thermoplastic Polymers. *Recycl.* 2017;2 (4) : 24.
- [12] Coppola S, Acierno S, Grizzuti N, Vlassopoulos D. Viscoelastic Behavior Of Semicrystalline Thermoplastic Polymers During The Early Stages Of Crystallization. *Macromolecules.* 2006; 39 (4) : 1507–14
- [13] Hotta A, Cochran E, Ruokolainen J, Khanna V, Fredrickson GH, Kramer EJ, Et Al. Semicrystalline Thermoplastic Elastomeric Polyolefins: Advances Through Catalyst Development And Macromolecular Design. 2006; 103 (42) : 153, 27–32.
- [14] Karsli NG, Aytac A. Composites : Part B Tensile And Thermomechanical Properties Of Short Carbon Fiber Reinforced Polyamide 6 Composites. *Compos Part B.* 2013; 51 : 2, 70–85.
- [15] Guedes RM. Creep And Fatigue In Polymer Matrix Composites. Woodhead Publishing. Woodhead Publishing; 2019.
- [16] Seydibeyoğlu MÖ, Doğru A, Kandemir MB, Aksoy Ö. Lightweight Composite Materials In Transport Structures. In: Sanjay Mavinkere Rangappa JPSK, Editor. *Lightweight Polymer Composite Structures.* CRC Press; 2020; P. 103–30.
- [17] Chalmers DW. The Potential For The Use Of Composite Materials In Marine Structures. *Mar Struct.* 1994;7(2–5):441–56.
- [18] Dhinakaran V, Surendar K V, Riyaz MSH, Ravichandran M. Materials Today : Proceedings Review On Study Of Thermosetting And Thermoplastic Materials In The Automated Fiber Placement Process. *Mater Today Proc.* 2020; (27) : 10–23.
- [19] Lees JK. Development In Thermoplastic Composites : A Review Of Matrix Systems And Processing Methods Recent. 1988;277–96.
- [20] Friedrich K, Zhang Z, Schlarb AK. Effects Of Various Fillers On The Sliding Wear Of Polymer Composites. *Compos Sci Technol.* 2005;65(15-16 SPEC.

ISS.):2329–43.

- [21] Tawfik BE, Leheta H, Elhewy A, Elsayed T. Weight Reduction And Strengthening Of Marine Hatch Covers By Using Composite Materials. *Int J Nav Archit Ocean Eng*. 2017 Mar 1;9(2):185–98.
- [22] George M, Chae M, Bressler DC. Composite Materials With Bast Fibres: Structural, Technical, And Environmental Properties. *Prog Mater Sci*. 2016;83:1–23.
- [23] Lotfi A, Li H, Dao DV, Prusty G. Natural Fiber – Reinforced Composites : A Review On Material , Manufacturing , And Machinability. 2019;
- [24] Marsh G. 50 Years Of Reinforced Plastic Boats. *Reinf Plast*. 2006 Oct;50(9):16–9.
- [25] Moreau R. Nautical Activities: What Impact On The Environment? A Life Cycle Approach For “Clear Blue” Boating - Commissioned By The European Confederation Of Nautical Industries - Ecn. 2009. 1–66 P.
- [26] Davies P, Verbouwe W. Evaluation Of Basalt Fibre Composites For Marine Applications. *Appl Compos Mater*. 2018; 25 (2) : 299–308.
- [27] Siró I, Plackett D. Microfibrillated Cellulose And New Nanocomposite Materials: A Review. *Cellul.*, 2010;17 (3) : 4, 59–94.
- [28] Henriksson M, Henriksson G, Berglund LA, Lindström T. An Environmentally Friendly Method For Enzyme-Assisted Preparation Of Microfibrillated Cellulose (MFC) Nanofibers. *Eur Polym J*. 2007; 43 (8) : 34–41.
- [29] Nechyporchuk O, Belgacem MN, Bras J. Production Of Cellulose Nanofibrils: A Review Of Recent Advances. *Ind Crops Prod*. 2016; 93 : 2–25.
- [30] Sathishkumar TP, Naveen J, Satheshkumar S. Hybrid Fiber Reinforced Polymer Composites - A Review. *J Reinf Plast Compos*. 2014; 33 (5) : 454–71.
- [31] Chu WS, Kim CS, Lee HT, Choi JO, Park J Il, Song JH, Et Al. Hybrid Manufacturing In Micro/Nano Scale: A Review. *Int J Precis Eng Manuf - Green Technol*. 2014; 1 (1) : 75–92.
- [32] Polyamide/Nylon (PA Plastic): Uses & Properties [Updated 2022] [Internet]. [Cited 2022 Apr 10]. Available From:

<https://Omnexus.Specialchem.Com/Selection-Guide/Polyamide-Pa-Nylon>

- [33] Rulkens R, Koning C. Chemistry And Technology Of Polyamides. Vol. 5, Polymer Science: A Comprehensive Reference, 10 Volume Set. Elsevier B.V.; 2012. 431–467 P.
- [34] Pan Z, Han S, Wang J, Qi S, Tian G, Wu D. Polyimide Fabric-Reinforced Polyimide Matrix Composites With Excellent Thermal, Mechanical, And Dielectric Properties. High Perform Polym. 2020; 32 (10) : 10, 85–93.
- [35] Jiang Y, Chen L, Xiao C, Zhou N, Qing T, Qian L. Friction And Wear Behaviors Of Steel Ball Against Polyimide-PTFE Composite Under Rolling-Sliding Motion. Tribol Lett. 2021; 69 (3) : 1–12.
- [36] Ghanta TS, Aparna S, Verma N, Purnima D. Review On Nano-And Microfiller-Based Polyamide 6 Hybrid Composite: Effect On Mechanical Properties And Morphology. Polym Eng Sci [Internet]. 2020; 60 (8) : 17, 17–59.
- [37] Szakács J, Mészáros L. Synergistic Effects Of Carbon Nanotubes On The Mechanical Properties Of Basalt And Carbon Fiber-Reinforced Polyamide 6 Hybrid Composites. J Thermoplast Compos Mater. 2018; 31 (4) : 5, 53–71.
- [38] Wohlers T. Additive Manufacturing Advances. Manuf Eng. 2012;148:55–6.
- [39] Kruth JP. Material Incess Manufacturing By Rapid Prototyping Techniques. CIRP Ann - Manuf Technol. 1991 Jan;40(2):603–14.
- [40] S A. Rapid Prototyping Systems. Mech Eng. 1991;113:34.
- [41] Wong K V., Hernandez A. A Review Of Additive Manufacturing. ISRN Mech Eng. 2012;2012:1–10.
- [42] Cooper K. Rapid Prototyping Technology: Selection And Application. Assem Autom. 2001 Dec;21(4):358–9.
- [43] Gibson I, Rosen D, Stucker B. Additive Manufacturing Technologies 3D Printing, Rapid Prototyping, And Direct Digital Manufacturing. 2015.
- [44] ASTM International ISO/ASTM 52921-13. Standard Terminology For Additive Manufacturing- Coordinate Systems And Test Methodologies,. 2013.
- [45] Guo N, Leu MC. Additive Manufacturing: Technology, Applications And Research Needs. Front Mech Eng. 2013; 8 (3) : 2, 15–43.



- [46] Wohlers T. Wohlers Report 2019: 3D Printing And Additive Manufacturing State Of The Industry Annual Worldwide Progress Report [Internet]. Wohlers Associates. Wohlers Associates; 2019. Available From: <https://Wohlersassociates.Com/2019report.Htm>
- [47] Najmon JC, Raeisi S, Tovar A. Review Of Additive Manufacturing Technologies And Applications In The Aerospace Industry. In: Additive Manufacturing For The Aerospace Industry. Elsevier Inc.; 2019; 13 : 7–31.
- [48] Brenken B, Barocio E, Favaloro A, Kunc V, Pipes RB. Fused Filament Fabrication Of Fiber-Reinforced Polymers: A Review. *Addit Manuf.*, 2018; 21 : 1–16.
- [49] Mishra M. Encyclopedia Of Polymer Applications, 3 Volume Set. Encyclopedia Of Polymer Applications, 3 Volume Set. CRC Press; 2018.
- [50] Paolini A, Kollmannsberger S, Rank E. Additive Manufacturing In Construction: A Review On Processes, Applications, And Digital Planning Methods. *Addit Manuf.* 2019; 30 : 80-94.
- [51] Almagour B. Additive Manufacturing Of Emerging Materials. Springer; 2018. 1–355 P.
- [52] Fernandes CP, Engineering M, Engineering M, Engineering BMSC. Use Of Recycled Poly Lactic Acid ( PLA ) Polymer In 3D Printing : A Review. *Int Res J Eng Technol.* 2019;06(09):1841–5.
- [53] Dizon JRC, Espera AH, Chen Q, Advincula RC. Mechanical Characterization Of 3D-Printed Polymers. *Addit Manuf.* 2018 ; 20 : 44–67.
- [54] Jia Y, He H, Peng X, Meng S, Chen J, Geng Y. Preparation Of A New Filament Based On Polyamide-6 For Three-Dimensional Printing. *Polym Eng Sci.* 2017; 57 (12) : 13-22.
- [55] Yao T, Ye J, Deng Z, Zhang K, Ma Y, Ouyang H. Tensile Failure Strength And Separation Angle Of FDM 3D Printing PLA Material: Experimental And Theoretical Analyses. *Compos Part B Eng.* 2020 May 1;188:107894.
- [56] Papon EA, Haque A. Fracture Toughness Of Additively Manufactured Carbon Fiber Reinforced Composites. *Addit Manuf.* 2019; 26 : 41–52.

- [57] Zaverl M, Seydibeyoğlu MÖ, Misra M, Mohanty AK. Studies On Recyclability Of Polyhydroxybutyrate-Co- Valerate Bioplastic: Multiple Melt Processing And Performance Evaluations. *J Appl Polym Sci*. 2011; 116 (5) :26, 58–67.
- [58] Dođru A, Kandemir B, Seydibeyoğlu MÖ. 3D Nanoprinting in the Aero-Industries, *Smart 3D Nanoprinting*. CRC Press,2022; 23-41.
- [59] ASTM. ASTM F2792-12a Standard Terminology For Additive Manufacturing Technologies [Internet]. 2015. Available From: [https://Www.Astm.Org/Standards/F2792.Htm](https://www.Astm.Org/Standards/F2792.Htm)
- [60] Tofail SAM, Koumoulos EP, Bandyopadhyay A, Bose S, O’Donoghue L, Charitidis C. Additive Manufacturing: Scientific And Technological Challenges, Market Uptake And Opportunities. *Materials Today*. 2018; 21 (1) : 22–37.
- [61] Huang SH, Liu P, Mokasdar A, Hou L. Additive Manufacturing And Its Societal Impact: A Literature Review. *Int J Adv Manuf Technol*. 2013;67(5–8):1191–203.
- [62] Ngo TD, Kashani A, Imbalzano G, Nguyen KTQ, Hui D. Additive Manufacturing (3D Printing): A Review Of Materials, Methods, Applications And Challenges. *Compos Part B Eng*. 2018;143 : 172–96.
- [63] Ryan J, Dizon C, Espera AH, Chen Q, Advincula RC. Mechanical Characterization Of 3D-Printed Polymers. *Addit Manuf*. 2018; 20 : 44–67.
- [64] Ning F, Cong W, Qiu J, Wei J, Wang S. Additive Manufacturing Of Carbon Fiber Reinforced Thermoplastic Composites Using Fused Deposition Modeling, *Composites Part B*. Elsevier Ltd; 2015; 80, 34-56
- [65] Ivey M, Melenka GW, Carey JP, Ayranci C. Characterizing Short-Fiber-Reinforced Composites Produced Using Additive Manufacturing. *Adv Manuf Polym Compos Sci*. 2017 Jul 3;3(3):81–91.
- [66] Zhong W, Li F, Zhang Z, Song L, Li Z. Short Fiber Reinforced Composites For Fused Deposition Modeling. *Mater Sci Eng A*. 2001;301:125–30.
- [67] Shofner ML, Lozano K, Rodríguez-Macías FJ, Barrera E V. Nanofiber-Reinforced Polymers Prepared By Fused Deposition Modeling. *J Appl Polym Sci*. 2003; 89 (11) : 30, 81–90.

- [68] Tekinalp HL, Kunc V, Velez-Garcia GM, Duty CE, Love LJ, Naskar AK, Et Al. Highly Oriented Carbon Fiber-Polymer Composites Via Additive Manufacturing. *Compos Sci Technol*. 2014; 105 : 144–50.
- [69] Love LJ, Kunc V, Rios O, Duty CE, Elliott AM, Post BK, Et Al. The Importance Of Carbon Fiber To Polymer Additive Manufacturing. *J Mater Res*. 2014;29(17):1893–8.
- [70] Ning F, Cong W, Hu Y, Wang H. Additive Manufacturing Of Carbon Fiber-Reinforced Plastic Composites Using Fused Deposition Modeling: Effects Of Process Parameters On Tensile Properties. *J Compos Mater*. 2017;51(4):451–62.
- [71] Anwer MAS, Naguib HE. Study On The Morphological, Dynamic Mechanical And Thermal Properties Of PLA Carbon Nanofibre Composites. *Compos Part B Eng*. 2016;91:631–9.
- [72] Ferreira RTL, Amatte IC, Dutra TA, Bürger D. Experimental Characterization And Micrography Of 3D Printed PLA And PLA Reinforced With Short Carbon Fibers. *Compos Part B Eng*. 2017; 124 : 88–100.
- [73] Papon EA, Haque A. Tensile Properties , Void Contents , Dispersion And Fracture Behaviour Of 3D Printed Carbon Nanofiber Reinforced Composites. *J Reinf Plast Compos*. 2018; 37 (6) : 381–95.
- [74] Lu T, Liu S, Jiang M, Xu X, Wang Y, Wang Z, Et Al. Effects Of Modifications Of Bamboo Cellulose Fibers On The Improved Mechanical Properties Of Cellulose Reinforced Poly(Lactic Acid) Composites. *Compos Part B Eng*. 2014; 62 : 191–7.
- [75] Yuan Y, Ruckenstein E. Polyurethane Toughened Polylactide. *Polym Bull*. 1998; 40 (4–5) : 485–90.
- [76] Melenka GW, Cheung BKO, Schofield JS, Dawson MR, Carey JP. Evaluation And Prediction Of The Tensile Properties Of Continuous Fiber-Reinforced 3D Printed Structures. *Compos Struct*. 2016; 153 : 8, 66–75.
- [77] Dickson AN, Barry JN, McDonnell KA, Dowling DP. Fabrication Of Continuous Carbon, Glass And Kevlar Fibre Reinforced Polymer Composites Using Additive Manufacturing. *Addit Manuf*. 2017; 16 : 146–52.

- [78] Justo J, Távora L, García-Guzmán L, París F. Characterization Of 3D Printed Long Fibre Reinforced Composites. *Compos Struct.* 2018; 185 : 537–48.
- [79] Peng Y, Wu Y, Wang K, Gao G, Ahzi S. Synergistic Reinforcement Of Polyamide-Based Composites By Combination Of Short And Continuous Carbon Fibers Via Fused Filament Fabrication. *Compos Struct.* 2019 Jan 1;207:232–9.
- [80] Araya-Calvo M, López-Gómez I, Chamberlain-Simon N, León-Salazar JL, Guillén-Girón T, Corrales-Cordero JS, Et Al. Evaluation Of Compressive And Flexural Properties Of Continuous Fiber Fabrication Additive Manufacturing Technology. *Addit Manuf.* 2018; 22 :157–64.
- [81] Basavaraj CK, Vishwas M. Studies On Effect Of Fused Deposition Modelling Process Parameters On Ultimate Tensile Strength And Dimensional Accuracy Of Nylon. In: *IOP Conference Series: Materials Science And Engineering* [Internet]. Institute Of Physics Publishing; 2016; 12, 10-35.
- [82] Badini C, Padovano E, De Camillis R, Lambertini VG, Pietroluongo M. Preferred Orientation Of Chopped Fibers In Polymer-Based Composites Processed By Selective Laser Sintering And Fused Deposition Modeling: Effects On Mechanical Properties. *J Appl Polym Sci.* 2020; 137 (38) : 41-52.
- [83] Hassen Aa, Lindahl J, Post B, Chen X, Love L, Kunc V. Additive Manufacturing Of Composite Tooling Using High Temperature Thermoplastic Materials Additive Manufacturing Coatings View Project Large Scale Reactive Polymer Additive Manufacturing View Project Additive Manufacturing Of Composite Tooling Using High Temperature Thermoplastic Materials, 2016; 124 (4); 56-67.
- [84] Carneiro OS, Silva AF, Gomes R. Fused Deposition Modeling With Polypropylene. *Mater Des.* 2015; 83 : 7, 68–76.
- [85] Gardner JM, Sauti G, Kim J-W, Cano RJ, Wincheski RA, Stelter CJ, Et Al. Additive Manufacturing Of Multifunctional Components Using High Density Carbon Nanotube Yarn Filaments. In: *NASA.* 2016.
- [86] Hou Z, Tian X, Zhang J, Li D. 3D Printed Continuous Fibre Reinforced Composite Corrugated Structure. *Compos Struct.* 2018; 184 : 10, 05–10.

- [87] Chabaud G, Castro M, Denoual C, Le Duigou A. Hygromechanical Properties Of 3D Printed Continuous Carbon And Glass Fibre Reinforced Polyamide Composite For Outdoor Structural Applications. *Addit Manuf.* 2019; 26: 94–105.
- [88] Chacón JM, Caminero MA, Núñez PJ, García-Plaza E, García-Moreno I, Reverte JM. Additive Manufacturing Of Continuous Fibre Reinforced Thermoplastic Composites Using Fused Deposition Modelling: Effect Of Process Parameters On Mechanical Properties. *Compos Sci Technol.* 2019; 181 : 10, 76-88.
- [89] Zhang J, Zhou Z, Zhang F, Tan Y, Tu Y, Yang B. Performance Of 3D-Printed Continuous-Carbon-Fiber-Reinforced Plastics With Pressure. *Materials (Basel).* 2020; 13(2).
- [90] Matsuzaki R, Ueda M, Namiki M, Jeong TK, Asahara H, Horiguchi K, Et Al. Three-Dimensional Printing Of Continuous-Fiber Composites By In-Nozzle Impregnation. *Sci Rep.* 2016; 6 : 1–7.
- [91] Li N, Li Y, Liu S. Rapid Prototyping Of Continuous Carbon Fiber Reinforced Polylactic Acid Composites By 3D Printing. *J Mater Process Tech [Internet].* 2016; 238 : 2, 18–25.
- [92] Hu Q, Duan Y, Zhang H, Liu D, Yan B, Peng F. Manufacturing And 3D Printing Of Continuous Carbon Fiber Prepreg Filament. *J Mater Sci.* 2018; 53 (3) : 18, 87–98.
- [93] Kabir SMF, Mathur K, Seyam AFM. A Critical Review On 3D Printed Continuous Fiber-Reinforced Composites: History, Mechanism, Materials And Properties. *Compos Struct.* 2020; 232 : 11, 14-76.
- [94] Caminero MA, Chacón JM, García-Moreno I, Reverte JM. Interlaminar Bonding Performance Of 3D Printed Continuous Fibre Reinforced Thermoplastic Composites Using Fused Deposition Modelling. *Polym Test.* 2018; 68:4, 15–23.
- [95] Tian X, Liu T, Wang Q, Dilmurat A, Li D, Ziegmann G. Recycling And Remanufacturing Of 3D Printed Continuous Carbon Fiber Reinforced PLA Composites. *J Clean Prod.* 2017; 142 : 1609–18.

- [96] Tian X, Liu T, Yang C, Wang Q, Li D. Interface And Performance Of 3D Printed Continuous Carbon Fiber Reinforced PLA Composites. *Compos Part A Appl Sci Manuf.* 2016; 88 : 198–205.
- [97] Sugiyama K, Matsuzaki R, Ueda M, Todoroki A, Hirano Y. 3D Printing Of Composite Sandwich Structures Using Continuous Carbon Fiber And Fiber Tension. *Compos Part A Appl Sci Manuf.* 2018; 1 : 14–21.
- [98] Silva M, Pereira AM, Alves N, Mateus A, Malça C. A Hybrid Processing Approach To The Manufacturing Of Polyamide Reinforced Parts With Carbon Fibers. *Procedia Manuf.* 2017; 12 : 195–202.
- [99] Brooks H, Molony S. Design And Evaluation Of Additively Manufactured Parts With Three Dimensional Continuous Fibre Reinforcement. *Mater Des.* 2016; 90 : 276–83.
- [100] Li J. Interfacial Studies On The O<sub>3</sub> Modified Carbon Fiber-Reinforced Polyamide 6 Composites. *Appl Surf Sci.* 2008;255(5 PART 2):2822–4.
- [101] Wojtuszewski R, Banaś A. Topology Optimization In Additive Manufacturing. *Annu Forum Proc - AHS Int.* 2017;1752–9.
- [102] Shi G, Guan C, Quan D, Wu D, Tang L, Gao T. An Aerospace Bracket Designed By Thermo-Elastic Topology Optimization And Manufactured By Additive Manufacturing. *Chinese J Aeronaut.* 2019
- [103] Mirzendehtel AM, Suresh K. Support Structure Constrained Topology Optimization For Additive Manufacturing. *CAD Comput Aided Des.* 2016;81:1–13.
- [104] Goh GD, Dikshit V, Nagalingam AP, Goh GL, Agarwala S, Sing SL, Et Al. Characterization Of Mechanical Properties And Fracture Mode Of Additively Manufactured Carbon Fiber And Glass Fiber Reinforced Thermoplastics. *Mater Des.* 2018; 137 : 79–89.
- [105] Ferro C, Grassi R, Secli C, Maggiore P. Additive Manufacturing Offers New Opportunities In UAV Research. In: *Procedia CIRP.* Elsevier B.V.; 2016; 27, 1004–10.
- [106] Lanzotti A, Martorelli M, Maietta S, Gerbino S, Penta F, Gloria A. A Comparison Between Mechanical Properties Of Specimens 3D Printed With

- Virgin And Recycled PLA. *Procedia CIRP*. 2019; 79 : 143–6.
- [107] Reese J, Vorhof M, Hoffmann G, Böhme K, Cherif C. Joule Heating Of Dry Textiles Made Of Recycled Carbon Fibers And PA6 For The Series Production Of Thermoplastic Composites. *J Eng Fiber Fabr*. 2020;15.
- [108] Yang Y, Boom R, Irion B, Van Heerden DJ, Kuiper P, De Wit H. Recycling Of Composite Materials. *Chem Eng Process Process Intensif*. 2012; 51 : 53 – 68.
- [109] Yousefian H, Rodrigue D. Effect Of Nanocrystalline Cellulose On Morphological, Thermal, And Mechanical Properties Of Nylon 6 Composites. *Polymer Composite*. 2016; 37 (5) : 1473–9.
- [110] Liu T, Tian X, Zhang M, Abliz D, Li D, Ziegmann G. Interfacial Performance And Fracture Patterns Of 3D Printed Continuous Carbon Fiber With Sizing Reinforced PA6 Composites. *Compos Part A Appl Sci Manuf*. 2018; 114 : 368–76.
- [111] Kim JS, Lee CS, Lee SW, Kim SM, Choi JH, Chung H, Et Al. Fabrication And Characterization Of Hollow Glass Beads-Filled Thermoplastic Composite Filament Developed For Material Extrusion Additive Manufacturing. *J Compos Mater*. 2020;54(5):607–15.
- [112] Hart KR, Dunn RM, Sietins JM, Hofmeister Mock CM, Mackay ME, Wetzel ED. Increased Fracture Toughness Of Additively Manufactured Amorphous Thermoplastics Via Thermal Annealing. Vol. 144, *Polymer*. 2018. P. 192–204.
- [113] Watson-Wright C, Singh D, Demokritou P. Toxicological Implications Of Released Particulate Matter During Thermal Decomposition Of Nano-Enabled Thermoplastics. *Nanoimpact*. 2017; 5 : 29 – 40.
- [114] Deloid G, Casella B, Pirela S, Filoramo R, Pyrgiotakis G, Demokritou P, Et Al. Effects Of Engineered Nanomaterial Exposure On Macrophage Innate Immune Function. *Nanoimpact*. 2016; 2: 70–81.
- [115] Benkaddour A, Demir EC, Jankovic N, Kim C, Mcdermott M, Ayranci C. Composites Part C : Open Access A Hydrophobic Coating On Cellulose Nanocrystals Improves The Mechanical Properties Of. *Compos Part C Open Access*. 2020;
- [116] Gardner DJ, Oporto GS, Mills R, Samir MASA. Adhesion And Surface Issues

- In Cellulose And Nanocellulose, Journal Of Adhesion Science And Technology. Taylor & Francis Group. 2008; 22. 45–67.
- [117] Sehaqui H, Zhou Q, Ikkala O, Berglund LA. Strong And Tough Cellulose Nanopaper With High Specific Surface Area And Porosity. Biomacromolecules. 2011; 12 (10) : 38–44.
- [118] Eichhorn SJ. Cellulose Nanowhiskers: Promising Materials For Advanced Applications. The Royal Society Of Chemistry; 2011; Vol. 7, 303–15.
- [119] Oksman K, Aitomäki Y, Mathew AP, Siqueira G, Zhou Q, Butylina S, Et Al. Review Of The Recent Developments In Cellulose Nanocomposite Processing. Compos Part A Appl Sci Manuf. 2016 Apr 1;83:2–18.
- [120] Chakrabarty A, Teramoto Y. Recent Advances In Nanocellulose Composites With Polymers: A Guide For Choosing Partners And How To Incorporate Them. Polymers (Basel). 2018; 10 (5) : 517.
- [121] Mao J, Abushammala H, Brown N, Laborie M-P. Comparative Assessment Of Methods For Producing Cellulose I Nanocrystals From Cellulosic Sources. In: ACS Symposium Series. 2017; 19–53.
- [122] Qua EH, Hornsby PR, Sharma HSS, Lyons G, Mccall RD. Preparation And Characterization Of Poly(Vinyl Alcohol) Nanocomposites Made From Cellulose Nanofibers. J Appl Polym Sci. 2009; 113 (4) : 38 – 47.
- [123] Mathew AP, Oksman K, Sain M. Mechanical Properties Of Biodegradable Composites From Poly Lactic Acid (PLA) And Microcrystalline Cellulose (MCC). J Appl Polym Sci. 2005; 97 (5) : 2014 – 25.
- [124] Wang D, Cheng W, Wang Q, Zang J, Zhang Y, Han G. Preparation Of Electrospun Chitosan/Poly(Ethylene Oxide) Composite Nanofibers Reinforced With Cellulose Nanocrystals: Structure, Morphology, And Mechanical Behavior. Compos Sci Technol. 2019 Sep 29;182:107774.
- [125] Fang H, Chen X, Wang S, Cheng S, Ding Y. Enhanced Mechanical And Oxygen Barrier Performance In Biodegradable Polyurethanes By Incorporating Cellulose Nanocrystals With Interfacial Polylactide Stereocomplexation. Cellulose. 2019; 26 (18) : 9751–64.
- [126] Hendren KD, Baughman TW, Deck PA, Foster EJ. In Situ Dispersion And



- Polymerization Of Polyethylene Cellulose Nanocrystal-Based Nanocomposites. *J Appl Polym Sci.* 2020; 137 (13) : 48500.
- [127] Sojoudiasli H, Heuzey M-C, Carreau PJ. Mechanical And Morphological Properties Of Cellulose Nanocrystal-Polypropylene Composites. *Polym Compos.* 2018; 39 (10) : 36, 05–17.
- [128] Zhang Z, Sèbe G, Wang X, Tam KC. UV-Absorbing Cellulose Nanocrystals As Functional Reinforcing Fillers In Poly(Vinyl Chloride) Films. *ACS Appl Nano Mater.* 2018; 1 (2) : 6, 32–41.
- [129] Neves RM, Lopes KS, Zimmermann MVG, Poletto M, Zattera AJ. Characterization Of Polystyrene Nanocomposites And Expanded Nanocomposites Reinforced With Cellulose Nanofibers And Nanocrystals. *Cellulose [Internet].* 2019; 26 (7) : 44, 17–29.
- [130] Corrêa AC, De Moraes Teixeira E, Carmona VB, Teodoro KBR, Ribeiro C, Mattoso LHC, Et Al. Obtaining Nanocomposites Of Polyamide 6 And Cellulose Whiskers Via Extrusion And Injection Molding. *Cellulose.* 2014; 21 (1):11–22.
- [131] Çetin NS, Tingaut P, Özmen N, Henry N, Harper D, Dadmun M, Et Al. Acetylation Of Cellulose Nanowhiskers With Vinyl Acetate Under Moderate Conditions. *Macromol Biosci.* 2009; 9 (10) : 997–1003.
- [132] Bendahou A, Hajlane A, Dufresne A, Boufi S, Kaddami H. Esterification And Amidation For Grafting Long Aliphatic Chains On To Cellulose Nanocrystals: A Comparative Study. *Res Chem Intermed.* 2015; 41 (7) : 4, 293–310.
- [133] Liu Y, Li M, Qiao M, Ren X, Huang T-S, Buschle-Diller G. Antibacterial Membranes Based On Chitosan And Quaternary Ammonium Salts Modified Nanocrystalline Cellulose. *Polym Adv Technol.* 2017; 28 (12) : 16, 29–35.
- [134] Kaboorani A, Riedl B. Surface Modification Of Cellulose Nanocrystals (CNC) By A Cationic Surfactant. *Ind Crops Prod.* 2015; 65 : 45–55.
- [135] Huang F-Y. Thermal Properties And Thermal Degradation Of Cellulose Tri-Stearate (Cts). *Polymers (Basel).* 2012; 4 (2) : 10, 12–24.
- [136] Ligon SC, Liska R, Stampfl J, Gurr M, Mülhaupt R. Polymers For 3D Printing And Customized Additive Manufacturing. *Chem Rev.* 2017; 117 (15) : 82–90.

- [137] Gibson I, Rosen D, Stucker B. Additive Manufacturing Technologies: 3D Printing, Rapid Prototyping, And Direct Digital Manufacturing, Second Edition. Additive Manufacturing Technologies: 3D Printing, Rapid Prototyping, And Direct Digital Manufacturing, Second Edition. 2015. P.1–498
- [138] Mard M. Use Of Rheological Properties To Predict Extrusion Parameters.
- [139] Friedrich K. Polymer Composites For Tribological Applications. *Adv Ind Eng Polym Res*. 2018; 1 (1) : 3–39.
- [140] Mazzanti V, Malagutti L, Mollica F. FDM 3D Printing Of Polymers Containing Natural Fillers: A Review Of Their Mechanical Properties. *Polymers (Basel)*. 2019;11(7).
- [141] Hajian A, Lindström SB, Pettersson T, Hamed MM, Wågberg L. Understanding The Dispersive Action Of Nanocellulose For Carbon Nanomaterials. *Nano Lett*. 2017; 17 (3) : 14, 39–47.
- [142] Wölfel B, Seefried A, Allen V, Kaschta J, Holmes C, Schubert DW. Recycling And Reprocessing Of Thermoplastic Polyurethane Materials Towards Nonwoven Processing. *Polymers (Basel)*. 2020; 12 (9) : 23-35.
- [143] Garces IT, Aslanzadeh S, Boluk Y, Ayranci C. Cellulose Nanocrystals (CNC) Reinforced Shape Memory Polyurethane Ribbons For Future Biomedical Applications And Design. *J Thermoplast Compos Mater*. 2020; 33 (3) : 77–92.
- [144] Huang S, Li H, Jiang S, Chen X, An L. Crystal Structure And Morphology Influenced By Shear Effect Of Poly(L-Lactide) And Its Melting Behavior Revealed By WAXD, DSC And In-Situ POM. *Polymer*. 2011; 52 (15) : 78–87.
- [145] Parandoush P, Lin D. A Review On Additive Manufacturing Of Polymer-Fiber Composites. *Compos Struct*. 2017; 182 : 36–53.
- [146] Galeja M, Hejna A, Kosmela P, Kulawik A. Static And Dynamic Mechanical Properties Of 3D Printed ABS As A Function Of Raster Angle. *Materials (Basel)*. 2020; 13 (2) : 56-64.
- [147] Goh GD, Yap YL, Agarwala S, Yeong WY. Recent Progress In Additive Manufacturing Of Fiber Reinforced Polymer Composite. *Adv Mater Technol*. 2019; 4 (1) : 33-40.

# Curriculum Vitae

Name Surname : Alperen DOĞRU

## Education:

- 2006–2010 Kocaeli University, Bachelor of Science, Aircraft Structures and System
- 2008–2013 Anadolu University, Bachelor of Science, Business and Administration
- 2010-2013 Sakarya University, Bachelor of Science, Industrial Eng.
- 2011-2014 Manisa Celal Bayar University, Master of Science, Mechanical Eng.

## Work Experience:

- 2009–2010 NDT Engineer / Turkish Technic
- 2010-2011 Instructor / TAI
- 2017-2018 Lecturer / National Defence University, Air Force HVS
- 2021-2022 Visiting Researcher / University of Alberta, Engineering Faculty
- 2010-... Lecturer / Ege University

## Publications (if any):

1. Lightweight Composite Materials in Transport Structures  
eBook ISBN: 9780429244087
2. 3D Nanoprinting in the Aero-Industries  
eBook ISBN: 9781003189404